UMBRELLA CELL MECHANOTRANSDUCTION AND STRETCH-REGULATED EXOCYTOSIS/ENDOCYTOSIS

by

Weiqun Yu

B.M., Zhejiang Medical University, 1993

M.S., Chongqing University, 1998

Submitted to the Graduate Faculty of

The Swanson School of Engineering in partial fulfillment

of the requirements for the degree of

Doctor of Philosophy

University of Pittsburgh

2008

UNIVERSITY OF PITTSBURGH

SWANSON SCHOOL OF ENGINEERING

This dissertation was presented

by

Weiqun Yu

It was defended on

December 10th, 2007

And approved by

Sanjeev G. Shroff, Professor, Department of Bioengineering

Lori Birder, Assistant Professor, Department of Medicine

Hai Lin, Assistant Professor, Department of Bioengineering

Dissertation Director: Gerard Apodaca, Professor, Department of Medicine

UMBRELLA CELL MECHANOTRANSDUCTION AND STRETCH-REGULATED EXOCYTOSIS/ENDOCYTOSIS

Weiqun Yu, Ph.D.

University of Pittsburgh, 2008

Cells interact with mechanical environments by mechanotransduction, a cellular process that converts mechanical signals into biochemical signals. Umbrella cells respond to mechanical stimuli by increasing exocytosis, endocytosis, and ion transport, but how these processes are coordinated and the mechanotransduction pathways involved are not well understood. By manipulating different forces and force parameters applied on umbrella cells, the responses of electrophysiological parameters (TEV, TER, and Isc) and apical membrane capacitance ($1\mu F \approx 1cm^2$ membrane surface area) are monitored through the modified Ussing chamber system. Stretch of the umbrella cells result in an acute change of electrical parameters, but not hydrostatic pressure. Further, the stretched response is sensitive to force direction, indicating that stretch of apical membrane causes umbrella cell TEV hyperpolarization, TER decrease, Isc increase, and apical membrane exocytosis, while stretch of basolateral membrane causes opposite effects, and this observation can be modeled mathematically. Stretch speed, which is defined by the filling rate, is further defined to play the key role in modulating the degree and time course of stretched umbrella cell responses, suggesting a mechnosensory function of umbrella cells.

Use of channel blockers and openers established that the stretch of apical membrane is likely dependent on cation transport pathway, while stretch of basolateral membrane is dependent on K^+ transport at the basolateral surface of the cells, indicating distinctive apical and basolateral membrane requirements for umbrella cell mechanotransduction. These results indicate that mechanotransduction in umbrella cells depends on the sequential activity of its distinct apical and basolateral membrane domains, which act in a collaborative manner to regulate apical membrane dynamics.

TABLE OF CONTENTS

LIST OF TABLES

LIST OF FIGURES

1.0 INTRODUCTION

The mammalian urinary bladder is a hollow organ that serves as a temporary storage site for urine, a function that greatly increases the sanitary conditions of an animal's living area. Coordinated action of the bladder and the nervous system is required to achieve this function. Briefly, the bladder wall is dynamically extended to accommodate the increased urine volume, and bladder fullness is sensed by bladder-associated nerve process that emanate from the sacral spinal cord. Voluntary signals from the brain act to override the sacral reflex and cause the bladder wall to contract while the external urinary sphincter relaxes. As a result, a sudden, sharp rise in intravesical pressure (from ~ 8 cm H_2O to ~ 30 cm H_2O) occurs and urine flows from the urinary bladder through the urethra. Various signals are required to control this coordinated actions, among which, mechanical signals are considered to play a critical role. However, the role of mechanical forces and the mechanotransduction pathways are still poorly understood.

Umbrella cells, which form the outer layer of the uroepithelium, line the luminal surface of the bladder and contact the urine, where they function as a physical barrier between the underlying tissue and urine. In addition to forming a barrier, emerging data

indicates that these cells may also play a key role in the coordinated action of the bladder by acting as a mechanosensor/transducer that senses bladder filling and communicates these changes to the nervous system (1-4).

1.1 URINARY BLADDER AND UMBRELLA CELLS

1.1.1 Urinary bladder: structure and function

The urinary bladder is a sac-shaped muscular sphere that sits in the middle of the urinary secretion pathway and resides on the pelvic floor. Urine enters the bladder via the two ureters that are connected to the upstream kidneys and exits via the urethra to the outside of the body. The trigone, which is a triangular shaped area on the postero-inferior wall of the bladder, is the place that ureters enter and the urethra exits the bladder (Figure 1.1). While both ureters and urethra are conductive tubes for urine, the urethra has a striated surrounding muscle called the sphincter that allows voluntary control over urination.

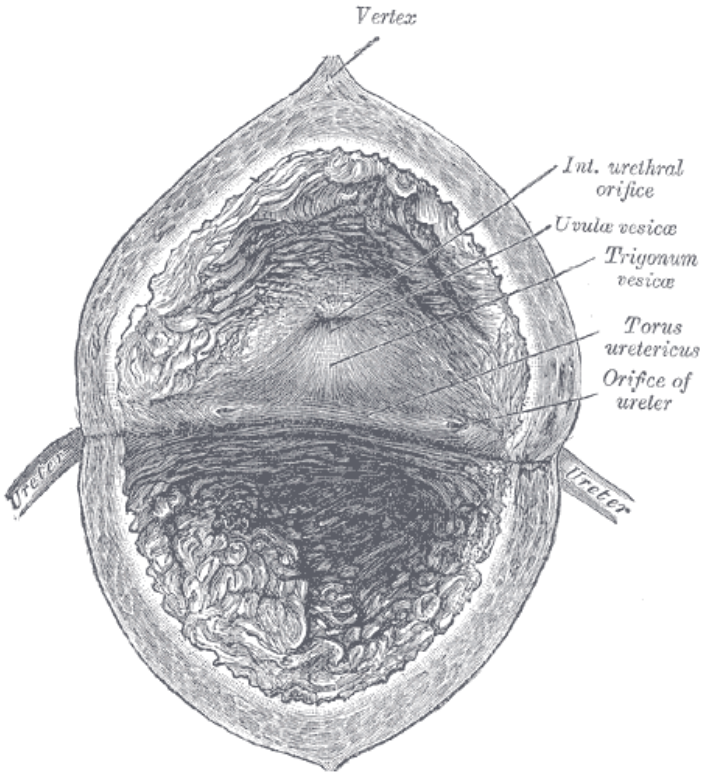

Figure 1.1 Anatomy of urinary bladder (copied from *Gray's Anatomy,* 39th edition, 2004, C.V. Mosby, US)

The thin wall of the urinary bladder consists of 3 layers: the transitional uroepithelial tissue that lines the inner surface of the bladder wall; a lamina propria that sits below the uroepithelium and is comprised of a loose connective tissue that contains a capillary bed, lymph vessels, and sensory neurons; a layer of smooth muscle known as the detrusor, which consists of an inner and outer longitudinal layer and a middle circular layer. (Figure 1.2).

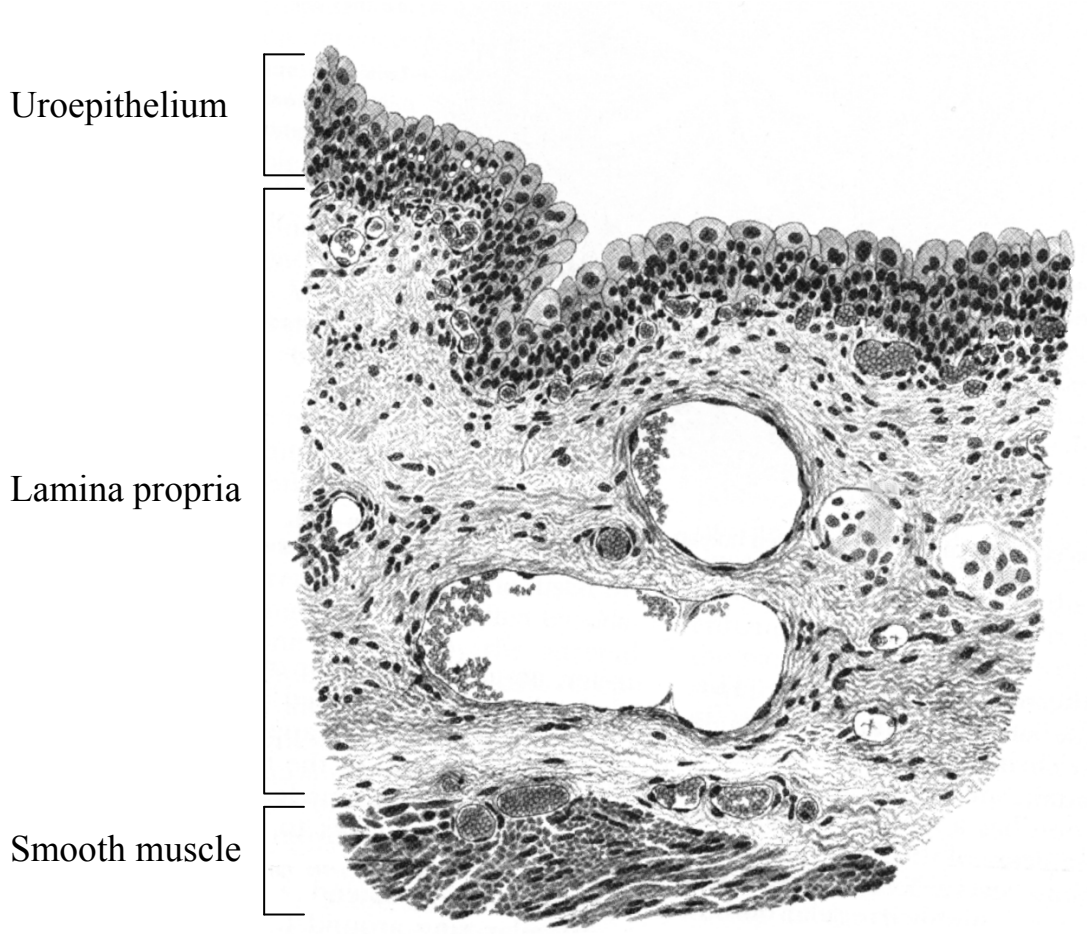

Figure 1.2 Structure of urinary bladder wall (Copied from Bloom *and Fawcett, A Textbook of Histology,* 12th edition, 1994 Chapman & Hall, New York)

This macrostructure enables the urinary bladder to be an ideal organ for urine storage and voiding. When relaxed, the bladder wall collapses and the inner mucosal surface infolds to form ruffles that minimize the bladder volume. During urinary instillation, the ruffles are unfolded and the compliance and elasticity of the bladder wall allow it to hold large volumes of urine, typically 400-600 ml in human. The stretch of the

bladder wall eventually initiates the micturition reflex, in which fullness of the urine is sensed and a voluntary signal is sent out, which contracts the detrusor, relaxes the sphincter, and allows for the expulsion of urine from the urethra.

1.1.2 Umbrella cell

1.1.2.1 Uroepithelium

The uroepithelium is the epithelial layer that covers the inner surface of urinary tract, including the renal pelvis, the ureters, the bladder, and the urethra. It is a stratified epithelial tissue comprised of three layers (5): basal cells, intermediate cells and umbrella cells (Figure 1.3). Basal cells sit on the connective tissue of the lamina propria. They are columnar with a diameter of 5-10 μM. Basal cells are germinal in nature and contain tissue-specific stem cells that are capable of cell proliferation and differentiation into intermediate cells and umbrella cells, thus generating a pool of maturing cells that maintains tissue homeostasis. Intermediate cells rise from basal cells, and they are ~20 μM in diameter. They may contain a pool of cytoplasmic vesicles as a distinctive feature from basal cells. Intermediate cells can form one to multiple cell layer(s), depending on the degree of bladder stretch. Intermediate cells can undergo quick differentiation into umbrella cells, especially when the umbrella cells are damaged. Umbrella cells form the superficial single epithelial layer that contacts the urine. They are hexagonal and have a diameter of 50-120 μM, depending on the degree of bladder stretch. Umbrella cells are fully differentiated and to form the barrier through their high resistance and impermeability of the apical membrane.

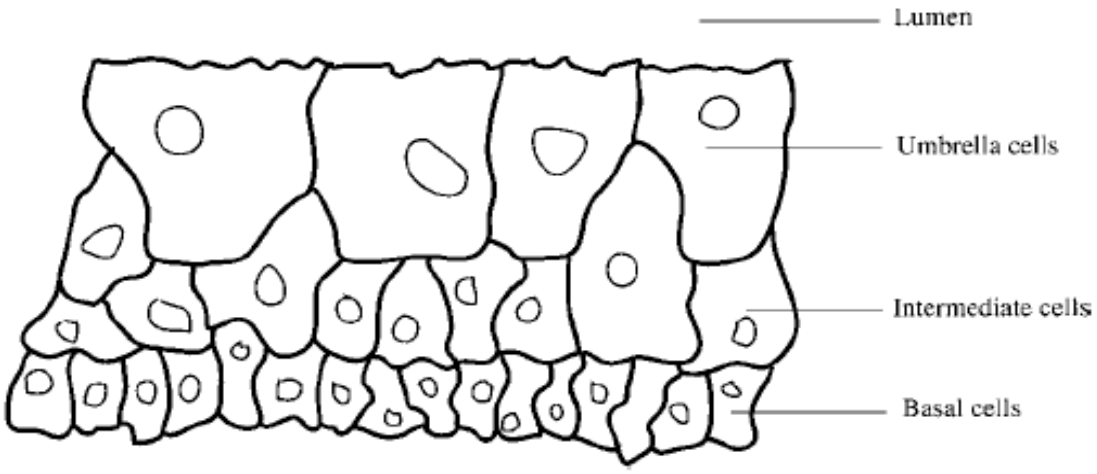

Figure 1.3 Schematic of the three layers of the uroepithelium (copied from reference 5)

1.1.2.2 Dynamic apical membrane

Umbrella cells are transitional epithelial cells. When relaxed, the cells appear to be cuboidal, and when stretched, they look flat and squamous. This dramatic morphological change enables umbrella cells to accommodate the varying urine volume. Like other polarized epithelia, umbrella cells have distinctive apical and basolateral plasma membrane domains, which are separated by tight junction (Figure 1.4). Two characteristics of the apical membrane of these cells contribute to the storage function of umbrella cells. During the initial phase of bladder filling, the unfolding of apical membrane ruffles (Figure 1.4) serves as one mechanism to accommodate increased urine

volume. The insertion of a pool of cytoplasmic vesicles (Figure 1.4) into the apical membrane provides additional mucosal expansion. During the voiding phase, the infolding and endocytosis of apical membrane reduces the bladder volume. While the recycling of endocytosed vesicles may provide a pool for additional rounds of bladder filling. The umbrella cell basolateral membrane, it is thought to undergo physical extension and contraction during cycles of bladder filling and voiding, but does not change surface area (5-7).

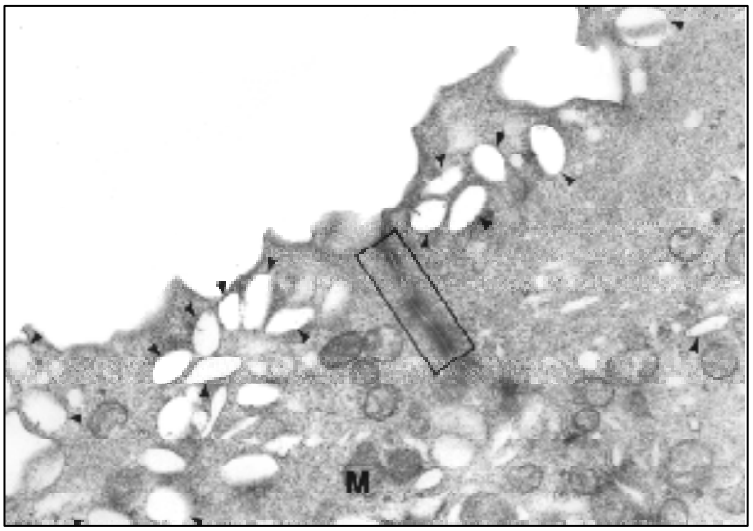

Figure 1.4 Umbrella cell apical membrane and cytoplasmic vesicles

1.1.2.2.1 Cytoplasmic vesicles

The umbrella cells contain a large pool of cytoplasmic vesicles that reside in the subapical domain (7). These vesicles can be either discoidal or fusiform-shaped, depending on the animal species. They are composed of two apposing plaques joined together by hinge membrane, and their protein composition appears to be similar with

those of apical membrane. Their exocytosis/endocytosis serves as an important mechanism for the adaptation of the apical membrane during bladder filling/voiding. These vesicles are tethered to the apical membrane by intermediate filaments, and these intermediate filaments are also associated with tight junctions and desmosomes along the basolateral membrane, suggesting an intriguing function of intermediate filaments in vesicles exocytosis/endocytosis.

1.1.2.3 Apical membrane permeability

The apical membrane of umbrella cells is impermeable to urine, a hypertonic solution containing many metabolites that are potentially toxic to underlying tissues. Several factors may contribute to this impermeabilitiy. Firstly, the surface of apical membrane is covered by a layer of glycosaminoglycan (GAG), a highly negatively charged polysaccharides that may function as the initial barrier by forming a non-adherent water layer to exclude salts and urinary proteins from the surface (8, 9). Secondly, the majority of the apical surface of umbrella cells is covered by scalloped-shaped plaques. These unit membrane of plaques have a thicker luminal leaflet compared to the inner leaflet, and is termed the asymmetrical unit membrane (AUM). The AUM forms an impermeable barrier to urine (5). Thirdly, the composition of the lipids associated with the AUM plaques is also believed to play a large role in determining the permeability barrier of the umbrella cells. Purified umbrella cell plaques are rich in both cholesterol and sphingolipids, which leads to a more ordered lipid structure, lowering membrane fluidity and permeability and favoring microdomain formation (10). Fourthly, the very high resistance of the apical membrane and the tight junctions provides a selective barrier to

ions (describe later). Collectively these features result in the apical membrane with low permeabilities to urea, ammonia, water and protons.

1.1.2.3.1 Uroplakins

The plaques of the AUM are composed of a paracrystalline array of subunits with center-to-center spacing of ~16 nM, and these subunits consist of 5 special transmembrane proteins known as uroplakins, including uroplakin Ia, Ib, II, IIIa, and IIIb (1). They can assemble into a hexagonal ribbon-like structure and form specific heterodimer pairs. Mice lacking expression of uroplakin II or uroplakin III hacce small or no plaques and develop vesicoureteral reflux and leaky plasma membranes (11, 12). The molecular mechanism of these defects is unknown.

1.1.2.4 Electrophysiological properties

Umbrella cells are classified as one of the tightest epithelia. The transepithelial resistance (TER) of the rabbit urinary bladder can be as high as 75,000 $\Omega \cdot cm^2$. TER is the sum of the resistances of the tight junctions and a parallel pathway comprised of the the apical and basolateral membranes. In rabbits, the tight junction connecting neighboring umbrella cells shows an extremely large resistance, approaching ∞ (13). The resistance of the basolateral membrane is ~1,500 $\Omega \cdot cm^2$, while the resistance of apical membrane is ~ 20,000 $\Omega \cdot cm^2$. Thus the TER essentially reflects the resistance of the apical membrane. The apical membrane of umbrella cells actively uptakes sodium from the mucosal solution by epithelium sodium channels (ENaC) as well as by some unknown cation

channel(s) expressed on this membrane (14). The absorbed sodium is pumped out the cell through the basal Na^+- K^+ ATPase (15). Potassium brought in by the pump exits the basolateral membrane by potassium-selective channels. These pump and ion channel activities generate a short circuit current ~2 $\mu A/cm^2$ and different apical (~ 40 mV) and basolateral (~ 70 mV) membrane potentials (13, 16). These electrophysiological activities are sensitive to external stimuli, such as aldosterone and mechanical stimuli (6, 17-19).

1.1.2.5 Innervation

The urinary bladder is innervated by parasympathetic (S2-S4) and sympathetic (T9-L1) nerves (20). Uroepithelia, including umbrella cells, are innervated by visceral afferent neurons for the bladder. The cholingeric and adrenergic efferent neurons are also present below the uroepithelium (2). The close contact of neurons and umbrella cells indicates intercommunication between them and further suggest a sensory function for umbrella cells (2, 21).

1.2 MECHANOTRANSDUCTION

1.2.1 Mechanical regulation of cellular function

1.2.1.1 Different mechanical forces

Cells live in a mechanical environment, and mechanical forces play a central role in a wide variety of cellular functions, including cell motility, growth, differentiation, and cell organization.

Different mechanical stimuli regulate cell functions differentially. For example, disturbed flow in blood vessels can increase endothelial monocyte chemotactic protein-1 (MCP-1) expression, which promotes endothelial proliferation, increases endothelial low-density lipoprotein (LDL) permeability and lipid synthesis, and place the vessel at risk for atherogenesis. In contrast, the sustained shear stress of laminar flow decreases endothelial MCP-1 expression, reduces endothelial proliferation, decreases endothelial LDL permeability and lipid synthesis, and is protective against atherogenesis (22, 23). The mammalian urinary bladder is also a mechanically regulated organ. The urinary bladder undergoes cycles of hydrostatic pressure fluctuation during filling and voiding, and as a result the wall of the urinary bladder is exposed to cycles of stretch and relaxation

according to the urinary volume. It is known that mechanical forces regulate umbrella cell apical surface area and that the increase in umbrella cell surface area is accompanied by a decrease in the number of subapical discoidal vesicles (6, 7). It is also known that mechanical sensitive channels exist in umbrella cells, and mechanical forces regulate ion transport in umbrella cells (19). However, whether hydrostatic pressure, or stretch, regulates membrane exocytosis/endocytosis and channel function in umbrella cells is unknown.

1.2.1.2 Different force parameters

The combination of force direction, magnitude, and frequency/speed, can modulate cellular functions differently. In the hair cell of the inner ear, the direction of stereocilla deflection is one of the key parameters that modulate channel activity and hair cell function. The deflection that stretches the tip link between adjacent stereocillia causes the transduction channel to open, while a deflection that relaxes the tip link closes the transduction channels (24). In rat fetal lung fibroblasts, epithelial cells, and human tendon fibroblasts, uniaxial stretch (magnitude: 5% strain and frequency: 1Hz) increases DNA synthesis and cell proliferation (25, 26), while in periodontal ligament cells, 9 or 18% uniaxial strain (0.1Hz) induces these cells to differentiate into osteoblasts and cementoblasts accompanied by decreased expression of EGF receptor (27). The possible effect of different force parameters on umbrella cells is a totally unexplored area.

1.2.2 Mechanosensors, transducers, and secondary messengers

The mechanical regulation of cellar functions is mediated through a process called mechanotransduction, in which a mechanical signal is sensed by cellular sensors and converted into biochemical signals. As numerous molecules have been identified to contribute to the mechanotransduction responses, such as ion channels, adhesive molecules, enzymes, the cytoskeleton, motor proteins, and the extracellular matrix, we are starting to understand some detail about these pathways. In the following sections, I will describe the role that these mechanosensors/transducers play in mechanotransduction.

1.2.2.1 Mechanical-sensitive ion channels

Mechanical-sensitive ion channels comprise one of the best understood models of mechanotransduction. In this case an ion channel is opened by an external mechanical force and stimulates the influx of ions such as Ca^{2+}. The mechanical sensitive ion channels can be directly activated through the increased tension exerted on the lipid bilayer, or through the force conveyed by structural proteins connected to the ion channel, such as the cytoskeleton. The mechanical sensitive ion channels can also be regulated indirectly through secondary messengers generated by other mechanosensors (28).

A growing list of mechanical sensitive ion channels has been identified in organisms ranging from prokaryotes to eukaryotes. There are three ion channels known to be associated with mechanosensitive activities in Escherichia coli (E.coli): MscL (MechanoSensitive Channel of Large conductance), MscS (Smaller conductance), and

MscK (K^+ regulated), and all three sense changes to membrane tension (29, 30). Sodium conductive channels, including the degenerins (DEGs), are expressed in the touch sensitive neuron of Caenorhabditis elegans and mutants in DEGs abolish their behavioral responses to touch (31). Vertebrate ENaCs have also been implicated in various mechanosensory modalities, such as in blood pressure sensing and cutaneous touch sensing (32). Recently, members of the transient receptor potential (TRP) channel superfamily and potassium channel superfamily have also been recognized as participating in mechanotransduction (33).

Hair cells, the mechanoreceptors of the inner ear, provide a classical model for ion channel mechanotransduction, where deflection of the hair bundles directly opens transduction channels through the stretch of the tip link between two stereocillia, and admit cations and depolarize the hair cell. These changes then increase neurontransmitter release from the synapses on basolateral surfaces of the hair cells (34). Umbrella cells are also sensitive to mechanical forces, and cation channels are believed to be expressed on apical membrane (35), but how they are respond to mechanical forces and the identity of the channel is not known.

1.2.2.1.1 TRP channels

The TRP channel superfamily contains 28 members (in mouse) of cation permeable channels, which have been divided into seven subfamilies: TRPC, TRPM, TRPV, TRPN, TRPA, TRPP and TRPML. They all share the common feature of six transmembrane domains and varying degrees of sequence similarity. They display numerous activating modes and physiological functions, particularly in sensory transduction for vision,

hearing, taste, olfaction, pheromone sensation, thermosensation, and mechanosensation (36-40).

Drosophila NompC is the first TRP channel identified to have a clear role in mechanosensation. The N terminus of NompC contains 29 ankyrin repeats that are suggested to function as a spring that transduces the mechanical force that results in channel opening (41, 42). In situ hybridization reveals expression of NompC in a variety of ciliated mechanoreceptor organs of fly and mutation in this protein show a defect in withdrawal from touch stimuli (42). NompC was also expressed in the hair cells of the zebrafish inner ear, and when zebrafish eggs are injected with morpholino oligonucleotides to block correct splicing of the NompC mRNA, the larvae were often deaf and display a balance disorder (43).

TRPV4 is another interesting TRP member. It is expressed in many tissues, such as kidney distal tubules, airway epithelium, and vascular epithelium. It is activated by osmotic stress and causes cell swelling (44). Mice lacking TRPV4 have reduced regulation of serum osmolarity and pressure sensation (45). The activation of TRPV4 by swelling is dependent on the generation of arachidonic acid by phospholipase A2, suggesting an indirect activation by lipid metabolism (46). TRPV4 is also expressed in umbrella cells and the TRPV4-selective agonist 4α-PDD evokes ATP release and increased maximal micturition pressure by 51%, suggesting TRPV4 channels in the urothelium could contribute to bladder activity (47).

PKD1 and PKD2 are TRPP subfamily members and mutants of any one of these two genes cause autosomal dominant polycystic kidney disease, a disease that is characterized by the development of large fluid-filled cysts in the kidney (48). PKD2

forms an ion channel and interacts with PKD1 (49). Together they act as a functional signaling complex. PKD1 and PKD2 are expressed in tissues like kidney, live, spleen, pancreas, and heart. Cysts may also develop in tissues other than kidney. Of particular interests, PKD1 and PKD2 are localized at the apical primary cilium of kidney and oviduct epithelium (50, 51). Bending of the primary cilium in cultured kidney epithelium by fluid flow causes calcium influx. Mutant epithelia lacking PKD1 do not show flow-activated calcium influx, nor do epithelia treated with blocking antibodies to either PKD1 or PKD2 (52, 53), indicating an essential role of PKD1 and PKD2 in primary cilia mechanotransduction. Their expression and function in urinary bladder is unclear.

Except TRPV4, TRPV1 is also expressed in urinary bladder epithelium and nerve fibers in the suburothelium. Activation of TRPV1 by the endogenous agonist anandamide evokes an increased bladder reflex activity. TRPV1 knockout mice display an increased bladder capacity and non-voiding bladder contraction (54). Currently, the mechanism of these phenotypes is still unresolved.

1.2.2.1.2 Potassium channels

Potassium channels are ubiquitous and key regulators of cellular electrophysiological properties. They are involved in almost every aspect of cellular functions, such as neuron transmitter and hormone release, regulation of vascular tone, and muscle contraction. Disruption of potassium genes can cause diseases such as cardiac arrhythmias, deafness, epilepsy, diabetes, and misregulation of blood pressure (55).

Over 80 potassium channel genes have been identified, and they can be classified as voltage-gated potassium channels (Kv, ~40 genes), calcium-activated potassium

channels (Kca, ~8 genes), two-pore potassium channels (K2P, ~15 genes), and inwardly rectifying potassium channels (Kir, ~15 genes). While K2P channels form dimers, all other potassium channels form tetramers (56-60).

Kv channels are activated by voltage depolarization which allows the outward flow of K^+ to repolarize the cell, while other potassium channels are gated by different chemical or physical stimuli, including mechanical forces, and this enables them to act as molecular sensors. Kca channels are activated by intracellular Ca^{2+} through either calmodulin binding or a Ca^{2+}-sensing cytoplasmic tail. A plethora of factors control the K2P channels, including oxygen tension, pH, lipids, mechanical stretch, neurotransmitters, G protein-coupled receptors, and anesthetics. Kir channels are gated by ligands such as G proteins, PIP2, and ATP (56-60).

ATP sensitive potassium (K_{ATP}) channels are an interesting example of molecular sensors (61). K_{ATP} channels are formed by 2 subunits: Kir6, a member of the Kir channel subfamily, and the sulphonylurea receptor (SUR), a member of the ATP binding cassette (ABC) proteins. There are two Kir subunits (Kir6.1 and Kir 6.2) and three SUR subunits (SUR1, SUR2A, and SUR2B), and the channel is formed by any combination of Kir and SUR subunits (62-64). Multiple regulatory sites exist in these two subunits. ATP inhibits, and PIP2 activates the channel, by direct interaction with the Kir subunits. Sulphonylureas inhibit, and K^+ channel-openers activate the channel by interaction with the SUR subunits. MgATP/ADP activate the channel through interaction with two nucleotide-binding folds in the SUR subunits. Inhibition by ATP binding to Kir and activation by MgADP is the primary regulatory mechanism of K_{ATP}. Actin filaments are another important regulator of the channel, but whether they directly couple to the K_{ATP}

channel or act through secondary messengers such as phospholipids, is unknown (61, 65, 66). An interesting example of K_{ATP} function is in the pancreatic β-cell. When glucose rises, metabolism is stimulated, raising the ratio of ATP to ADP, and this closes the K_{ATP} channels, which depolarizes the cell and opens Ca^{2+} channels, triggering insulin secretion. Mutation of K_{ATP} in pancreatic β-cell causes decreased insulin secretion and diabetes (61).

Multiple potassium channels are expressed in bladder smooth muscle and may play functional roles in regulating bladder smooth muscle tension and contraction. Pharmacologic studies indicate that BK and SK channels have prominent roles as negative feedback elements to limit bladder smooth muscle contraction amplitude and duration (67-69). BL-1249, a K^+ channel opener, produces a concentration-dependent membrane hyperpolarization of bladder myocytes and a concentration-dependent relaxation of KCl-induced contraction in rat bladder strips, possibly through $K_{2P}2.1$ (TREK-1) (70). Opening of SK/IK by NS309, a SK/IK opener, increases bladder capacity, micturition volume and inter-contraction intervals in a concentration-dependent way (71). K_{ATP}, which is inhibited by binding to ATP and links energy state (ATP concentration) to cellular function, is present in guinea pig bladder smooth muscle cells (72, 73), and activation of <1% of K_{ATP} channels is sufficient to inhibit significant action potentials and related phasic contractions of guinea pig bladder smooth muscle (74). The expression of K^+ channels in the uroepithelium and their functional role in modulating umbrella cell mechanotransduction and exocytosis/endocytosis is unknown.

1.2.2.2 Adhesive molecules

Adhesive molecules are also important participants in mechanotransduction. They mediate cell-cell interactions, cell-matrix interactions, cell shape control, cell migration and motility (75-80). Diverse groups of adhesive molecules have been identified, such as immunoglobulin superfamily cell adhesive molecules (IgCAM), selectins, cadherins, and integrins. There are extensive studies showing adhesive molecule function in mechanotransduction. For example, platelet endothelial cell adhesion molecule (PECAM-1) (a immunoglobulin family receptor), vascular endothelial cell cadherin and VEGFR2 comprise a mechanosensory complex to confer the shear stress force to endothelial cells and initiate the intracellular pathway for atherogenesis (81).

The best understood model of adhesive molecule-mediated mechanotransduction is integrin signal pathway. Integrins are a class of transmembrane glycoproteins that link extracellular matrix to the cytoskeleton. Integrins are composed by α and β subunits and form heterodimers, and the $\beta1$ integrins (a heterodimer formed by the $\beta1$ subunit and $\alpha1$-10 subunits) are predominantly responsible for binding to the extracellular matrix. For example, the $\alpha1\beta1$ integrin binds to collagen and laminin, and the $\alpha3\beta1$ integrin binds to fibronectin (82). Integrins can transduce the extracellular force to actin filaments through adaptor protein such as talin, paxillin, and α-actinin (77, 79, 80, 82, 83). The β subunit of intergins can also bind to different intercellular signal molecules including kinases that can activate a series of pathways, such as focal adhesion kinase (FAK), Fyn, and Shc. For example, FAK becomes activated through autophosphoylation after binding to integrins, and this allows the recruitment and activation of signaling molecules such as Src, p130Cas, and phosphoinositide-3 kinase (PI3K) to form a signaling complex. Multiple

signal pathways then may be activated to regulate cellular functions, such as the Rac pathway to modulate cellular migration, Ras and MAPK/ERK pathway to regulate cellular proliferation and differentiation, and the PI3K pathway to modulate protein synthesis and membrane traffic (77, 79, 80, 82, 83).

Little is known about adhesion molecules expression and function in uroepithelium, especially their possible function in umbrella cell mechanotransduction.

1.2.2.3 Cytoskeleton

Cells respond to external forces by reorganizing their cytoskeleton. Actin filaments, microtubules, and intermediate filaments all may play some function in this process. As described above, actin filaments can regulate ion channels and signal molecules, and physical stress has been shown to induce changes in actin polymerization. Mechanical forces may directly activate signaling pathways by unfolding or distortion of force sensitive proteins. For example, when the membrane and soluble proteins of L929 cells were removed by Triton X-100 extraction, the remaining cytoskeleton activated a Rap1 signal pathway by direct stretch (84). In a more recent report, the cytoskeletal protein spectrin was increasingly labeled by cysteines as a function of shear stress and time, indicative of forced unfolding of specific domains (84). Single molecule measurements also showed that domain unfolding occurred in response to the reversible extension of purified cytoskeleton proteins (85-87).

In umbrella cells, intermediate filaments are physically connected with vesicles and the apical membrane (5), and cytokeratin 20 (CK20), 1 component of the intermediate filaments, is expressed specifically in the umbrella cell subapical region (88,

89). Actin filaments, another important component of the cytoskeletons, are involved in hypoosmolarity induced-exocytosis in umbrella cells (6). In umbrella cells, there is a distinctive distribution of actin filaments, with a dense network clustered under the basolateral membrane and only sparse filaments seen in the subapical region (90). These data suggest that the cytoskeleton may also play an important function in umbrella cell mechanotransduction.

1.2.2.4 Myosins

Myosins are ubiquitously expressed motor proteins that generate force. There are ~40 myosin genes in humans (91). Myosins are active participants in integrin- or actin-mediated mechanotransduction pathways (77). In hair cells of the inner ear myosin 1c is important for stereocilia adaptation, myosin 7a forms the ankle-link complex in stereocilia, and myosin 6 and myosin 15 may participate in stereocillia bundle formation and maintenance. Mutation of these genes results in shortened or disordered stereocillia bundles that may cause deafness (34). Studies have shown that myosins are strain sensitive, and a load against the myosin motor increases its bound time to actin filament (92-94). Myosin II directly responds to mechanical forces and may play critical role in cellular mitosis. When challenged by an externally applied mechanical load, a high mitosis failure rate and grossly asymmetric cell division is observed (95, 96). Myosin II also plays important role in integrin-mediated cell migration and contraction (78, 97). Furthermore, myosin II is implicated in mechanosensing of substrate stiffness and may contribute to stem cell differentiate in response to different mechanical environments (75, 76).

In urinary bladder, myosins, including members of myosin II are expressed in smooth muscle (98, 99). But their expression and possible function in mechanotransduction and membrane traffic in umbrella cells is not known.

1.2.2.5 Tyrosine kinases

Membrane bound enzymes such as phospholipase A2, phospholipase C and tyrosine kinases are also implicated in mechanotransduction (80).

Epidermal growth factor (EGF) receptor is a receptor tyrosine kinase, which may be activated by ligands through paracrine or autocrine pathways in response to mechanical stimuli. In human bronchial epithelial cells, compressive stress shrinks the lateral intercellular space surrounding epithelial cells, and triggers cellular signaling via autocrine binding of EGF to its receptor (100). Mechanical stimuli are also reported to activate the EGF signal pathways in human epidermal keratinocytes and rabbit proximal tubule cells (101, 102). In bladder smooth muscle cells, cyclic mechanical stretch activates p38 SAPK2, and ErbB2, and increased transcription of the gene for heparin-binding EGF (103). In bladder umbrella cells, EGF receptor was identified on the apical surface of umbrella cells, and EGFR downstream MAPK pathway activation is required for umbrella cell mechanotransduction and apical membrane exocytosis (104).

1.2.2.6 Purinergic receptor

Extracellular purines such as ATP can function as signaling molecules to modulate cellular function by binding their receptors. There are two families of purinergic receptors or P2 receptors based on their differences in molecular structure and signal

transduction mechanisms: the P2X ligand-gated ion channels and the G protein-coupled P2Y receptors. There are currently eight P2X receptors (P2X1-7 and P2XM) and eight P2Y receptors (P2Y1, P2Y2, P2Y4, P2Y6, P2Y11, P2Y12, P2Y13 and P2Y14) identified (105-107). P2X receptors are non-selective cation channel and binding of ATP increases their permeability to Ca^{2+} and Na^{+}. P2Y receptors are mainly coupled to G_q protein and can cause PLC-IP_3 induced intracellular Ca^{2+} release. Purinergic receptors are ubiquitously expressed and play diverse effects on many cellular functions including smooth muscle contraction, neurotransmission, exocrine and endocrine secretion, inflammation, platelet aggregation, pain, and modulation of cardiac function (105, 107).

In the urinary bladder, P2 receptors are also extensively expressed. A range of P2X (P2X1, P2X2, P2X3, P2X4, P2X5, P2X6, and P2X7) and P2Y (P2Y1, P2Y2, and P2Y4) receptor subtypes are expressed throughout the bladder urothelium (4). P2X and P2Y receptors participate in umbrella cell membrane traffic induced by mechanical stimuli, possibly through a Ca^{2+} and protein kinase A (PKA) dependent secondary messenger cascades (108). Furthermore, P2X and P2Y receptors are expressed by cholinergic parasympathetic neurons innervating the urinary bladder in the cat (109), suggesting that the parasympathetic pathways in cat bladder may be modulated by complex purinergic synaptic mechanisms. For tubular and hollow organs, model involving purinergic mechanosensory transduction has been put forward. In this model distension is sensed by the epithelium and tranduced through epithelial ATP release and ATP binding to the underlying P2X2/3 expressing afferent neurons (110). P2X3 is expressed exclusively by a subset of sensory neurons (111), and coexpression of P2X2 and P2X3 receptor subunits account for the ATP-gated currents in sensory neurons (112),

suggesting they function as molecular sensors. In the urinary bladder, ATP is released from the uroepithelia by mechanical stimuli (17, 113). Furthermore, P2X3-deficient mice show a bladder hyporeflexia (114). These data suggest that the purinergic mechanosensory transduction pathway also exist in urinary bladder (115). But whether hydrostatic pressure or stretch induces the ATP release, and how ATP release is correlated with mechanical stimuli, is not clear.

1.2.2.7 Adenosine receptor

Another family of purinoceptors is the P1 or adenosine receptors, a family of 4 G-protein coupled receptors. They play important functions in modulating blood vessel tone and smooth muscle relaxation (105, 116). In epithelial cells, adenosine receptors also play a role in regulating ion transport and epithelial secretion, especially in the gastrointestinal, airway and kidney epithelia (106). In chapter 3, I show that they are also expressed and play a functional role in the uroepithelium (see chapter 3).

1.2.3 Epithelial sensory transduction

Classically, epithelia are divided into excitable and non-excitable according to their electrophysiological properties, and excitable epithelia are considered to play a sensory function by releasing neurontransmitters to adjacent afferent neuron in response to external stimuli, such as hair cells to sound, gustatory cells to tastes, olfactory cells to smell. While non-excitable epithelia, such as keratinocytes that line on the surface of the skin, and epithelia that line the inner wall of respiratory tracts, gastrointestine,

reproductive tracts, urinary tracts, and blood vessels, are not considered to have sensory function and in most cases mainly play a protective role. Recent studies suggest that they might also have sensory function. Afferent neurons are well known to innervate the skin, gastrointestine, blood vessels, and urinary tract epithelia (21, 110, 117-119). Sensory molecules are also identified in those epithelia. TRPV3, a temperature sensitive ion channel is expressed in keratinocytes (120). TRPV4, an osmotic sensitive ion channel is expressed in kidney and urinary bladder epithelium (47, 121, 122). Furthermore, neurontransmitters such as ATP are released by these epithelia (keratinocytes, endothelium, uroepithelium) and allow communication with the nervous system (17, 110, 115, 117). Considering the universal existence of temperature and mechanical sensation, the position of epithelia at the interface with the external environment, suggests that they may also have sensory functions for temperature and mechanical stimuli.

Umbrella cells line the inner surface of the urinary bladder and form the interface of the urine and underlying tissue, including sensory afferent neuron. Umbrella cells sense the mechanical signal in response to urine volume change. They may also sense the biochemical signals contained in the urine by surface receptors. These signals may not only modulate umbrella cell function, but also modulate the state of nerves and detrusor activity by umbrella cell released signaling molecules, such as acetylcholine, adenosine, ATP, NO, and prostaglandins (2). Although a sensory function of umbrella cell is becoming clear, functional evidence is still absent. For example, how mechanical stimuli impact umbrella cell responses, like neurontransmitter release is not reported. This is a crucial point to answer whether umbrella cells have mechanical sensory function.

1.3 GOALS OF THIS DISSERTATION

Umbrella cells exist in a changing mechanical environment and mechanotransduction plays the key role in modulating umbrella cells apical membrane excytosis and endocytosis. How umbrella cells respond to external mechanical stimuli is still not well understood. My first goal was to determine whether stretch or hydrostatic pressure modulated umbrella cell electrophysiological properties and membrane traffic, and to determine how umbrella cells responded to different force parameters, including force direction, magnitude, and speed. The inter-relationship between force parameters and umbrella cell functional changes will be defined, which may provide important clues for the mechanotransduction pathways and help us to understand the possible underlying mechanisms. My second goal was to understand the mechanotransduction mechanism involved, and to identify the possible mechanosensors, transducers, and secondary messengers that may participate in mechanically induced umbrella cell responses. Multiple molecules and messengers were examined, including ion channels, the cytoskeleton, Ca^{2+}, adenosine receptors, adenosine release. Their functional relationship with external mechanical force parameters provides important information for our understanding of the mechanotransduction mechanisms in umbrella cells.

2.0 DISTINCT APICAL AND BASOLATERAL MEMBRANE REQUIREMENT FOR STRETCH-INDUCED MEMBRANE TRAFFIC AT THE APICAL SURFACE OF BLADDER UMBRELLA CELLS

2.1 INTRODUCTION

Mechanotransduction, the ability of cells to sense and respond to mechanical stimuli, depends on the polarized distribution and action of stretch-activated channels, the cytoskeleton, cell adhesion proteins, signaling molecules, and other cell-associated components that include the extracellular matrix (80). These diverse elements must act in a harmonized manner to modulate mechanically-responsive processes such as gene expression, cell signaling, ion transport, and membrane trafficking events like exocytosis and endocytosis (80, 123). Mechanotransduction is by necessity more intricate in epithelial cells, which form cell-cell and cell-matrix interactions, and have a complex cytoarchitecture that includes distinct apical and basolateral plasma membrane domains. How mechanical stimuli that initiate at one plasma membrane domain of an epithelial cell

are propagated and coordinated with events that occur at the other cell surface to regulate processes such as ion and membrane transport is an open question.

The uroepithelium, which lines the inner surface of the bladder, ureters, and renal pelvis, is a useful model to study epithelial mechanotransduction. The outermost layer of this tissue is lined by a single layer of polarized umbrella cells, which are known to respond to mechanical stimuli by augmented ion transport and membrane traffic (6, 7, 19); however, the relationship of these two processes and the mechanical force (stretch and/or pressure) that acts upon the umbrella cell to stimulate these events is not well understood. When isolated uroepithelial tissue is experimentally bowed outwards towards its serosal surface (mimicking bladder filling) the umbrella cells increase their apical surface area in a two-stage manner. The initial "early" stage may occur in response to a changing mechanical environment and is characterized by relatively rapid increases in surface area. In the subsequent "late" stage, which occurs after the tissue has reached a mechanical equilibrium, the surface area increases slowly over several hours (104). The late stage is temperature sensitive, and dependent on extracellular Ca^{2+}, purinergic signaling pathways, the cytoskeleton, activation of the EGF receptor, and protein synthesis and secretion (7, 18, 104, 108). In contrast, the early stage is largely unexplored but appears to be insensitive to temperature and does not require EGF signaling or protein synthesis (104). In addition to stimulating apical exocytosis, mechanical stimuli also trigger increased endocytosis, which modulates the increase in apical surface area (7); however, the relationship of endocytic and exocytic events, and the mechanisms by which they are coordinated is not known. Previous studies showed that the electrophysiological responses of the uroepithelium are dependent on the direction the

tissue is bowed (17); however, the physiological significance of these differences and the role of the distinct surface domains of umbrella cells in mechanotransduction is yet to be defined.

By studying the responses of umbrella cells to different force parameters (direction, magnitude, and speed) we established that the early stage depends on distinct events at both plasma membrane domains of the umbrella cell. In response to apical membrane tension, but not pressure, we observed increased ion transport and exocytosis at the apical surface of the umbrella cell layer. Exocytosis was dependent on the cytoskeleton and the activity of the apically distributed epithelial sodium channel (ENaC) and a non-selective cation channel (NSCC). The increases in exocytosis and ion transport were reversed when tension was increased in the basolateral membrane of the cells, which stimulated apical membrane endocytosis. These events could be further modulated by opening K^+ channels at the basolateral surface of the cell. Our results indicate that in response to a dynamic mechanical environment, such as that observed during bladder filling and voiding, the apical membrane dynamics of umbrella cells are governed by sequential and coordinated mechanotransduction events at its distinct apical and basolateral membrane domains.

2.2 RESULTS

2.2.1 Stretch, but not hydrostatic pressure, stimulates ion transport and membrane turnover in umbrella cells

To determine which mechanical force(s), pressure or stretch, stimulated ion transport and membrane traffic in the umbrella cells we used isolated uroepithelium mounted in Ussing stretch chambers. In control experiments the tissue was equilibrated for 30 min (Figure 2.1A), and then left unperturbed for up to 3h, during which time the umbrella cells maintained a relatively stable transepithelial voltage (TEV) of -15 – -20 mV, a transepithelial resistance (TER) of ~ 20 kΩ•cm^2, a low short-circuit current (I_{sc}) of ~ 2 μA/cm^2, and a stable apical membrane capacitance (C_a; absolute value was ~ 2.0 μF) (Figure 2A). We previously mimicked bladder filling by manually increasing the amount of fluid in the mucosal hemichamber, which caused the tissue to visibly bow outward toward the serosal hemichamber (18, 19). However, in the present studies we found that the manual method made it difficult to reproducibly achieve a range of hydrostatic pressures. To overcome these problems, we attached tubing to Luer ports at the tops of the hemichambers, and positioned the tubing at varying preset heights to accurately produce graded changes in hydrostatic pressure (Figure 2.1B).

When hydrostatic pressure in the mucosal chamber was raised to 4 cm H_2O, the tissue visibly bowed outwards (data not shown) and electrophysiological changes were observed including a rapid decrease in TEV and TER and a transient increase in I_{sc} (Figure 2.2A). Further increasing the hydrostatic pressure in the mucosal hemichamber to 8, 16, 32, or 64 cm in a step-wise fashion did not induce further changes in these parameters (Figure 2.2A), indicating that once the tissue was bowed outwards further changes in hydrostatic pressure had no effect on these parameters. The C_a increased as the pressure head was raised to 4 cm H_2O and slowly rose during the next 150 min. Next, we simultaneously raised the pressure head in both the mucosal and serosal hemichambers (Figure 2.1C), which prevented tissue bowing, but allowed for pressure to be increased to 4, 8, 16, 32, or 64 cm H_2O against both surfaces of the tissue. Intriguingly, no change in any of the electrical parameters was noted (Figure 2.2A). These results provide evidence that it was increased stretch (and the resulting bowing of the epithelium) and not changes in hydrostatic pressure that induced electrophysiological changes in the umbrella cell layer.

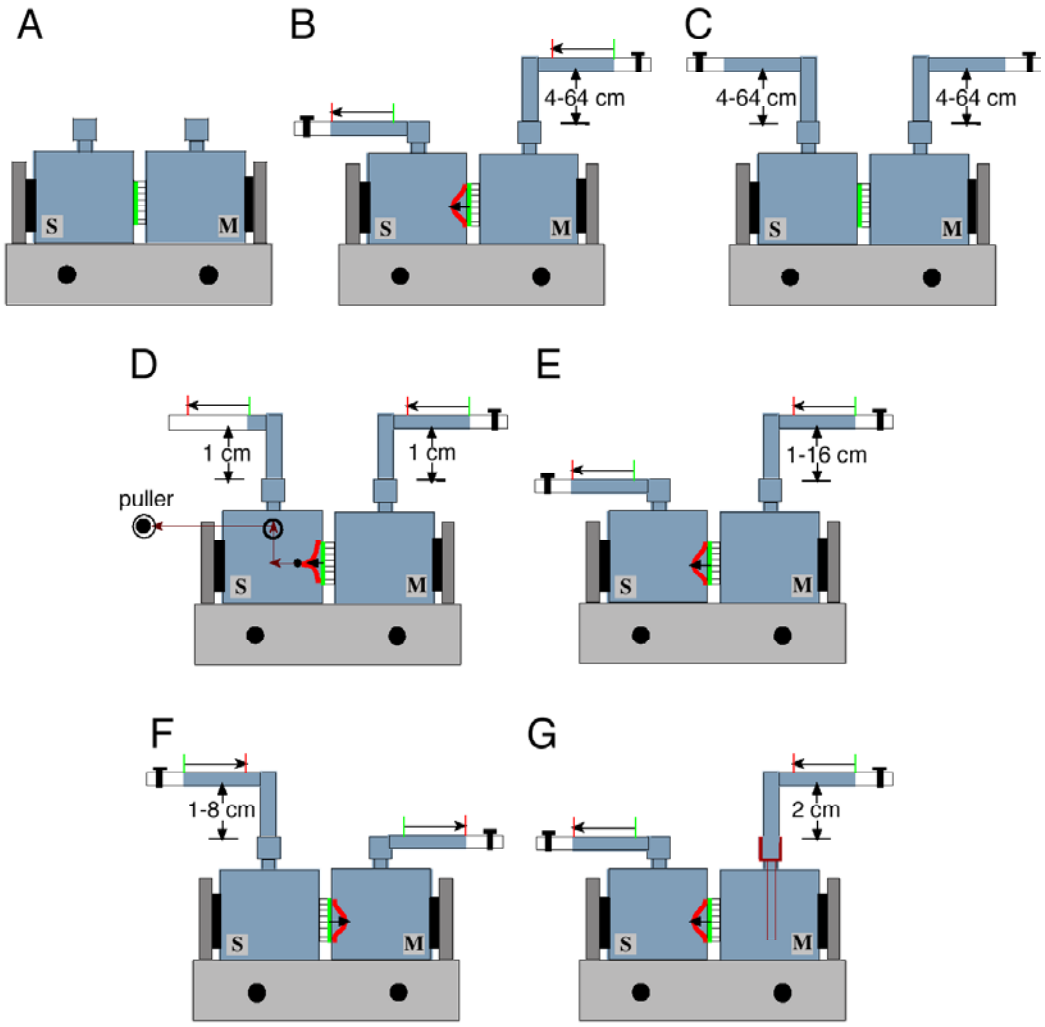

Figure 2.1. System for stretching the uroepithelium

Uroepithelial tissue was mounted between two closed Ussing stretch chambers, which were filled with Krebs buffer and equilibrated for 30-45 min. (A) Control tissue was not exposed to mechanical stimuli. (B) Tissue was bowed outward in response to stepwise increases in the hydrostatic pressure head. (C) Hydrostatic pressure was simultaneously raised stepwise in both mucosal and serosal hemichambers. (D) Both the mucosal and serosal hermichambers were maintained at 1 cm H_2O pressure and the tissue was pulled

by a filament toward the serosal hemichamber. (E) Tissue was bowed outward in response to raising hydrostatic pressure in the mucosal hemichamber. (F) Tissue was bowed inward in response to raising hydrostatic pressure in the serosal hemichamber. (G) Tissue was bowed outward as the mucosal hemichamber filled at different rates. Legend: M, mucosal hemichamber; S, serosal hemichamber. The green line between the chambers shows the initial position of uroepithelium while the red curve shows the position of the tissue upon bowing.

To further confirm that stretch is the relevant mechanical force in umbrella cells the following experiment was performed. A suture thread was attached to a small pad of muscle that was left on the serosal surface of the tissue during the dissection of the uroepithelium. The epithelium was mounted between the Ussing stretch chambers and the thread was passed through a Luer port on the serosal hemichamber and pulled at different speeds (0.1, 0.5, 1.0, or 2.0 cm/min). Tubing was attached to both the mucosal and serosal hemichambers, which maintained the same hydrostatic pressure (1 cm H_2O) as the epithelium was pulled toward the serosal hemichamber (Figure 2.1D). Slow speeds of pulling induced relatively gradual changes in the electrophysiological properties, while rapid pulling induced quick changes (Figure 2.2B). Regardless of speed, we observed that stretch was accompanied by TEV hyperpolarization, a decrease in TER, and an increase in I_{sc} and C_a, consistent with our previous published observations that experimental filling stimulates ion transport and capacitance changes in the uroepithelium (18, 19). The release of stretch was accompanied by a rapid return of the parameters to near baseline values, indicating that the tissue was not disrupted by the treatment. In summary, our data

indicate that stretch, but not hydrostatic pressure, is the mechanical force responsible for stimulating events in the umbrella cell layer.

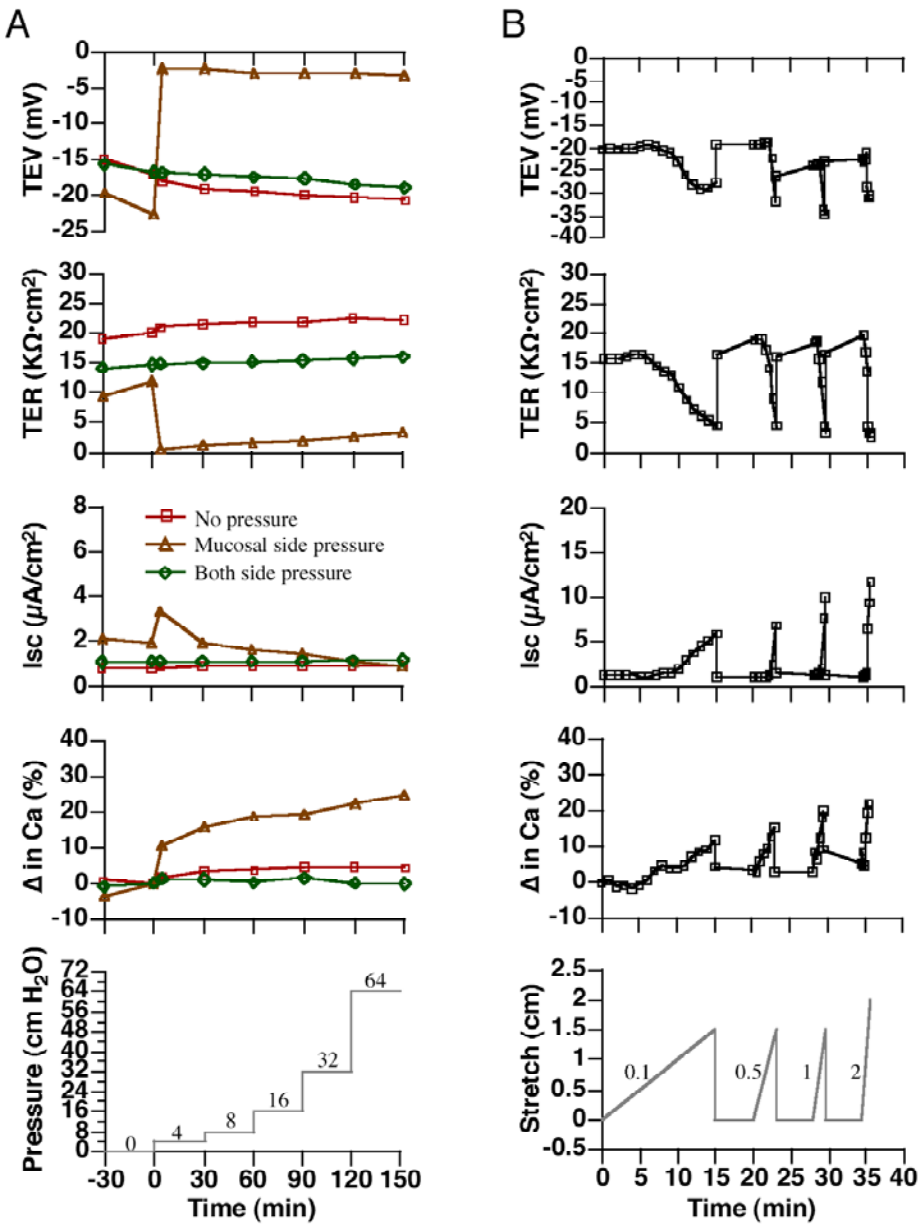

Figure 2.2. Modulation of electrophysiological parameters in response to mechanical stimuli

(A) Responses in tissue exposed to step-wise increases in pressure. (B) Responses to pulling the tissue toward the serosal chamber under constant pressure. The experiments were repeated ≥ 3 times and representative results are shown.

2.2.2 Umbrella cell electrophysiological properties are sensitive to the direction, magnitude, and rate of the applied force

In the next experiments we examined the effects of three force parameters (direction, magnitude, and rate) on tissue that was bowed outwards toward the serosal hemichamber or bowed inwards toward the mucosal hemichamber. We theorized that as the mucosal hemichamber is filled, tension in the apical plasma membrane of the umbrella cells would increase first (see supplementary Figure S2.1A). This increase in tension would be dissipated to some extent by the ability of the umbrella cell to modulate (i.e. increase) its apical surface area, as well as by outward bowing of the tissue. As the stretch increases further one would expect the basolateral surface to also experience increased tension (Figure S2.1A). However unlike the apical membrane, the ability of the basolateral membrane to accommodate tension would be constrained by its apparent lack of surface area change in response to stretch (6, 7, 124). In a reciprocal manner, bowing the tissue inwards by increasing the pressure head in the serosal hemichamber, would increase tension in the basolateral membrane first, but would eventually increase apical membrane tension if the tissue was further stretched toward the mucosal hemichamber (Figure S2.1C).

Using the setup shown in Figure 2.1E we monitored the electrical parameters of tissue that bowed outward in response to increasing the pressure head in the mucosal hemichamber to 2 cm H_2O. We observed responses that were temporally separated into three phases. In the first phase the TEV hyperpolarized, the TER decreased, the I_{sc} increased, and the C_a increased to ~ 100 % over starting values (Figure 2.3A). Because the apical membrane resistance of the umbrella cell is the primary contributor to the TER (13), and because C_a increased, the changes we observed in phase 1 likely reflected increased ion transport and membrane traffic at the apical plasma membrane domain of the umbrella cells (see also discussion below). During the second phase of outward bowing the parameters rapidly reversed course (Figure 2.3A). The decrease in C_a is consistent with our previous finding that in addition to stimulating exocytosis, stretch also increases endocytosis (the net effect is membrane addition) (7). The decrease in I_{sc} may reflect the internalization of ion channels, changes in their open probability, or changes in the electrochemical gradients across the epithelium. By 5 min and beyond (phase 3) the tissue had reached a mechanical equilibrium and the late stage response was observed, which was characterized by a slow increase in C_a and TER and a decrease in I_{sc} and TEV over the next 60-180 min (Figure 2.3A and data not shown).

The reversal in parameters that we observed during the second phase of outward bowing may reflect events that occur in response to increased tension in the basolateral membranes of the umbrella cells. This possibility became apparent when we used the setup in Figure 2.1F to raise the pressure head in the serosal hemichamber to 1 cm H_2O. As described above this would likely increase tension across the basolateral membrane of the umbrella cells, causing the tissue to bow inwards. Consistent with a two-membrane

model, the first phase of inward bowing (like the second phase of outward bowing) resulted in a decrease in TEV, Isc, and C_a (compare these parameters in Figure 2.3A and B). The TER responses in tissue bowed inwards or outwards were of opposite magnitudes, likely reflecting the fact that outward bowing stimulated increased ion transport across the epithelium. Following phase 1 of inward bowing, the tissue reached an equilibrium (phase 2) in which the electrical parameters remained relatively constant (Figure 2.3B). In summary, apical membrane tension resulted in increased ion transport and apical membrane exocytosis, while increased basolateral membrane tension lead to decreased I_{sc} and increased apical membrane endocytosis.

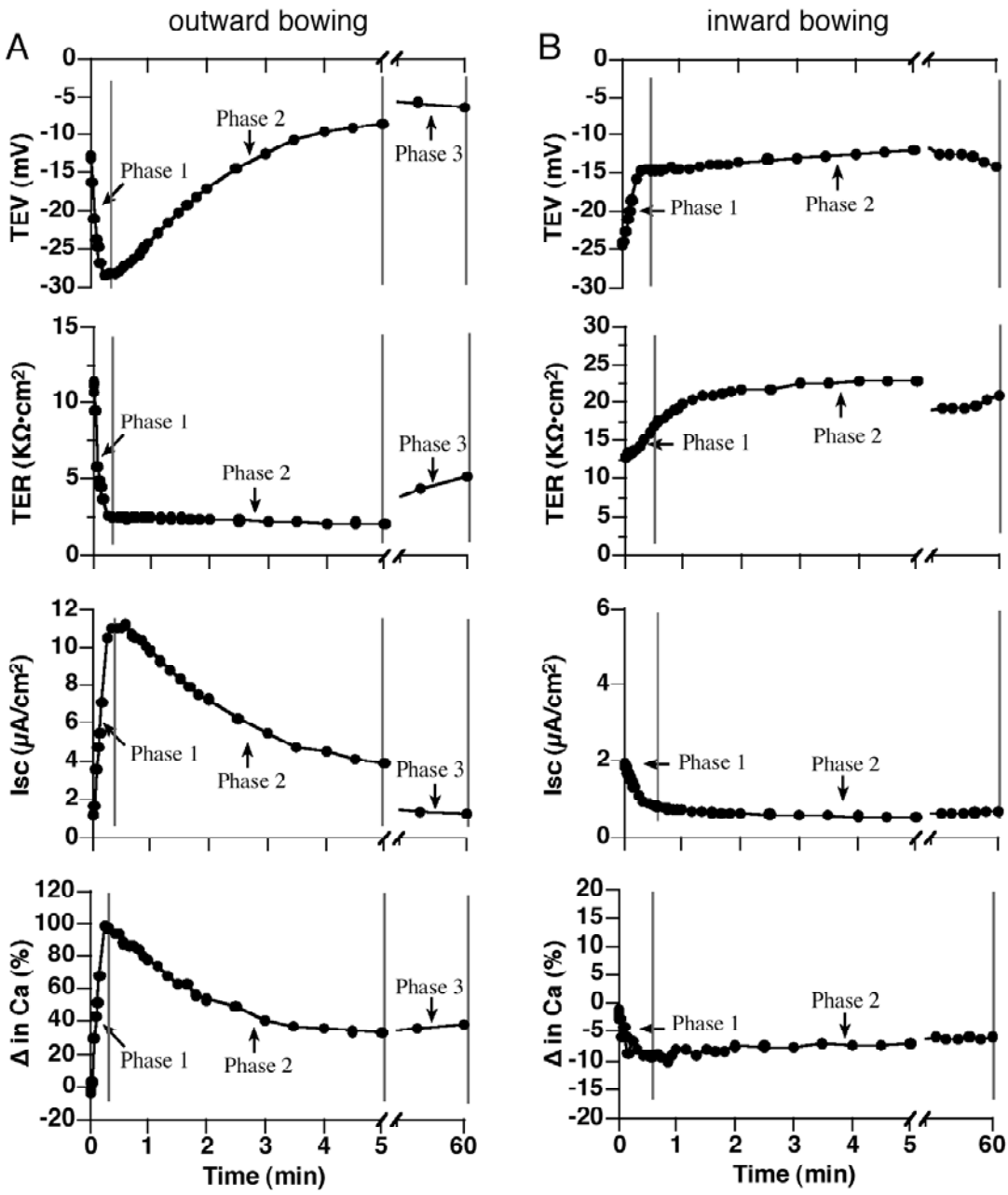

Figure 2.3. Modulation of umbrella cell electrophysiological parameters by changes in the direction of the mechanical force

(A) Responses in tissue bowed outward in response to a 2 cm H_2O pressure head in the mucosal hemichamber. (B) Responses in tissue bowed inward in response to a 1 cm H_2O pressure head in the serosal hemichamber. The experiments were repeated ≥ 3 times and representative results are shown.

If our dual-membrane model was correct then we expected that the responses to apical membrane tension would be limited, regardless of pressure head, by increased tension in the basolateral membrane (Figure S2.1B). As we showed above, increased tension in this membrane stimulated apical membrane endocytosis and decreased I_{sc}. In fact, the peak values for each of the parameters were similar irrespective of the magnitude of the mucosal pressure head (1-16 cm H_2O; Figure 2.4A and Table 2.1). The increased pressure not only changes the magnitude of the force but according to Poiseuille's Law (which relates changes in pressure to rates of fluid flow), higher pressures induce more rapid rates of chamber filling (and vice-versa). In turn, faster rates of chamber filling would act to more quickly increase membrane tension and tissue bowing. In fact we observed that the phase 1 response to 8 cm H_2O was complete in ~ 0.02 min (see inset in Figure 2.4A), but took a full minute to peak in tissue exposed to a pressure head of 1 cm H_2O (Figure 2.4A).

To examine further the relationship between filling rates, the degree of tissue stretch, and the tissue responses, the following experiments were performed. We maintained a constant pressure head in the mucosal hemichamber (2 cm H_2O), and then varied the rate of buffer flow into the mucosal hemichamber by inserting different gauge needles between the end of the tubing and the Luer port at the top of the mucosal

hemichamber (Figure 2.1G). Consistent with the hypothesis that the rate of filling (and degree of stretch) will affect the kinetics of the filling response, we observed that use of an 18 g needle, which allows a relatively rapid flow rate of ~ 3400 µl/min, resulted in rapid changes in the electrophysiological parameters during phase 1 and 2 (Figure 2.4B and Table 2.1). In contrast, when we filled the chamber with a 25 g needle (flow rate of ~ 65 µl/min), we observed gradual changes in electrophysiological responses and a dramatic increase in the length of the phase 1 response (see inset in Figure 2.4B). Under these conditions the phase 2 response was only observed after ~ 15 min (see inset in Figure 2.4B). By multiplying the maximum response time (end of phase 1) by the corresponding filling rate, a relative constant value of ~1 ml was obtained, indicating a constant fill volume was needed to fully stretch the umbrella cells. Regardless of filling speed, the magnitude of the responses was similar. These data provide further evidence in support of our two-membrane model and demonstrate that the timing of the responses was dependent on a dynamic mechanical environment and the speed of tension development across the apical and then basolateral membrane domains of the umbrella cell.

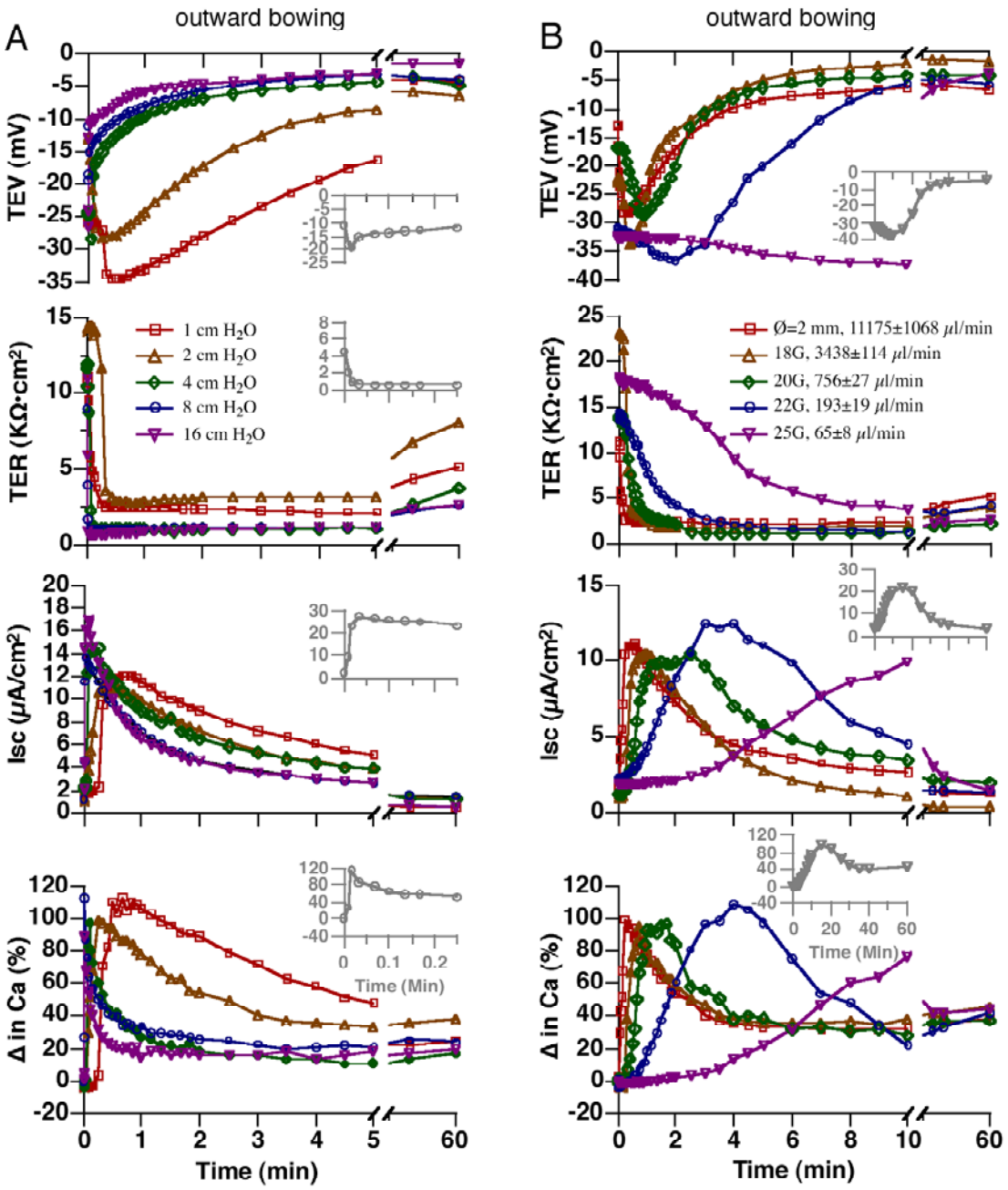
A
outward bowing
TEV (mV)
TER (KΩ·cm²)
1 cm H2O
2 cm H2O
4 cm H2O
8 cm H2O
16 cm H2O
Isc (μA/cm²)
Δ in Ca (%)
Time (Min)
Time (min)
B
outward bowing
TEV (mV)
TER (KΩ·cm²)
Ø=2 mm, 11175±1068 μl/min
18G, 3438±114 μl/min
20G, 756±27 μl/min
22G, 193±19 μl/min
25G, 65±8 μl/min
Isc (μA/cm²)
Δ in Ca (%)
Time (Min)
Time (min)

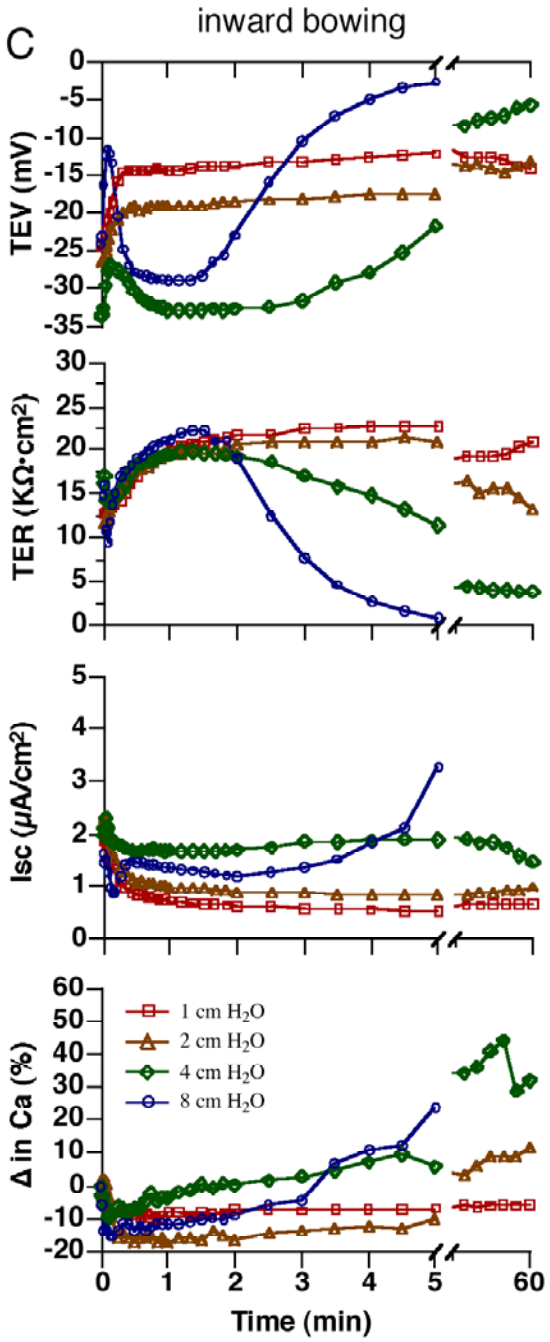

Figure 2.4. Electrophysiological responses to different pressure heads and rates of chamber filling

(A) Effect of different pressure heads on electrophysiological parameters as the tissue was bowed outwards. Insets show responses observed when the hydrostatic pressure was raised to 8 cm H_2O. (B) Responses to different rates of filling when the pressure head was maintained at 2 cm H_2O in the mucosal hemichamber. The legend shows the gauge of needle and approximate rate of filling. The insets show data for the 25-gauge needle. (C) Effect of different pressure heads on electrophysiological parameters as the tissue was bowed inwards. The experiments were repeated ≥ 3 times and representative results are shown. Data for the responses to 2 cm H_2O (outward bowing) and 1 cm H_2O (inward bowing) are reproduced from Figure 2.3.

We also monitored the electrophysiological parameters when the tissue bowed inwards at different pressure heads (Figure 2.4C). At a relatively low pressure head of 2 cm H_2O we observed similar responses to those observed for 1 cm H_2O. The TEV decreased in magnitude, the TER increased, and the I_{sc} and C_a decreased. In contrast, when the pressure head was increased to 8 cm H_2O we observed a complex response. Initially, there was a change similar to that described for 1 or 2 cm H_2O (decreased TEV, I_{sc}, and C_a). However, the subsequent response was similar to that observed when apical membrane tension was increased: an increase then decrease in the magnitude of the TEV, the TER rose but then fell, and the I_{sc} and C_a gradually increased (Figure 2.4C). As proposed in Figure S1, the response to 8 cm H_2O likely resulted from the initial increase in tension at the basolateral membrane followed by a subsequent increase in apical membrane tension, which we showed stimulated ion transport and apical exocytosis. These data are consistent with the idea that tension can develop in a sequential fashion

when the tissue is bowed in either direction. We were unable to test higher pressures, as the epithelium rapidly lost resistance and it was no longer possible to accurately measure the physiological parameters.

2.2.3 Stretch stimulates rapid membrane turnover at the apical surface of umbrella cells, which is dependent on the cytoskeleton

An intriguing finding in our analysis was that rapid changes in membrane tension were accompanied by rapid and relatively large increases in C_a. Consistent with our previous findings (104), the early stage response (i.e phase 1) was insensitive to the secretory inhibitor brefeldin-A, while the late stage response (i.e. phase 3) was significantly inhibited (compare C_{max} vs C_{60} in Table 1). To confirm that the phase 1 response reflected real changes in exocytosis at the apical surface of the umbrella cells we initially assessed whether C_a was sensitive to incubation at 4˚ C, a temperature routinely used to block exocytosis and endocytosis in quiescent cells. Surprisingly, the initial change in C_a (at the end of phase 1) was similar at 37˚ C or 4˚ C (Table 2.1), possibly indicating that the mechanical energy provided by stretching the tissue was sufficient to drive the exocytic response by overcoming the normal energy barrier observed in cells incubated at a reduced temperature. The lower temperature did alter the change in C_a observed during the phase 2 response and inhibited C_a during the phase 3 response (Table 2.1). As further confirmation of our findings, we used a biotinylation approach to show that exocytosis was stimulated during phase 1 and this increase occurred in a temperature independent fashion (supplementary Figure S2.2).

Table 2.1. Effect of various treatments on C_a

Experimental manipulation		n	C_{max} (%)	C_{min} (%)	C_{60} (%)
Force magnitude	1 cm H_2O	3	112.0 ± 8.5	25.7 ± 6.0	23.0 ± 1.7
	2 cm H_2O†	3	108.0 ± 35.2	25.0 ± 6.6	30.7 ± 7.5
	4 cm H_2O	3	128.0 ± 30.5	16.0 ± 2.7	19.7 ± 4.6
	8 cm H_2O	3	112.3 ± 14.5	17.3 ± 0.6	25.7 ± 6.7
	16 cm H_2O	3	101.7 ± 6.7	11 ± 5.2	20.3 ± 0.6
Fill speed	2 cm H_2O/2 mm†	3	108.0 ± 35.2	25.0 ± 6.6	30.7 ± 7.5
	2 cm H_2O/18 g	4	93.3 ± 14.2	32.8 ± 3.0	41.3 ± 6.6
	2 cm H_2O/20 g‡	7	114.4 ± 30.7	31.4 ± 9.7	43.9 ± 12.1
	2 cm H_2O/22 g	3	95.7 ± 13.5	25.7 ± 5.5	50.0 ± 7.0
	2 cm H_2O/25 g	3	88.3 ± 7.6	36.0 ± 5.6	50.3 ± 6.1
Temp or BFA	Control‡	7	114.4 ± 30.7	31.4 ± 9.7	43.9 ± 12.1
	4° C	3	126.7 ± 27.5	61.3 ± 23.2*	16.7 ± 10.1*
	BFA	3	107.9 ± 33.0	18.0 ± 3.24	26.2 ± 6.3
Cytoskeleton disruptors	cytochalasin D	5	38.0 ± 4.7*	25.4 ± 10.3	42.8 ± 20.2
	latrunculin A	3	60.3 ± 6.4*	33.0 ± 9.9	54.0 ± 10.1
	colchicine	3	97.7 ± 9.0	28.7 ± 1.5	44.3 ± 4.7
	thioglycolate	4	44.3 ± 5.4*	27.8 ± 10.7	46.8 ± 12.7
	okadaic acid	5	40.0 ± 3.0*	28.3 ± 5.5	46.3 ± 6.0
Channel blockers	Gd_3Cl - mucosal	3	39.8 ± 3.3*	28.4 ± 5.2	46.7 ± 6.1
	La_3Cl - mucosal	4	54.0 ± 11.9*	22.0 ± 5.7	35.3 ± 4.8
	100 μM amiloride - mucosal	3	41.3 ± 4.7*	24.0 ± 9.2	40.3 ± 6.4
	1 μM amiloride - mucosal	4	46.7 ± 14.1*	15.0 ± 12.6	39.9 ± 12.5
	benzamidine - mucosal	4	33.9 ± 16.6*	20.8 ± 7.6	42.4 ± 5.8
	Gd_3Cl - serosal	4	105.5 ± 11.9	30.8 ± 6.1	42.3 ± 6.0
	La_3Cl - serosal	3	97.7 ± 29.6	23.0 ± 9.2	29.7 ± 12.3
	100 μM amiloride - serosal	3	90.7 ± 7.4	25.0 ± 6.6	39.0 ± 7.0
Ca^{2+}	No apical Ca^{2+}	3	28.8 ± 14.1*	18.4.0 ± 2.6	32.4 ± 4.0
	2-APB	3	41.7 ± 4.6*	23.3 ± 10.3	23.7 ± 9.2
	ryanodine	3	86.7 ± 11.1	28.3 ± 6.7	41.3 ± 6.4
K^+ channels	NS1619	3	80.7 ± 11.0	31.0 ± 4.6	50.0 ± 5.3
	NS309	3	93.0 ± 6.1	45.3 ± 4.7*	78.7 ± 4.5*
	chromakalim	6	99.8 ± 17.6	44.7 ± 4.1*	82.3 ± 13.8*
	arachadonic acid	3	95.7 ± 9.0	32.3 ± 7.5	45.3 ± 5.0
	halothane	3	114.3 ± 15.3	27.3 ± 2.1	42.0 ± 5.6
	glyburide + chromakalim	3	100.7 ± 10.1	29.3 ± 5.0	55.0 ± 7.9
	glyburide	4	85.3 ± 12.7	26.4 ± 7.2	32.6 ± 8.5

Table 2.1. Effect of various treatments on C_a. Tissue was bowed outwards at the indicated pressure head, speed, temperature, or in the presence of the indicated drug. C_{max} was measured at the end of phase 1, C_{min} was measured at the end of phase 2, and C_{60} was measured 60 min after initiation of the mechanical stimulus. Data are mean ± SEM. * $p < 0.05$ relative to control. †,‡ data are identical and reproduced for clarity.

Furthermore, we observed that pretreatment with the actin disrupting agent cytochalasin D (cytoD), which was previously reported to block exocytosis in umbrella cells (6), prevented the phase 1 increase in exocytosis (Figure S2.3 and Table 2.1). We also observed that the actin depolymerizing drug latrunculin A also inhibited stretch-induced changes in C_a (Table 2.1 and Figure S2.3), further implicating actin filaments in this process. Intermediate filaments are physically associated with the discoidal vesicles and apical membrane of umbrella cells (125, 126), but their function is poorly understood. We observed that treatment with thioglycolic acid, a reagent that reduces sulfhydryl bridges and disorganizes the cytokeratin network (89, 127), inhibited the stretch-induced responses (Table 2.1 and Figure S2.3). A similar response was observed upon treatment with okadaic acid, a protein serine/threonine phosphatase inhibitor that is reported to fragment intermediate filaments (128) (Table 1 and Figure S2.3). However, this drug has many effects that are independent of the cytoskeleton (129). In contrast, treatment with the microtubule depolymerizing agent colchicine had no significant effect on C_a (Table 2.1 and Figure S2.3). In summary, the early stage exocytic response was dependent on the cytoskeleton, but independent of temperature.

2.2.4 Roles for ENaC, an NSCC, and $[Ca^{2+}]_i$ in the phase 1 response to outward bowing

Na^+ conductance is a major contributor to I_{sc} in quiescent and stretched umbrella cells (14, 19, 35), and mathematical modeling showed that Na^+ permeable ion channels, possibly in conjunction with K^+ conducting channels, could account for the phase 1 response of outward bowing (see supplementary Figure S2.4). Consistent with a role for ENaC in these responses we observed that 1 μM amiloride or 1 μM benzamil (a highly selective inhibitor of ENaC) inhibited the phase 1 response of outward bowing (Figure 2.5A and Table 2.1). However, these inhibitors had no effect on the late stage (phase 3) changes in C_a (Table 2.1).

In addition to ENaC, we have also described an apically localized NSCC that may also play an important role in the processes we described (19). In fact, we observed that mucosal addition of 1 mM Gd^{3+} or La^{3+} (inhibitors of the NSCC) (19, 130), or 100 μM amiloride (an inhibitor of ENaC and the NSCC when used at this concentration) (19), impaired the phase 1 response of outward bowing (Figure 2.5A and Table 2.1), but had little effect on C_a changes during phase 2 or phase 3 (Table 2.1). The lack of effect of these channel blockers on the phase 2 and 3 responses indicates that they occur as a result of basolateral membrane stretch and not simply signaling that occurs downstream of opening apical channels. When Gd^{3+}, La^{3+}, or amiloride was added to the serosal hemichamber they had only small effects on the phase 1 parameters and no significant effects on C_a (Figure 2.5B and Table 2.1), further indicating that the basolateral membrane events were differentially regulated.

NSCCs often conduct extracellular Ca^{2+} into the cell, stimulating Ca^{2+}-dependent increases in $[Ca^{2+}]_i$. Consistent with this possibility we observed that depleting the apical Krebs solution of Ca^{2+} blocked the phase 1 response (Figure 2.5C and Table 2.1), but not phase 2 or 3 responses (Figure 2.5C and data not shown). Ca^{2+}-dependent Ca^{2+} release can occur downstream of IP_3 receptor or ryanodine receptor activation. We observed that the IP_3 receptor inhibitor 2-APB inhibited the phase 1 response while the ryanodine receptor inhibitor ryanodine had little effect (Figure 2.5C and Table 2.1). These data are consistent with the possibility that extracellular Ca^{2+} enters through the apical pole of the cell and stimulates $[Ca^{2+}]_i$ downstream of an IP_3-receptor-dependent pathway.

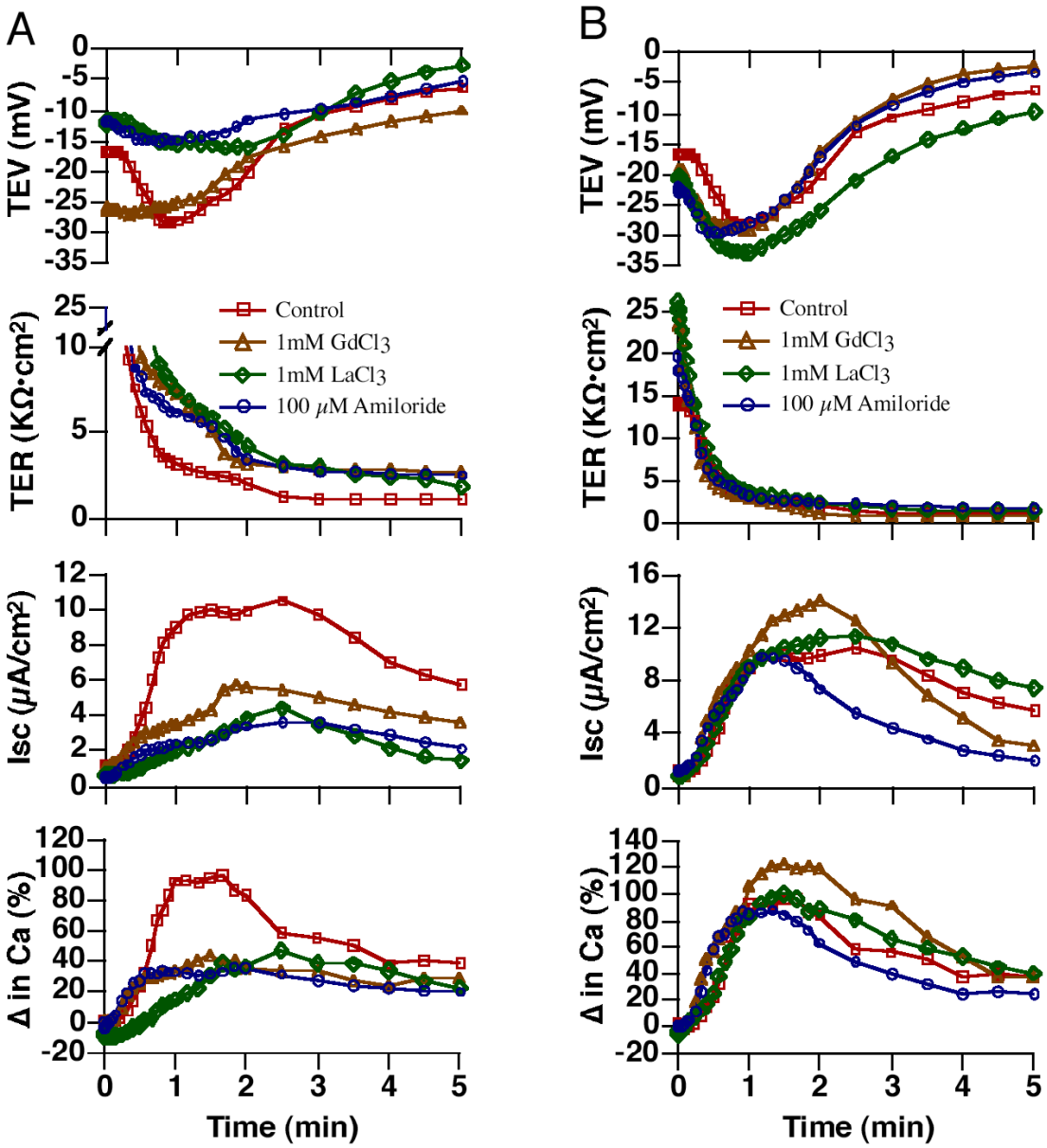
A
B
TEV (mV)
TER (KΩ·cm²)
Isc (μA/cm²)
Δ in Ca (%)
Time (min)
Control
1mM GdCl3
1mM LaCl3
100 μM Amiloride

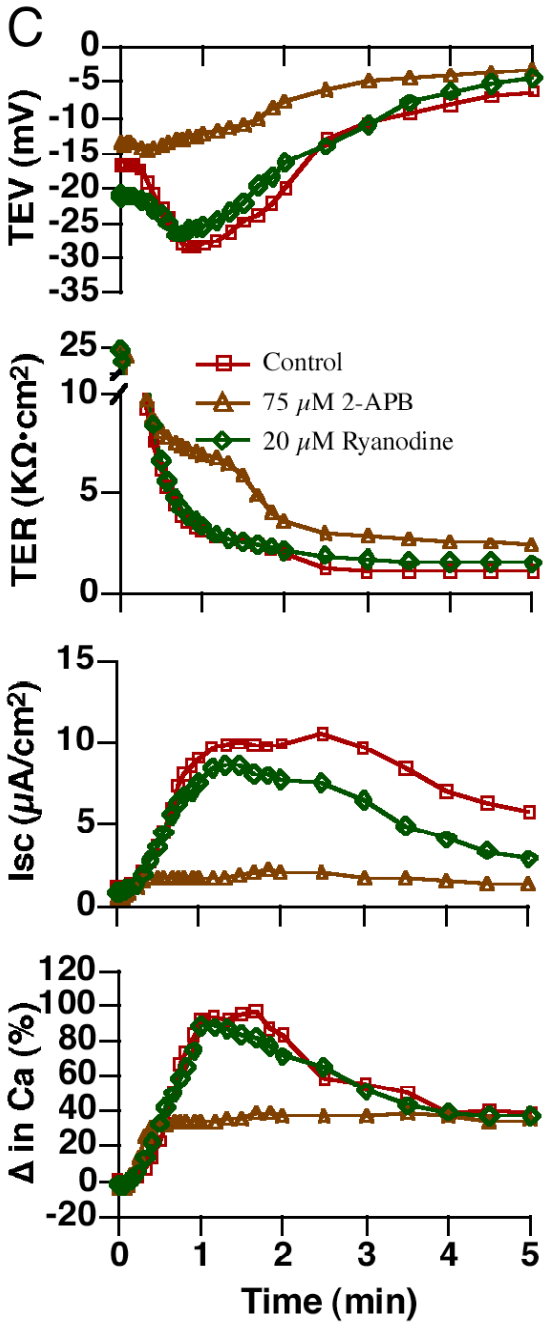

Figure 2.5. Requirement for apical membrane cation channels and intracellular Ca^{2+} release in the Phase 1 response to outward bowing

(A-B) The indicated channel blockers were added to the mucosal (A) or serosal (B) chamber and pre-incubated for 30 min at 37˚ C. The tissue was then bowed outward using a 20-gauge needle to fill the mucosal hemichamber at a 2 cm H_2O pressure head. Untreated tissue served as a control. (C) Tissue was pre-treated with 2-APB or ryanodine for 1 h and then stretched as described in A-B. The experiments were repeated ≥ 3 times and representative results are shown.

2.2.5 Basolateral K^+ channels modulate stretch induced-responses in umbrella cells

We previously reported that stretch-sensitive K^+ channels are present on the basolateral surface of umbrella cells (19). RT-PCR of uroepithelial-derived mRNA was used to identify 11 possible stretch-modulated K^+ channels that are expressed in the bladder. Ten of them were detected in uroepithelium, including the calcium-activated potassium channels KCNMA1 (BK), KCNN1-4 (SK/IK), the two-pore potassium channels KCNK2 (TREK-1), KCNK4 (TRAAK), and the inwardly rectifying potassium channels KCNJ8 (Kir6.1) and KCNJ11 (Kir6.2). Only KCNK10 (TREK-2) was not detected in the uroepithelium (Figure 2.6A); however, we confirmed that its expression was detected in the heart (data not shown). Kir6.1 and Kir6.2 are subunits of ATP sensitive potassium channels (K_{ATP} channels). K_{ATP} has important roles in bladder function and can regulate membrane traffic in other cell types (72, 73, 131). To further establish that K_{ATP} was expressed in the uroepithelium, and determine its localization in umbrella cells, western blots and immunofluorescence were performed using antibodies against Kir6.1. Western blot analysis confirmed the expression of an expected 44.7 KD protein species (Figure

2.6B). Furthermore, immunofluorescence staining showed expression of Kir6.1 in the uroepithelium, including at the basolateral membrane of the umbrella cell layer (Figure 2.6C).

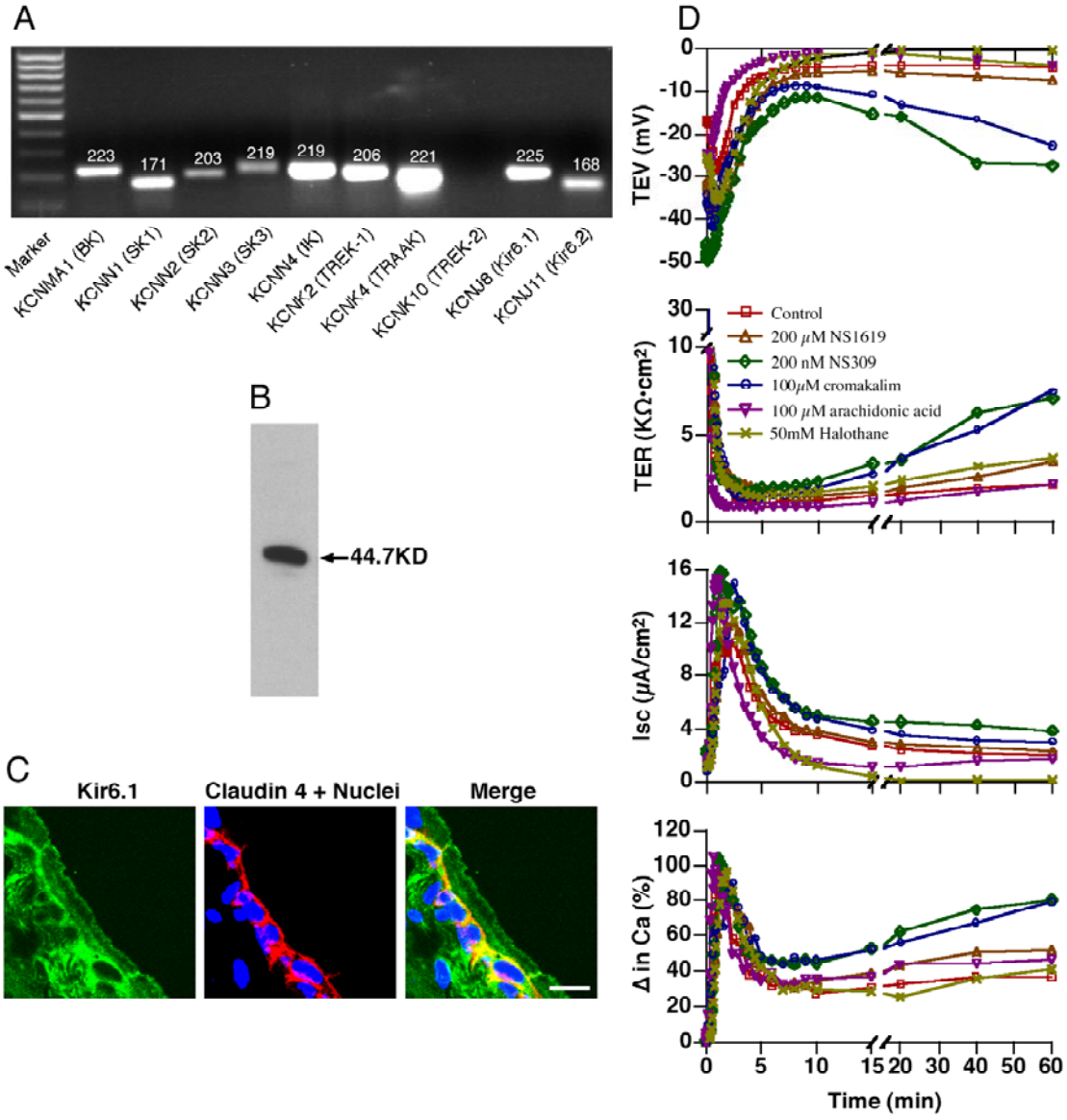

Figure 2.6. K_{ATP} is expressed in umbrella cells and modulates the stretch response

(A) Expression of the indicated K^+ channels was detected by RT-PCR of total RNA isolated from mouse bladder uroepithelium. Numbers above the DNA species are the

expected product sizes of the RT-PCR reaction (in bp). (B) A lysate of rat uroepithelium was resolved by SDS-PAGE and a western blot probed with antibody specific for the Kir6.1 subunit of K_{ATP}. The nominal mass of the major protein detected in the lysate is indicated to the right of the panel. (C) Frozen thin sections of rat bladder tissue were labeled with an antibody to the Kir6.1 subunit of K_{ATP} (green), rhodamine phalloidin to label the actin cytoskeleton (red), and Topro-3 to label the cell nuclei (blue). A merged panel is shown at the right. Bar = 10 μm. (D) The indicated K^+ channel openers were added to the serosal hemichamber and incubated with tissue for 30 min. The tissue was then bowed outward by filling the chamber with a 20-gauge needle at a 2 cm H_2O pressure head. The experiments were repeated ≥ 3 times and representative results are shown.

The mathematical model shown in Figure S2.4 predicts that opening K^+ channels at the basolateral surface of the umbrella cells may effect the phase 2 and possibly phase 3 responses upon outward bowing. We used K^+ channel openers to determine which K^+ channel(s) was functional in modulating the stretch-induced umbrella cell response. NS1619, a potent BK opener, had no effect on stretch-induced responses (Figure 2.6D and Table 2.1). Arachidonic acid or halothane, which open channels such as TREK-1 and TRAAK, also had no effect (Figure 2.6D and Table 2.1). In contrast, the SK/IK channel opener NS309 modulated the phase 2 and 3 responses, and increased the magnitude of the TEV, TER, and C_a (Figure 2.6D and Table 2.1). We also observed that cromakalim, a K_{ATP} channel opener, changed the stretch-induced responses in a manner similar to NS309 (Figure 2.6D and Table 2.1). Glyburide, a K_{ATP} inhibitor, blocked the cromakalim

effect (Table 2.1); however, glyburide itself had no effect on the stretch responses (Table 2.1). Our data indicate that SK/IK and K_{ATP} may modulate the basolateral membrane responses to umbrella cell stretch.

2.3 DISCUSSION

Several insights have emerged from our studies of umbrella cell mechanotransduction: First, stretch, not pressure, is the relevant mechanical stimulus that regulates ion and membrane transport in the umbrella cell. Second, during the previously described early stage the apical and basolateral membranes of the umbrella cell have discrete functions that act in concert to regulate membrane turnover at the apical surface of the umbrella cell. Third, we established that ion channels likely act as mechanotransducers to regulate changes in umbrella cell apical membrane traffic. Fourth, the responses we observed may be physiologically relevant to the dynamic processes of bladder filling and voiding. Overall our results provide increased understanding of how changes in the mechanical environment of umbrella cells are transduced by discrete membrane domains to coordinate ion transport and membrane traffic.

2.3.1 Role of stretch in promoting changes in umbrella cell function

Previous studies have established that umbrella cells are mechanosensitive and in response to mechanical stimuli show increased ion transport (6, 19), apical membrane turnover (exocytosis and endocytosis) (6, 7, 18), and release of various mediators and

neurotransmitters including ATP and adenosine (17, 113, 132). We observed that increased membrane tension (i.e. stretch) and not pressure was likely responsible for stimulating these changes. Stretch, but not pressure, was previously reported to open the MscL channel (133) and to increase endothelial connexin 43 expression (134). In a similar manner, stretch of the apical or basolateral membranes of umbrella cells may modulate ion channel activities that regulate apical membrane transport. While increased membrane tension (i.e. stretch) may be the physiologically relevant stimulus in these and other cells it is possible that pressure itself may play some role in other responses.

2.3.2 Distinct effects of increasing apical or basolateral membrane tension on umbrella cell apical membrane traffic

Our data indicates that the previously described early stage of surface area increase occurs when the distinct apical and basolateral membrane domains of the umbrella cell react to a changing mechanical environment. Consistent with this possibility we showed in Figure 2.4B that by changing the filling rate we could alter the time scale of phase 1 and 2 responses by several orders. In this dynamic environment we observed that exocytic events were triggered by increases in apical membrane tension and could be blocked by agents that perturbed the cytoskeleton, prevented rises in $[Ca^{2+}]_i$, or inhibited channel function (see discussion below). Intriguingly, exocytosis under these conditions was independent of temperature and was not sensitive to treatment with brefeldin-A. We further observed that the exocytic response was modulated by endocytosis, which was stimulated by increased basolateral membrane tension, occurred after the first phase of

outward bowing, and predominated during the second phase of this response. In contrast to the dynamic responses we observed in the early stage, the previously described late stage (i.e. phase 3 response to outward bowing) appears to reflect the responses of umbrella cells that have reached a mechanical equilibrium, when the uroepithelium is fully bowed outwards and tension is present in both umbrella cell membranes.

The increase in the apical surface area of umbrella cells is thought to reflect fusion of a subapical pool of discoidal/fusiform-shaped vesicles with the apical plasma membrane of these cells (1). If discoidal/fusiform vesicles are important for both the early stage and late stage responses, then what accounts for the differences in the regulation of these processes? We suggest that the early stage events reflect trafficking of a preexisting pool of vesicles (i.e. those present at steady state). Consistent with this possibility we observed that the early stage changes in surface area can occur on a rapid time scale and do not require new protein synthesis or secretion (7, 104). In contrast, the timing of the late stage events and their dependence on protein synthesis and secretion indicate that are likely mediated by a newly synthesized pool of vesicles. Further exploration is required to understand the relationship of the two exocytic responses, the membrane pools involved in these two processes, and how they are regulated.

2.3.3 Regulation of umbrella cell apical membrane traffic by ion channels

Like those in other cells (135-137), stretch-modulated channels may act as mechanotransducers to signal increased exocytosis at the apical surface of the umbrella cell. Likely candidates include an NSCC and ENaC. In response to stretch, the NSCC

conducts Ca^{2+}, which could stimulate exocytosis directly or indirectly by promoting Ca^{2+}-dependent Ca^{2+} release from IP3-receptor dependent stores in the endoplasmic reticulum (Figure 2.7). In addition $[Ca^{2+}]_i$ could also allow for crosstalk between the apical channels and basolateral K^+ channels (138), which we also showed may play a regulatory role in modulating the exocytic response. As well, K^+ channels are known to modulate Ca^{2+} responses in cells (131). The identity of the NSCC is unknown; however, TRP family channels such as PKD1/PKD2 may be candidates, as PKD1 is expressed in the uroepithelium (139). Ferguson et al. previously proposed that ENaC may act as a mechanosensor to regulate ATP release from the uroepithelium (140), and data from other cell types indicates that ENaC activity may be triggered by membrane stretch (6, 14, 17, 35, 141-143). Our data indicates that ENaC, acting downstream or in conjunction with the NSCC, could play a role in mechanotransduction by modulating membrane potential or crosstalk between ion channels at the apical and basolateral membrane domains.

We do not know the identity of the mechanotransduction pathway(s) that functions at the basolateral surface of the umbrella cell to regulate apical endocytosis. One possibility is that it involves the closing of one or more basolaterally localized K^+ channels including SK/IK and/or K_{ATP}. Intriguingly, our data showed that openers of these channels modulated the second and third phases of outward bowing, and stimulated a significant increase in C_a. The increase may represent a slowing in the endocytic rate or an increase in exocytic rate. An additional mechanosensor may include the actomyosin cytoskeleton, which is required for mechanosensation in both anchored and non-anchored cells (34, 76-78, 80, 95-97), and is prominently associated with the basolateral membrane

of the umbrella cell (see supplementary Figure S2.1D). Treatment with cytochalasin D or latrunculin impairs exocytosis and endocytosis in umbrella cells (6). While this may reflect effects on discoidal/fusiform vesicle dynamics, it is plausible that it may also result from defects in mechanotransduction.

2.3.4 Physiological relevance of the early and late stage response

The bladder fills in a multi-phase manner. An initial filling phase, marked by a rapid rise in pressure to 2-5 cm H_2O, is followed by a long storage phase, when the pressure rises only slowly. The subsequent mictruition phase is characterized by rapid spikes in bladder pressure (which can rise to $>$ 100 cm H_2O) as the smooth muscle contracts and ultimately terminates with voiding. We suggest that the early stage events we described may be important to all three phases of bladder filling. In the filling and storage phases the uroepithelium is in a dynamic mechanical state as the mucosa is actively unfolding and is slowly bowed outwards in response to increased urine volume, while in the micturition phase the epithelium must maintain patency in the face of rapid pressure changes. In all cases the increase in apical surface area would help dissipate the pressure (allowing the cells to maintain their barrier function) and stimulate the surface expression of apical membrane channels and receptors that would sense bladder filling as well as urine contents (sensory function). Increases in basolateral tension would modulate the apical membrane responses and signal the onset of the late stage of surface area modulation. This late stage may be important during the mid to late portions of the storage phase,

when the mucosa is bowed outwards and must accommodate the increasing urinary volume.

The dual-membrane response we observed is not only relevant to bladder filling, but may also be important for the relatively rapid process of bladder voiding. Upon release of the bladder contents, the epithelium is rapidly refolded, which would dissipate any apical membrane tension. Furthermore, it would also likely increase tension at the basolateral surface of the uroepithelial cells in the forming crest regions of the folds, which would be actively pushed by the underlying matrix and musculature toward the lumen of the bladder. As we observed, increased tension in the basolateral surface of the umbrella cells would promote endocytosis of membrane and associated sensory receptors and channels, returning the umbrella cell layer to its basal state prior to another cycle of bladder filling.

2.3.5 Summary and model

We propose a model in which the polarized membrane domains of the umbrella cell act in concert to regulate apical membrane dynamics in this cell during bladder filling and voiding (Figure 2.7). While increased tension in the apical membrane of the umbrella cell stimulates opening of stretch-sensitive channels that induce exocytosis, subsequent increases in tension across the basolateral membrane stimulate apical membrane endocytosis. The latter process would ensure membrane turnover and would act in combination with exocytosis to modulate the sensory and barrier functions of the epithelium as the bladder fills and empties. It likely that the mechanisms we observe in umbrella cells will apply to other mechanically sensitive epithelial cells (e.g. those that

line the urinary tract, gastrointestinal tract, respiratory tract, and vascular system), whose distinct membrane domains likely also act in concert to modulate the function of these cells and their end organs.

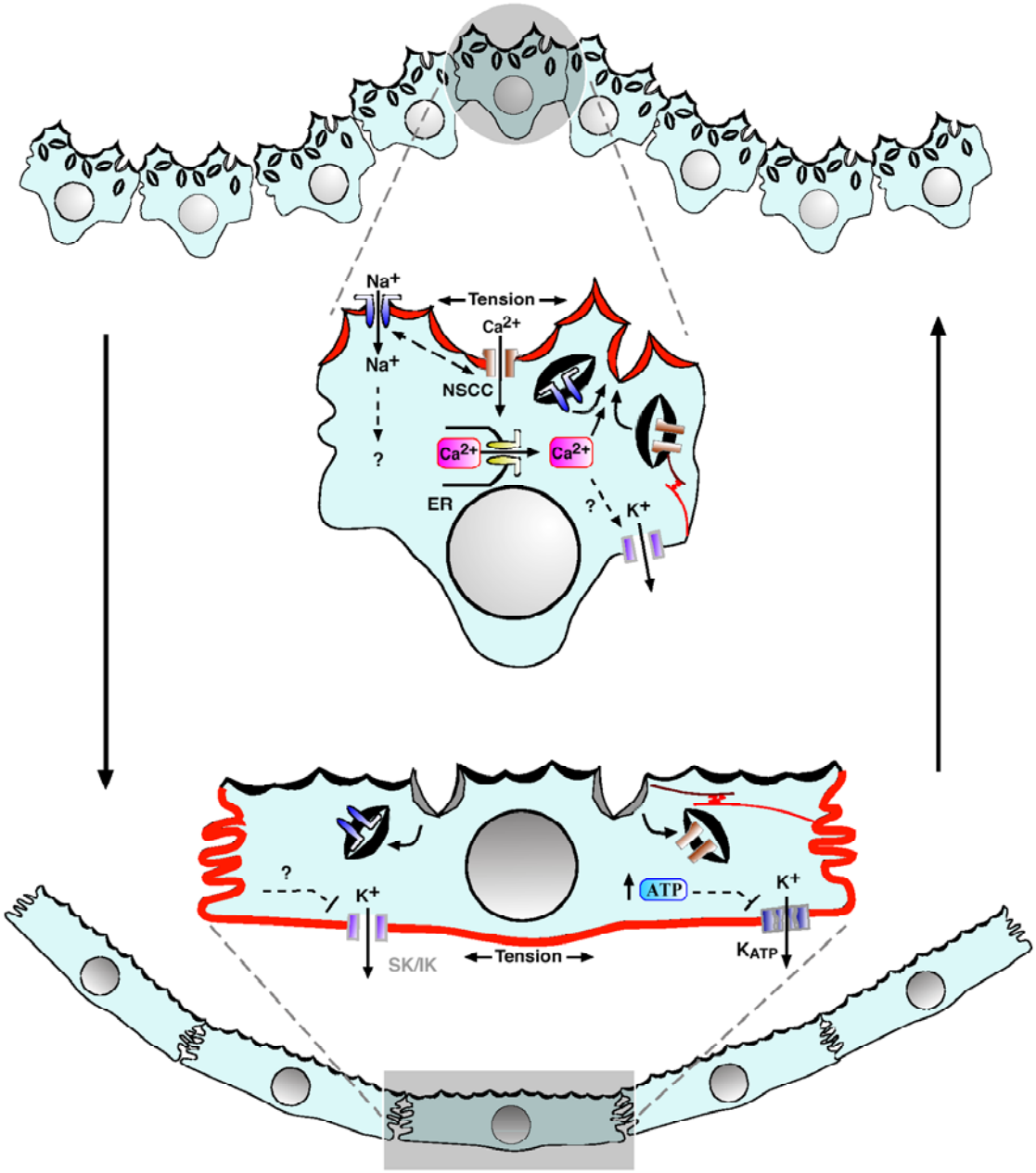

Figure 2.7. Model for stretch-induced umbrella cell responses

As the bladder fills, the increased tension at the apical membrane causes opening of an NSCC, stimulating influx of extracellular Ca^{2+}. The increased $[Ca^{2+}]_i$ triggers Ca^{2+}-dependent Ca^{2+} release from IP_3 dependent stores, which stimulates exocytosis and may modulate the activity of other channels. Exocytosis may amplify the initial response by stimulating delivery of additional stretch sensing channels to the apical surface of the cell. ENaC, perhaps acting downstream of the NSCC, is also opened and may modulate the exocytic response by changing the membrane potential or the driving force for the entry of other ions (e.g. by modulating the activity of the Na^+,K^+ ATPase). As the epithelium bows further outward tension in the basolateral membrane would subsequently increase. This would cause an increase in apical membrane endocytosis, which would modulate the exocytic response by stimulating internalization of apical membrane channels and other sensory molecules (not shown). The mechanosensor at this membrane is unknown but may include the cytoskeleton or stretch-modulated K^+ channel(s), which may close in response to the increased tension or other intracellular mediators such as ATP. During voiding, tension would increase in the basolateral membrane as the mucosa refolds. The increased tension would further stimulate endocytosis of apical membrane and its constituents, readying the umbrella cell for the next cycle of filling. For clarity we do not include the underlying cell layers or connective tissue; however, the umbrella cell may transmit tension to the interconnected matrix, intermediate cells, and basal cells and they, in turn, may impact or promote events in the overlying umbrella cell layer.

2.4 EXPERIMENTAL PROCEDURES

2.4.1 Materials, reagents, and animals

Unless described otherwise all reagents and chemicals were obtained from Sigma (St. Louis, MO). Anti-chicken Kir6.1 antibody CAF-1 was raised against a peptide corresponding to residues 20–31 of the Kir6.1 N-terminus (ENLRKPRIRDRLP) and was kindly provided by Dr. Coetzee (New York University). It was used at a 1:400 dilution for western blot analysis and a 1:200 dilution for immunofluorescence. Female New Zealand white rabbits (3-4 kg) were obtained from Myrtle's Rabbitery (Thompson Station, TN), C57BL/6J mice (3-4 months old) were obtained from the Jackson Labs (Bar Harbor, ME), and Sprague-Dawley rats (weighing 250-300 g) were obtained from Harlan (Indianapolis, IN). All animal studies were approved by the University of Pittsburgh Animal Care and Use Committee.

2.4.2 Isolation and mounting of uroepithelial tissue

The preparation and mounting of rabbit uroepithelium in Ussing stretch chambers was performed as described previously (18); however, we used two closed Ussing stretch

chambers in our analysis. The tissue was bowed slightly inwards during the equilibration period.

2.4.3 Mechanical stretch of tissue

Tissue manipulations are shown graphically in Figure 1 and are described in detail in the supplementary text.

2.4.4 Electrophysiological data acquisition and capacitance measurements

The measure of TEV and C_a were described previously (18, 19, 104). Changes in capacitance reflect changes in the apical cell surface area of the umbrella cells, where 1 $\mu F \approx 1\ cm^2$ of membrane area. According to two exponential equation: $V(t) = I(t)\,[Ra\,(I\text{-}e^{-t/RaCa}) + Rb\,(I\text{-}e^{-t/RbCb})]$, apical membrane capacitance was measured by nonlinear regression curve fit the voltage response with Prism GraphPad software. Isc was calculated from the voltage response to a 1 μA square current pulse using Ohm's law (6).

2.4.5 RT-PCR analysis

Bladders were excised from euthanized mice, the uroepithelium was recovered by scrapping and RNA purified and RT-PCR performed as described previously (104).

2.4.6 Western blot and immunofluorescence

Rat uroepithelial cells were isolated by gentle scraping, lysed in SDS lysis buffer, resolved by SDS page, and subjected to western blot analysis as described previously (7). Rat tissue was prepared for immunofluorescent labeling as described previously (7); however, tissue was fixed in 10% (v/v) acetic acid, 40% (v/v) ethanol in phosphate buffered saline for 40 min at 4˚ C. Images were acquired using a Leica (Leica, Dearfield, IL) TCS-SL scanning-laser confocal microscope as described previously (7).

2.4.7 Statistical Analysis

Data were analyzed using Student's t test and $p < 0.05$ was taken as significant. ANOVA and Bonferroni's correction were used when making multiple comparisons.

2.5 SUPPLEMENTARY MATERIALS

2.5.1 Supplementary Figure S2.1 legend

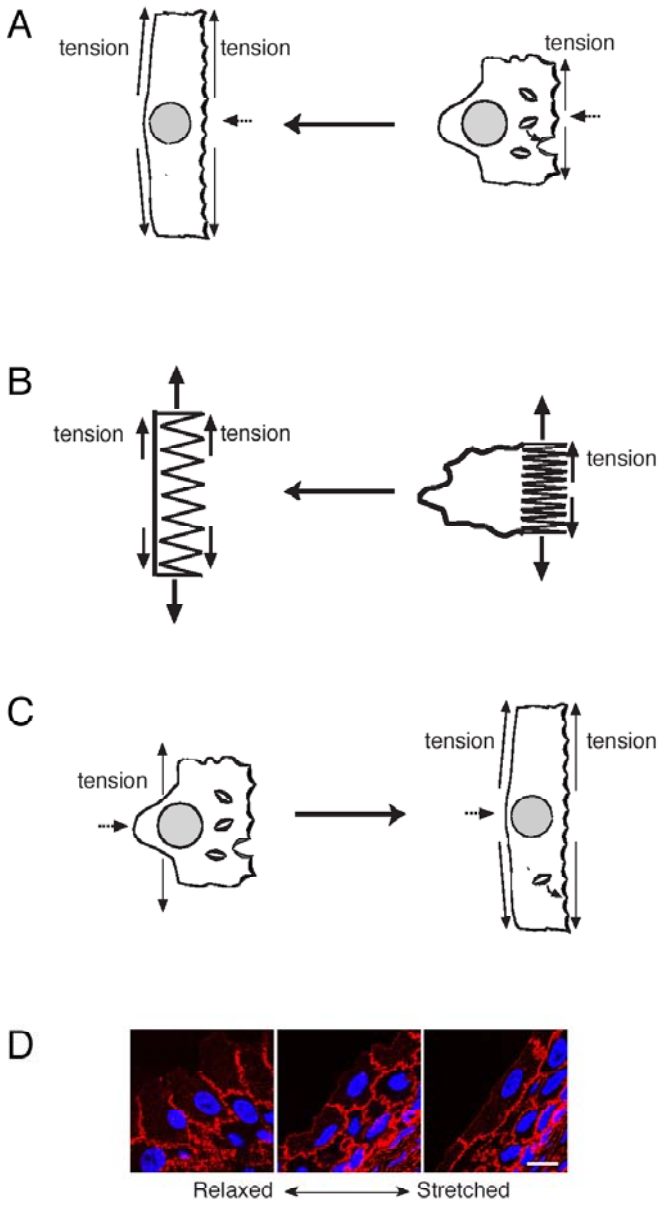

Figure S2.1. Mechanical and morphological features of distended umbrella cells

(A) In response to filling the mucosal hemichamber, tension develops in the apical membrane, which causes the tissue to bow outwards. The apical membrane tension can be dissipated in part by increased exocytosis. Subsequently, tension increases in the basolateral membrane, which unlike the apical membrane does not accommodate increased tension by modulating surface area. (B) The apical membrane acts like a spring that can accommodate heightened tension by increasing apical surface area, but the spring is limited by the basolateral membrane, which may act like a rope to further constrain tension release (in the case of the umbrella cell by promoting endocytosis of apical membrane). (C) In response to filling the serosal hemichamber, tension is increased in the basolateral membrane, which cause the tissue to bow inwards. As the tissue bows further, tension increases in the apical membrane. (D) Morphology of umbrella cells in relaxed state (fixed after bladder is cut open) or when the tissue was stretched and then fixed. Red staining, rhodamine phalloidin; blue staining, Topro-3. Bar = 10 μm.

2.5.2 Supplementary Figure S2.2 legend

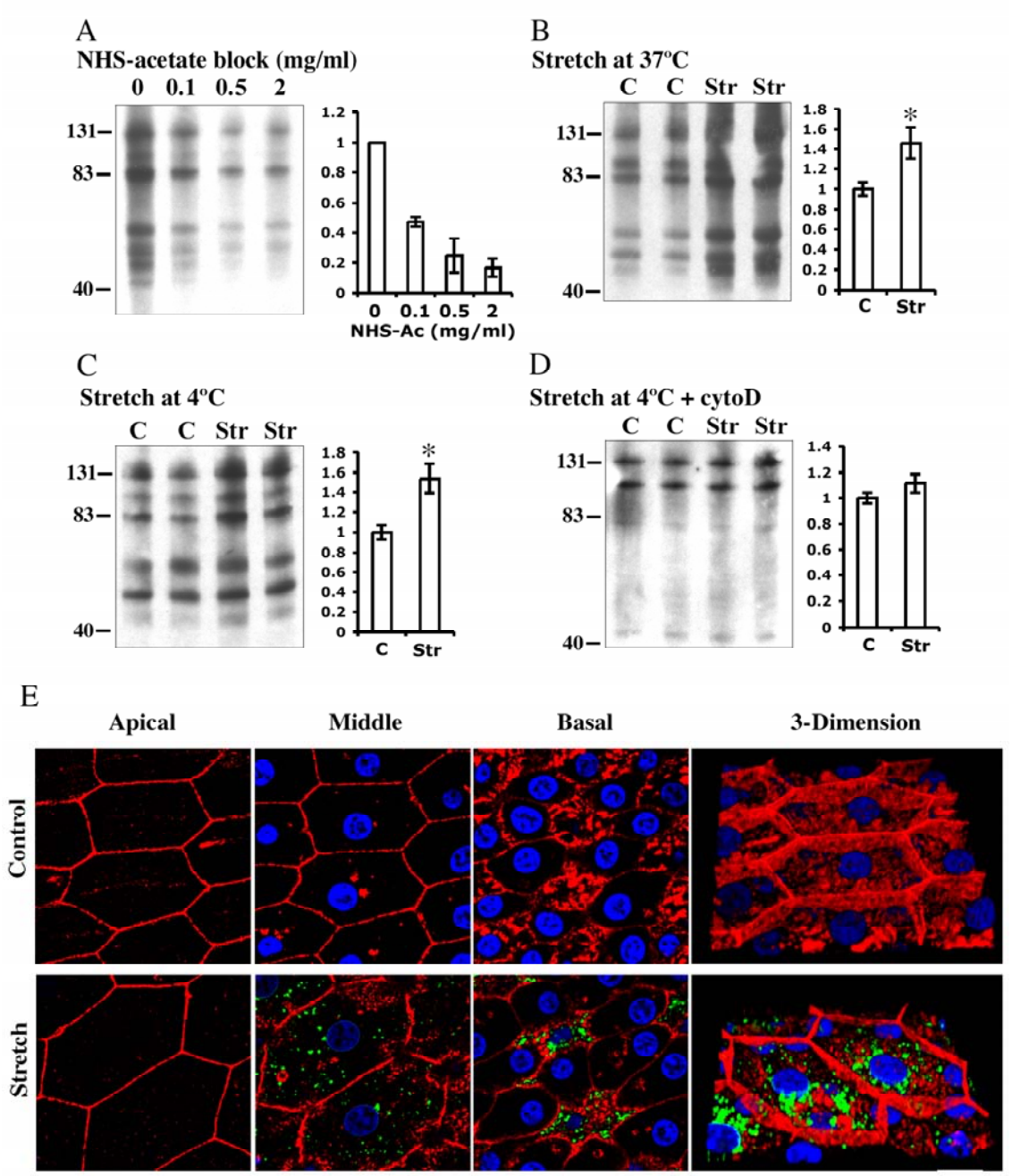

Figure S2.2. Increased membrane turnover in response to acute changes in hydrostatic pressure

(A) Tissue was mounted, equilibrated, and then cooled to 4°C for 30 min. The apical surface of the cells was treated with the indicated concentration of sulfo-NHS acetate for 60 min, washed, and then incubated with 0.5mg/ml sulfo-NHS-SS-biotin for 15 min to biotinylate unblocked apical membrane proteins. The percent change in biotinylated proteins way quantified by densitometry and is plotted in the graph to the right. (B-C) The apical surface of the umbrella cells was incubated with 1 mg/ml sulfo-NHS acetate for 60 min at 4˚C, and then the tissue was bowed outwards (2 cm H_2O pressure using a 20-gauge needle) for 5 min at 37˚C (B) or 10 min at 4˚C (C). The apical surface of tissue was then incubated with 0.5 mg/ml sulfo-NHS-SS-biotin for 15 min to biotinylate newly inserted apical membrane proteins. The percent change in biotinylated proteins is shown in the panel to the right. (D) The tissue was incubated with 1 mg/ml sulfo-NHS acetate, treated with cytochalasin D for 60 min at 37˚ C, stretched 10 min at 4˚ C, and the apical surface biotinylated. The percent change in biotinylated proteins is shown in the panel to the right. (A-D) Data are expressed as mean ± SEM ($n \geq 3$). *Statistically significant difference ($p < 0.05$) relative to control. Representative lysates from two control (C) or stretched (S) samples are shown in panels B-D. (E) Tissue was mounted, equilibrated, and then cooled to 4°C for 30 min. WGA was added to the mucosal hemichamber, incubated for 30 min, and the tissue was bowed outwards for 10 min at 4˚ C by filling the chamber using a 20-gauge needle at a 2 cm H_2O pressure head. Unstretched tissue served as control. Shown are individual optical sections taken from the apical, middle, and basal regions of stretched umbrella cells. Rhodamine phalloidin was used to label the actin cytoskeleton (red), and Topro-3 was used to label the nuclei (blue). A 3-dimensional reconstruction of the cell is shown at the right. Bar = 20 μm.

2.5.3 Supplementary Figure S2.2 discussion

The temperature independence of the phase 1 response prompted us to use a different approach to confirm increased membrane turnover under our experimental conditions. We first blocked the majority of NHS-reactive groups on the apical surface of quiescent umbrella cells using NHS-acetate (up to 2 mg/ml), a treatment that effectively prevented apical membrane proteins from being subsequently labeled with an NHS-S-S-biotin reagent (Figure S2.2A). Next, the tissue was bowed outward and incubated for either 5 min at 37˚ C (Figure S2.2B) or for 10 min at 4˚ C (Figure S2.2C). We reasoned that if stretch stimulated increased exocytosis then new proteins would appear at the cell surface and expose new reactive groups that could be identified using the NHS-S-S-biotin reagent. Indeed, we observed a significant increase in the surface expression of several protein species both at 37˚ C and 4˚ C (Figure S2.2B-C), confirming that exocytosis occurred under these conditions. Our data also indicates that acute stretch is accompanied by increased endocytosis. Consistent with this possibility, we observed that FITC-labeled wheat germ agglutinin was endocytosed at either 4˚ C (Figure S2.2E) or at 37˚ C (data not shown).

2.5.4 Supplementary Figure S2.3 legend

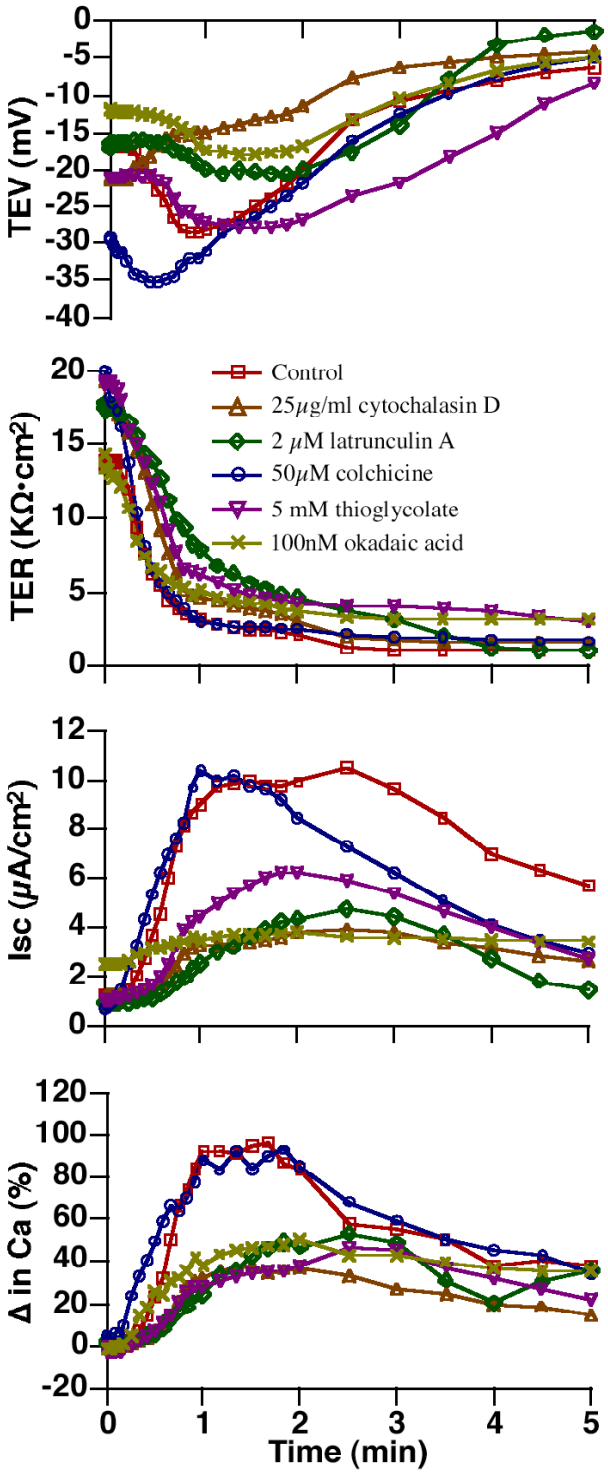

Figure S2.3. Role of the cytoskeleton in the electrophysiological responses to outward bowing

The tissue was pre-treated with the indicated blocker for 30 min at 37˚ C. The tissue was then bowed outward using a 20-gauge needle to fill the mucosal hemichamber at a 2 cm H_2O pressure head. Untreated tissue served as a control. The experiments were repeated $\geq$ 3 times and representative results are shown.

2.5.5 Supplementary Figure S2.4 legend

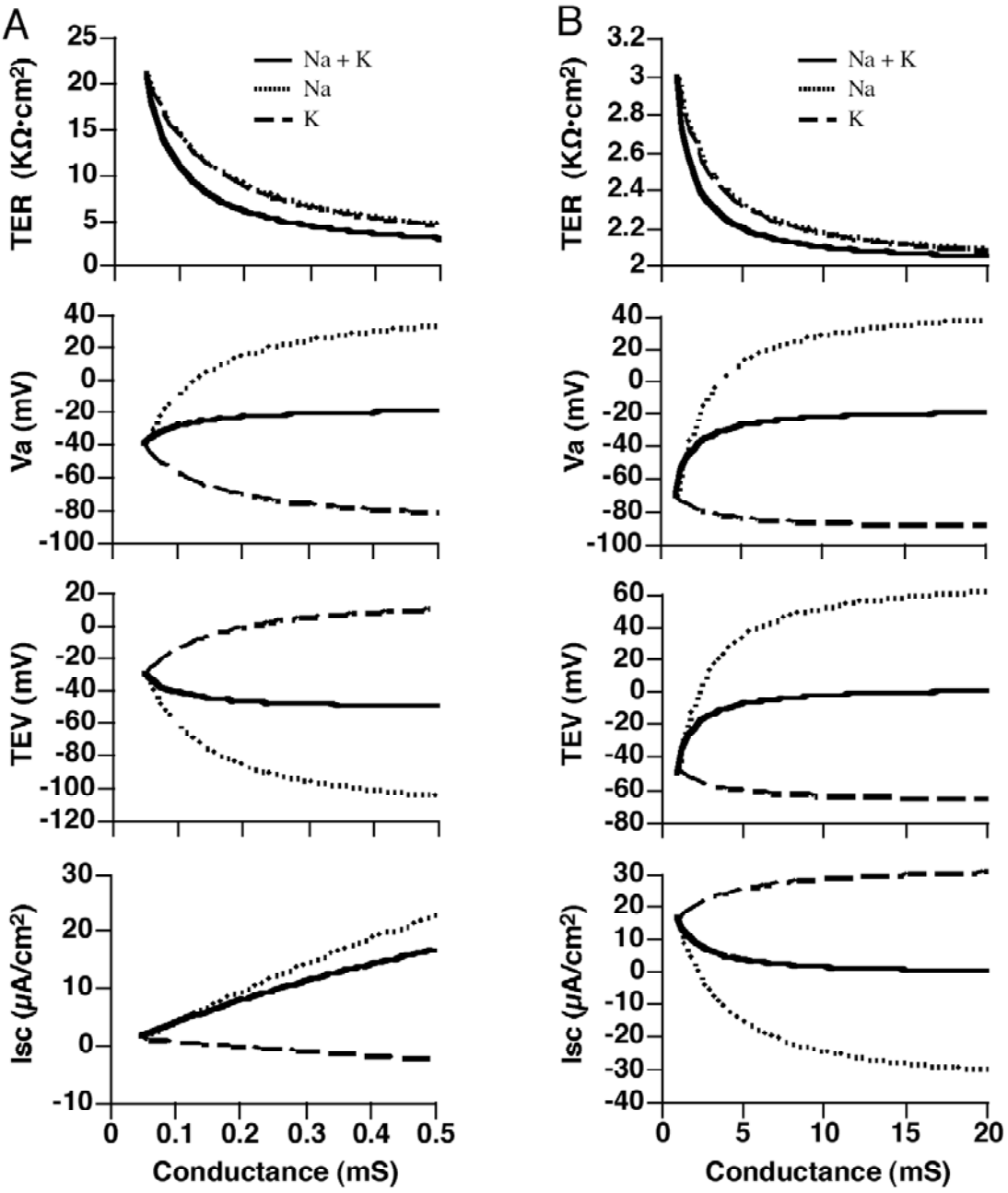

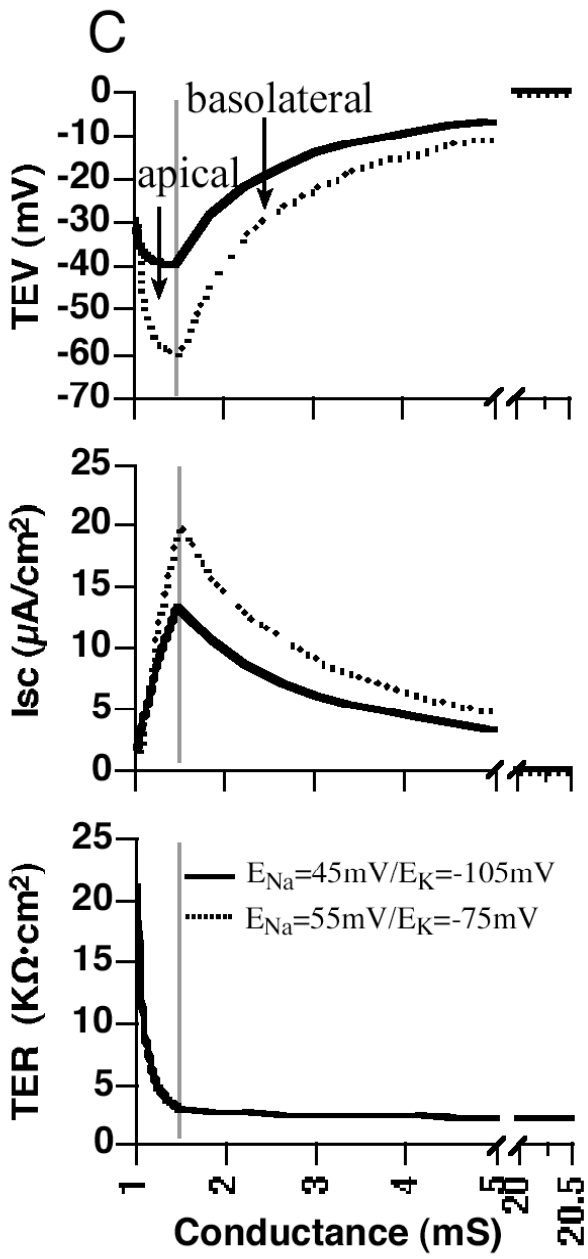

Figure S2.4. Mathematical modeling of umbrella cell electrophysiological parameters

(A) Predicted changes in TER, V_a, TEV, and I_{sc} upon increased apical conductance of Na^+ or/and K^+ ions. (B) Predicted changes upon increased basolateral conductance of Na^+

or/and K^+ ions. (C) Predicted changes in TEV and Isc upon sequentially increasing apical and then basolateral conductance of Na^+ and K^+ ions using two values for E_{Na} and E_K.

2.5.6 Supplementary Figure S2.4 discussion

2.5.6.1 The apical and basolateral membrane contributions to the observed electrophysiological properties can be modeled mathematically

Our data indicate that the phase 1 response of outward bowing and subsequent reversal of the electrophysiological parameters during phase 2 may result from the successive stretch of the apical and then basolateral membranes of the umbrella cell layer. To further confirm this possibility and also gain insight into the molecular mechanisms involved, we modeled umbrella cell electrophysiological responses assuming that apical and basolateral membrane are stretched sequentially and Na^+ and K^+ permeable ion channels are modulated upon stretch.

We and others have previously reported that stretch stimulates Na^+ absorption via the amiloride-sensitive ENaC in apical membranes of the umbrella cell layer (13, 14, 19, 35). Therefore, we first modeled the impact that an increase in the apical membrane conductance of Na^+ would have on several electrophysiological parameters. In addition to causing apical membrane depolarization (V_a), the increase in Na^+ absorption would result in TEV hyperpolarization, an increase in I_{sc}, and a drop in TER (supplementary Figure S2.4A), a response identical to that observed during phase 1 of outward bowing. We also modeled the condition where the apical membrane conductance was limited to an increase in K^+ conductance via K^+-permeable ion channels. A response largely opposite

of that observed for increased Na^+ conductance was predicted (Figure S2.4A). If the increase in apical membrane conductance was contributed equally by both Na^+ and K^+ permeable ion channels, a response similar to that observed for opening of Na^+ permeable ion channels was observed (Figure S2.4A), indicating that Na^+ permeable ion channels may play a major role in the response observed when the apical membrane is stretched.

We also modeled events at the basolateral membrane, and observed that absorption of just Na^+ permeable ion channels resulted in basolateral membrane and TEV depolarization, decreased TER, and increased I_{sc} (Figure S2.4B), a response similar to that observed during phase 2 of outward bowing. Likewise, if stretch of the basolateral membrane resulted in an equal increase in conductance through both Na^+ and K^+ permeable channels, we would observe a decrease in TER, TEV, and I_{sc}. In contrast, opening of K^+ channels alone gave an opposite response to that we observed, with the exception of TER, which remained depressed (Figure S2.4B). Taken together these data indicated that the second phase of outward bowing may occur in response to closing of K^+ channels or increasing the fraction of Na^+ transport. Finally we modeled the situation where the apical membrane response predominated initially followed by a predominant basolateral membrane response using different values for E_{Na} (45 or 55 mV) and E_K (-75 or -105mV). The results of this analysis showed an initial phase marked by hyperpolarization of TEV, a rise in I_{sc}, and decreased TER, followed by a second phase characterized by depolarization of TEV and a fall in I_{sc} (Figure S2.4C). In summary, mathematical modeling provides further support of the distinctive function of the apical and basolateral membranes in modulating the electrophysiological responses to umbrella cell stretch.

2.5.7 Supplementary Methods

2.5.7.1 Mechanical stretch of tissue

Tissue manipulations are shown graphically in Figure 2.1. Control tissue was left at 37˚ C and was not exposed to mechanical stimuli (Figure 2.1A). In some experiments tissue was bowed outwards by attaching 4 mm diameter Tygon tubing to the top Luer fitting of the mucosal hemichamber. The tubing, filled with Krebs buffer, was placed at the indicated height above an additional piece of tubing (filled with Krebs buffer) that was attached to the serosal hemichamber. The free end of the mucosal tubing was attached to a master stopcock. At the start of the experiment the master stopcock was opened, which allowed the back pressure in the mucosal hemichamber to be increased in a step-wise fashion by raising the height of the mucosal tubing 4-64 cm H_2O above the starting point (Figure 2.1B). In some experiments the tubing attached to both hemichambers was simultaneously raised to increase pressure in both hemichambers to 4-64 cm H_2O (Figure 2.1C). To stretch the uroepithelium in the absence of pressure change, a filament (silk surgical suture thread) was sutured onto a 2.5 mm diameter pad of muscle let on the serosal surface of the tissue during dissection. A 1-cm H_2O pressure head was maintained in each chamber, and the filament, threaded through the side port of the serosal hemichamber, was attached to an NE-1600 syringe pump (New Era Pump Systems, Inc.; Farmington, NY) and pulled at a constant speed of 0.1- 2.0 cm/min (Figure 2.1D). In some experiments the tissue was bowed outward (Figure 2.1E) or inward (Figure 2.1F) to discrete pressure heads of 1-16 cm H_2O using a setup similar to that

described for Figure 2.1B. According to LaPlace's law (where T = PR/2) the tension inside a spherical wall will increase proportionally to the pressure (P) and the radius of curvature (R). Assuming the degree of tissue bowing is similar, which is generally true in our system at all pressure heads examined, then changing the pressure will increase tension in the tissue. In other experiments we maintained a constant pressure head of 2 cm H_2O in the mucosal hemichamber, but changed the rate of filling by attaching different gauge needles to the end of the tubing feeding the mucosal hemichamber (Figure 2.1G). According to Poiseuille's law, where $dV/dt = \pi/8(R^4/\eta)(dP/L)$, if the length of the needle (L) is kept constant then the filling rate (dV/dt) will be dependent on the pressure difference (dP), the radius of the needle (R), and the viscosity of the Krebs buffer (η). Changing R (by using different gauge needles) while maintaining the other parameters constant will only change the filling rate.

2.5.7.2 Measurement of exocytosis and endocytosis at the apical surface of umbrella cells

Tissue was mounted and equilibrated as described and then cooled to 4° C for 30 min. After incubating apical surface of umbrella cells with sulfo-NHS acetate (1 mg/ml) for 60 min, tissue was then stretched by 2 cm H_2O pressure with 20 gauge needle either at 37˚ C for 5 min or at 4˚ C for 10 min, the apical surface of tissue was then incubated with 0.5mg/ml sulfo-NHS-SS-biotin for 15 min to biotinylate newly turnover apical membrane proteins. Tissue without stretch served as control. The uroepithelium was washed with ice-cold Krebs, removed from the chamber, the tissue recovered by scraping and lysed in 0.5% SDS lysis buffer (0.5% w/v SDS, 100 mM triethanolamine, pH 8.6, 0.5

mM EDTA, 1 mM phenylmethylsulfonyl fluoride, 5μg/ml leupeptin, 5μg/ml antipain, and 5μg/ml pepstatin). Equal amounts of protein from the tissue lysates were resolved SDS-PAGE, and proteins transferred and probed with streptavidin-HRP as described previously (7). To measure endocytosis, tissue was mounted, equilibrated and cooled to 4° C for 30 min. FITC-WGA (50 μg/ml) was then added to the mucosal chamber and incubated for 30 min, and the tissue was stretched for 10 min using a 20-gauge needle at a 2 cm H_2O pressure head. Tissue was then fixed, prepared, and stained with rhodamine phalloidin and Topro-3 as described previously (132). Unstretched tissue served as control.

2.5.7.3 Mathematical modeling of electrophysiological parameters

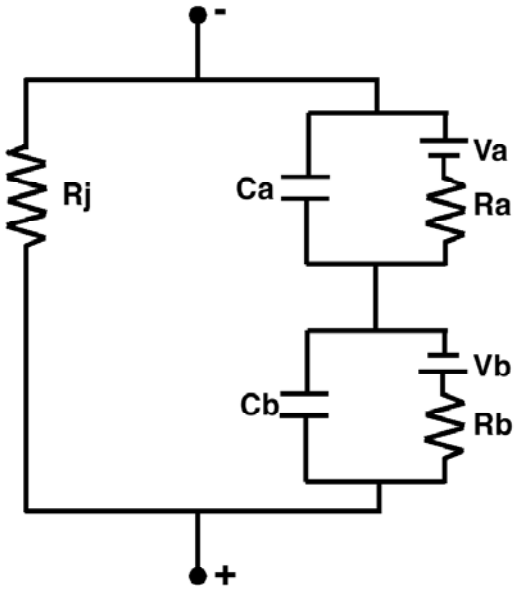

Figure. S2.5 circuit diagram of umbrella cells

Our mathematical model was based on previously described electrophysiological analysis of umbrella cells (13-16, 35). The TER and TEV were estimated from the following equations: TER = $(R_a+R_b)*R_j/(R_a+R_b+R_j)$ and TEV = $(V_a+V_b)*R_j/(R_a+R_b+R_j)$, where R_j = the tight junction resistance, V_a = the apical membrane voltage, and V_b = the basolateral membrane voltage. Because Rj ≅ ∞ (13, 14, 35), the above equations can be simplified to TER = R_a+R_b and TEV = V_a+V_b. Estimates of R_a (20000 Ω•μF), R_b (1000 Ω•μF), V_a (40 mV) and V_b (70 mV) were described previously (13-16, 35). V_a and V_b are essentially dependent on the potential difference of Na^+ and K^+ and their relative conductances according to the following equation: $V_{a/b} = (G_{a/bNa}*E_{Na} + G_{a/bK}*E_K)/(G_{a/bNa} + G_{a/bK})$, where Gi_{Na} and Gi_K are the respective conductances of Na^+ or K^+ at the apical (a) or basolateral (b) membrane domain. The equilibrium potential for Na^+ (E_{Na}) or K^+(E_K) was determined using the Nernst equation and typical values of E_{Na} (45 – 55 mV) and E_K (-75 – -105 mV). Isc was calculated by $(V_a + V_b)/ (R_a + R_b)$.

2.5.7.4 Primers used for PCR of K^+ channels

Table S2.1. Primers used for PCR of K^+ channels

K^+ channel	Sequence of Primers (5'-3')	Expected Product size (bp)
Kcnma1 (BK)	CGTACTGGGAATGTGTCTACTT ACTACAATGTGCTTTCTTCCAC	223
Kcnn1 (SK1)	GGCTTTTCTTCAGGATCTATCT GTGTCCTTACTTTGACATCAGG	171
Kcnn2 (SK2)	ATCCCATACCTGGGAATTATAC TATCTTATTAAGTGCCCCAATG	203
Kcnn3 (SK3)	ACCTACGAGCGTATCTTCTACA ATCAGTGAAGAGTTTGCTATGG	219
Kcnn4 (IK1)	CACAGAAGAACCAGGCTAAGTA CTGATGAGGGCATATGTGTAGT	219
Kcnk2 (TREK-1)	AAAGGGAAAGCAAATAGAAAAC AGCATTCAGATTCATTCATAGG	206
Kcnk4 (TRAAK)	GGCGTCTCTTTTGTATCTTCTA GAAGGTAGGAGTGAGGACAAA	221
Kcnk10 (TREK-2)	AAGAGAAGAAAGAGGACGAGAC ACACATAGTCCAATTCCAATGT	201
Kcnj8 (Kir6.1)	AACTCCATCAGGAGGAATAACT CAATATTTTGATCATCGGAACT	225
Kcnj11 (Kir6.2)	CAAATGATTGGAGACCTTTCTA ATCCAGGTATATCAGTGTTTGC	168

3.0 ADENOSINE RECEPTOR EXPRESSION AND FUNCTION IN BLADDER UROEPITHELIUM

*Reprinted from *American Journal of Physiology – Cell Physiology*, (2006, Volume 291, Page C254-C265), with permission by the American Physiology Society

3.1 INTRODUCTION

Adenosine is a universally produced nucleoside that participates in the normal function of the cardiovascular, immune, neuronal, and renal systems where it regulates diverse phenomena including tubuloglomerular feedback, neuronal hyperpolarization, vasodilation, smooth muscle relaxation, protection against ischemic damage, and release of vasoactive substances (144-146). Adenosine is generated within the cell from the hydrolysis of S-adenosyl-L-homocysteine, and is also formed both extracellularly and intracellularly from the hydrolysis of ATP, ADP, AMP, or cAMP (144, 147). Once produced, adenosine has several fates including bidirectional translocation between the cytoplasm of the cell and the extracellular fluid (through equilibrative or concentrative transport proteins), conversion by adenosine deaminase to inosine, phosphorylation by adenosine kinase to generate AMP, or interaction with cell surface adenosine receptors (144). Four subtypes of adenosine receptors have been defined: A_1, A_{2a}, A_{2b}, and A_3, all of which are G-protein coupled receptors with 7 transmembrane domains. A_1 and A_3 receptors preferably interact with members of the G_i family and inactivate adenylate

cyclase to decrease the production of cAMP, while A_{2a} and A_{2b} receptors are coupled to G_s and stimulate cAMP production. All four receptors activate phospholipase C (PLC), resulting in inositol-3,4-,5-trisphosphate (IP_3) production and increased cytoplasmic Ca^{2+} (146, 148), and can also stimulate mitogen-activated protein kinase cascades (148).

Adenosine may regulate normal bladder function. Message for all four adenosine receptor subtypes is detected in whole rat bladders by RT-PCR analysis (149), and northern blot analysis confirms that A_{2b} receptors are abundantly expressed in the detrusor muscle (150); however, the tissue distribution of A_1, A_{2a}, and A_3 receptors within the bladder has not been defined. Studies thus far indicate that adenosine inhibits contraction of isolated rat detrusor muscle exposed to carbachol, acetylcholine, potassium depolarization, or field stimulation, a function that has been variously ascribed to A_{2a} and/or A_{2b} receptor activation (151-155). The involvement of adenosine in the inhibition of muscle contraction may be the consequence of membrane hyperpolarization as a result of K_{ATP} activation (73), a downstream effect of A_{2a} activation. In contrast, A_1 receptor activation may have a role in stimulated detrusor muscle contraction in cat bladder muscle (156). Adenosine also acts to regulate bladder function by inhibiting the contraction of the detrusor muscle via A_1 receptors present at the neuromuscular junctions and in the central nervous system via activation of A_1 and A_2 receptors (157-159). The latter act to increase the urine volume necessary to induce volume-evoked micturition reflex in rats (159). Whether adenosine affects other bladder functions is unknown.

The interface between the urine and the underlying nervous tissue and musculature of the bladder is the uroepithelium (1). This stratified tissue, comprised of

basal, intermediate, and umbrella cell layers, not only forms a dynamic barrier that maintains the composition of the urine, but also may communicate the contents of the urine and the degree of bladder filling to sensory afferents that underlie the epithelium (1). The uroepithelium can release ATP (17, 108), but it is unknown whether this contributes to the high concentrations of adenosine found in urine. As the bladder fills, the apical surface of umbrella cells becomes flattened and cytoplasmic discoidal/fusiform-shaped vesicles fuse with the apical plasma membrane, which increases the lumenal surface area of the bladder and may allow the bladder to accommodate increased urine volumes (7). Beyond bladder filling and its associated mechanotransduction pathways that increase cAMP and Ca^{2+} within the uroepithelium (7, 18), few physiological regulators of umbrella cell discoidal/fusiform vesicle exocytosis are known. We have recently shown that ATP, released from the bladder epithelium, binds to cell surface P2X receptors on uroepithelium and acts as an autocrine regulator of membrane traffic in the umbrella cell (108).

Our studies indicate that the uroepithelium is a source of adenosine biosynthesis, that all four adenosine receptors are expressed in the uroepithelium, and that adenosine/adenosine agonists stimulate umbrella cell exocytosis possibly through a Ca^{2+}-dependent signaling pathway. These observations reveal a previously undescribed role for adenosine as an autocrine/paracrine modulator of exocytosis in the umbrella cell layer.

3.2 MATERIALS AND METHODS

3.2.1 Materials

Unless specified otherwise, all chemicals were obtained from Sigma (St. Louis, MO) and were of reagent grade or better. Stock solutions of adenosine, adenosine receptor agonists/antagonists, and other reagents were prepared in Krebs solution (110 mM NaCl, 5.8 mM KCl, 25 mM $NaHCO_3$, 1.2 mM KH_2PO_4, 2.0 mM $CaCl_2$, 1.2 mM $MgSO_4$, 11.1 mM glucose, pH 7.4) or DMSO as follows: adenosine, 10 mM in Krebs solution; brefeldin A (BFA), 10 mg/ml in DMSO; 2-chloro-N^6-cyclopentyladenosine (CCPA), 10 mM in Krebs solution; 2-[p-2-carboxyethyl]phenylethylamino-5'-N-ethylcarboxamidoadenosine (CGS21680), 1 mM in Krebs solution; N^6-(3-iodobenzyl)adenosine-5'-N-methyluronamide (Cl-IB-MECA), 10 mM in DMSO; (9-chloro-2-(2-furyl[1,2,4]triazolo[1,5-c]quinazolin-5-amine) (CGS15943), 10 mM in DMSO; 1,3-dipropyl-8-cyclopentylxanthine (DPCPX), 5 mM in Krebs solution; 4-(2-[7-amino-2-[2-furyl]-[1,2,4]triazolo[2,3-a][1,3,5]triazin-5-yl-amino]ethyl)phenol (ZM241385), 10 mM in DMSO; N-(4-cyano-phenyl)-2-4-(2,6-dioxo-1,3-dipropyl-2,3,4,5,6,7-hexahydro-1H-purin-8-yl)-phenoxy]acetamide (MRS1754), 2.5 mM in DMSO; N-(2-methoxyphenyl)-N-(2-(3-pyridyl)quinazolin-4-yl)urea (VUF5574), 4 mM in DMSO; adenosine deaminase, 90 U/ml in Krebs solution; iodotubericidin, 1 mM in

DMSO; erythro-9-(2-Hydroxy-3-nonyl)adenine (EHNA), 10 mM in Krebs solution; 2-aminoethoxydiphenylborate (2-APB); 10 mM in DMSO; 1-[6-((17b-3-Methoxyestra-1,3,5(10)-trien-17-yl)amino)hexyl]-1H-pyrrole-2,5-dione (U73122), 5 mM in DMSO; and xestospongin C, 1 mM in ethanol. All stock solution were freshly prepared just prior to use.

3.2.2 Animals

Animals used in this study were female New Zealand White rabbits (3-4 kg; Myrtle's Rabbitry, Thompson Station, TN), female Sprague-Dawley rats (weighing 250-300 g), and female C57BL/6J mice (3-4 months old). Rabbits were euthanized by injection of 300 mg sodium pentobarbital into the ear vein, while rats and mice were euthanized by inhalation of 100% CO_2. Following euthanization and thorocotomy the bladders were rapidly excised and processed as described below. All animal studies were carried out with the approval of the University of Pittsburgh Animal Care and Use Committee.

3.2.3 Antibodies and labeled probes

Affinity-purified rabbit polyclonal anti-rat adenosine A_1 receptor antibody and corresponding control peptides were purchased from Novus Biologicals, Inc (Littleton, CO). Rabbit polyclonal antibodies to the A_{2a}, A_{2b}, and A_3 receptors and antigenic peptides were purchased from Chemicon International (Temecula, CA). Secondary goat anti-rabbit antibodies conjugated to FITC or horseradish peroxidase were purchased from

Jackson Immunoresearch Laboratories, Inc (West Grove, PA). Topro-3 and TRITC-phalloidin were purchased from Invitrogen/Molecular Probes (Carlsbad, CA).

3.2.4 Western blot analysis of adenosine receptors in uroepithelium

Rat bladder uroepithelial tissue was obtained by gently scraping the epithelium using a 17-mm cell scraper (Sarstedt, Inc., Newton, NC). The collected cells were lysed in 0.5% SDS lysis buffer (100 mM NaCl, 50 mM triethanolamine, 5 mM EDTA, and 0.5% [w/v] SDS) containing a protease inhibitor cocktail (5µg/ml leupeptin, 5µg/ml antipain, 5µg/ml pepstatin, and 1 mM phenymethysulfonyl fluoride). Proteins were resolved by SDS-PAGE, transferred to Immobilon-P, and the blots were probed with adenosine receptor specific antibodies using our previously described techniques (7, 108). In some experiments, primary antibody was combined with antigenic peptide (1:100) for 2 h at room temperature prior to incubation with the transferred proteins. Images were scanned using an ArtixScan 1800f flatbed scanner (Microtek International. Carson, CA), the contrast was corrected using Photoshop (Adobe Systems Inc., San Jose, CA) and the images were imported into Freehand (Macromedia, San Francisco, CA).

3.2.5 Immunofluorescence analysis of adenosine receptors in uroepithelium

Excised bladders were fixed in 4% (w/v) paraformaldehyde dissolved in 100 mM sodium cacodylate, pH 7.4 buffer for 2 h at room temperature, the tissue was cut into small pieces with a razor blade and then cryoprotected, sectioned, and incubated with primary

antibodies (1:250 – 1:500 dilution) preincubated with or without immunogenic peptide (1:50-100) for 2 h at room temperature as described previously (7). After washing, the sections were incubated with a mixture of FITC-conjugated goat-anti rabbit secondary antibody (diluted 1:100), rhodamine-phalloidin (1:50), and Topro-3 (1:1000). The sections were washed with PBS, post fixed with 4% (w/v) paraformaldehyde, and mounted under coverslips using *p*-diaminobenzidine-containing mounting medium (7).

3.2.6 Scanning laser confocal analysis of fluorescently labeled cells

Imaging was performed on a TCS-SL confocal microscope equipped with argon and green and red helium-neon lasers (Leica, Dearfield, IL). Images were acquired by sequential scanning using a 100 × (1.4 numerical aperature) planapochromat oil objective and the appropriate filter combination. Settings were as follows: photomultipliers set to 600–800 V, 1 Airy disk, and Kalman filter ($n = 4$). Serial (z) sections were captured with a 0.25-μm step size. The images (512 × 512 pixels) were saved as TIFF files. The OpenLab program (Improvision, Lexington, MA) was used to project the serial sections into one image. The contrast level of the final images was adjusted in Photoshop, and the contrast-corrected images were imported into FreeHand.

3.2.7 Mounting of rabbit uroepithelium in ussing stretch chambers

Excised rabbit bladders were cut open longitudinally, then washed in Krebs solution and mounted on custom-made Teflon racks with the mucosal side down. The smooth muscle

layers were removed using sharp scissors and forceps. The remaining mucosal tissue, containing the uroepithelium, was mounted on plastic rings with a 2-cm^2 opening and then was sandwiched between two halves of a modified Ussing stretch chamber as described previously (18). Each hemichamber (mucosal and serosal) was filled with 12.5 ml of Krebs solution, the serosal hemichamber was bubbled with gas containing 5% (v/v) CO_2 and 95% (v/v) air, and the tissue was equilibrated for 30-60 min. In some experiments, the hydrostatic pressure in the mucosal hemichamber was increased as described previously (18).

3.2.8 Measurement of extracellular adenosine

Following mounting in Ussing stretch chambers and a 30-min period of equilibration, the tissue was isovolumetrically washed three times with 60 ml of Krebs solution. Following an additional 30-min incubation, hydrostatic pressure was increased as described above. Aliquots (1000 μl) were taken with replacement from the serosal and mucosal hemichambers at the designated time points (0, 5, 30, 60, and 120 min). Adenosine, AMP, and inosine were measured with an LCMS assay on a ThermoFinnigan LCQ mass spectrometer with electrospray ionization. To 60 μl of sample, 10 μl of 140 pg/ μl internal standard (9-β-D arabinofuranoside) were added, and 50 μl injected for analysis. Purines were resolved on a C-18 reverse phase column (Eclipse Zorbax XDB, 4.6 mm x 150 mm) with water/methanol 0.1% formic acid as the mobile phase at a flow rate of 0.5 ml/min. The mobile phase was held at 100% water for 1.5 min, changed to 90:10 water:methanol over 0.5 min and held at this composition for an additional 8 minutes.

The analytes were monitored using single ion monitoring: for AMP, mass-to-charge ratios (m/z) = 348; for adenosine and adenine 9-β-D arabinofuranoside (internal standard), m/z = 268; and for inosine, m/z = 291.

3.2.9 Capacitance measurements

Changes in capacitance primarily reflect changes in the apical cell surface area of the umbrella cells, where 1 $\mu F \approx 1\ cm^2$ of membrane area (18). Capacitance was measured as described previously (18).

3.2.10 Data Analysis

Non-linear regression analysis built into the Graphpad Prism program (San Diego, CA) was used to determine EC_{50} values for adenosine and adenosine agonists. Statistically significant differences between means were determined by Student's t test, or when multiple comparisons were made, significant differences were assessed using ANOVA with Bonferroni's correction.

3.3 RESULTS

3.3.1 Adenosine receptors are expressed in the uroepithelium

To determine the adenosine receptor expression profile in the uroepithelium, cell lysates of rat uroepithelium were probed with adenosine receptor specific antibodies. Rat tissue was used as rats are readily accessible and the currently available antibodies are all rabbit in origin. Western blot analysis revealed that all four adenosine receptors were present in uroepithelium (Fig. 3.1). As previously reported (160, 161), a predominant molecular mass species of ~ 38 kDa was detected using an anti-A_1 receptor antibody (Fig. 3.1A), which is close to the calculated molecular mass of the A_1 receptor (36.5 kDa). Two protein species were detected using an A2a receptor antibody (Fig. 3.1B). The larger molecular mass species coincided with the reported molecular mass of the protein (44.7 kDa), while the other smaller molecular mass species (~ 38 kDa), was reported previously and may represent proteolytic processing of the larger precursor (160, 162, 163). The A_{2b} receptor antibody recognized a single molecular weight species of 52 kDa, which is greater than the calculated mass of 36.3 kDa (Fig. 3.1C), but is identical to the reported mass of A_{2b} receptors detected in bovine corneal endothelium and kidney vasculature (160, 161). The A_3 specific antibody detected a protein species of 52 kDa,

consistent with previous reports (160), and a species of 36.2 kDa, the nominal molecular mass of the protein (Fig. 3.1D). The signals for each antibody reaction were significantly attenuated in the presence of antigenic peptide, confirming the specificity of the reactions. Taken together, these results indicate that all four adenosine receptor species are expressed in the uroepithelium.

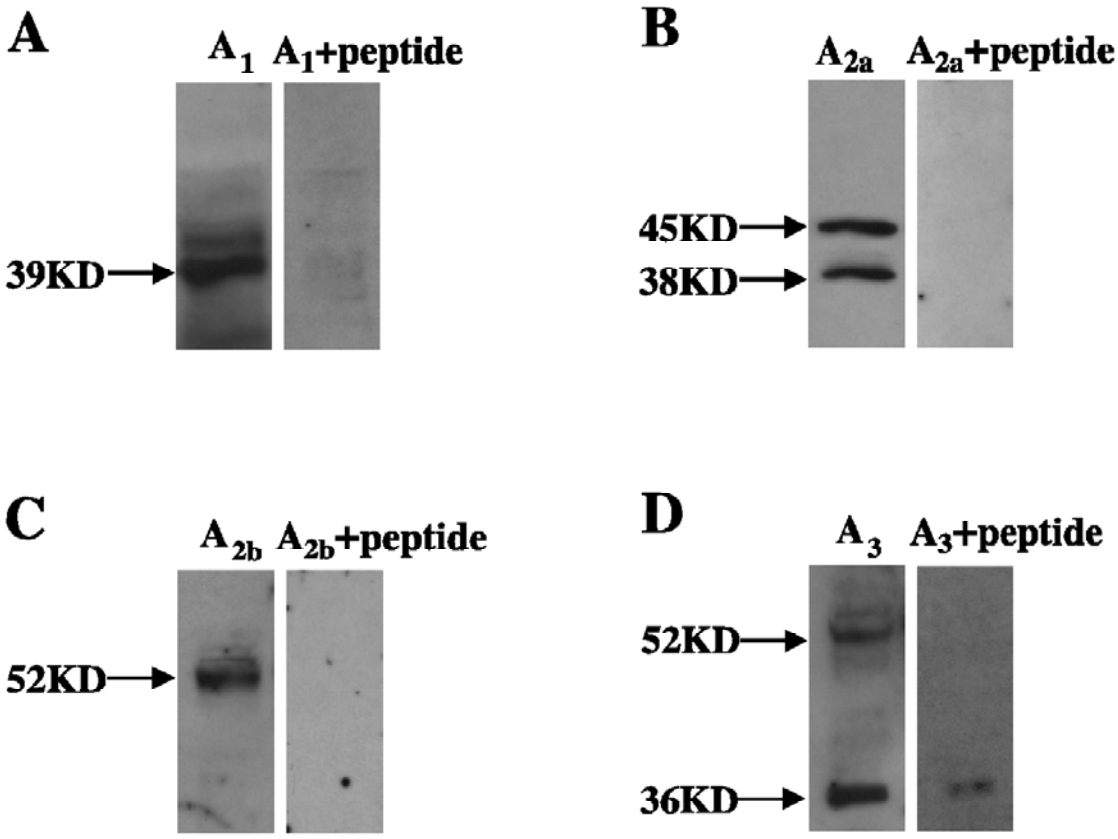

Figure 3.1. Expression of adenosine receptors in rat uroepithelium

Lysates of rat uroepithelium were resolved by SDS-PAGE and western blots were probed with antibodies specific for A_1 (**A**), A_{2a} (**B**), A_{2b} (**C**), or A_3 (**D**) receptors (± antigenic peptide). The nominal mass for each receptor is shown to the right of each

panel, and the major protein species detected in rat uroepithelial lysates are marked to the left of each panel.

3.3.2 Adenosine receptors show a polarized distribution in the uroepithelium

The uroepithelium is stratified, and the outermost umbrella cells have distinct apical and basolateral plasma membrane domains. To confirm the expression of adenosine receptors in the uroepithelium and to analyze the cellular distribution of these receptors, we immunolabeled cryosections of frozen rat bladder tissue using adenosine receptor-specific antibodies. The tissue was stained with rhodamine-phalloidin to define the regions of cell-cell contact in the different cell layers and to identify the apicolateral junctional complex in the umbrella cell layer (164). Topro-3 was used to label cell nuclei.

Consistent with the western blot analysis, all four adenosine receptors were localized within the uroepithelium (Fig. 3.2). The A_1 receptor antibody strongly labeled the apical plasma membrane of umbrella cells. In contrast, less staining was observed along the basolateral plasma membrane of the umbrella cell layer, and there was little staining of the underlying intermediate and basal cell layers (Fig. 3.2A). Signal for the A_1 receptor was also observed in the underlying submucosal connective tissue (data not shown). The A_{2a} receptor antibody labeled the cytoplasm of all three types of uroepithelial cells, and also strongly labeled a layer of tissue elements below the epithelium, possibly connective tissue cells, myofibroblasts, or blood vessels (Fig. 3.2B). By immunofluorescence it was difficult to tell if A_{2a} was localized to the plasma

membrane. The A_{2b} receptor antibody stained the apical cytoplasm and the basolateral plasma membrane of the umbrella cells, and also appeared to label the cytoplasm of the intermediate/basal cells (Fig. 3.2C). Consistent with previous reports of A_{2b} gene expression in the detrusor muscle (150), intense A_{2b} receptor staining was also observed in bladder smooth muscle tissue (data not shown). The A_3 receptor antibody specifically labeled the basolateral plasma membrane of umbrella cells and the plasma membranes of the underlying epithelial cell layers (Fig. 3.2D). Staining of the submucosa or detrusor muscle was not observed. In all cases, antibody signal for all 4 receptors was blocked upon addition of the immunogenic peptide (data not shown). A similar distribution of adenosine receptors was observed in mouse uroepithelium (data not shown).

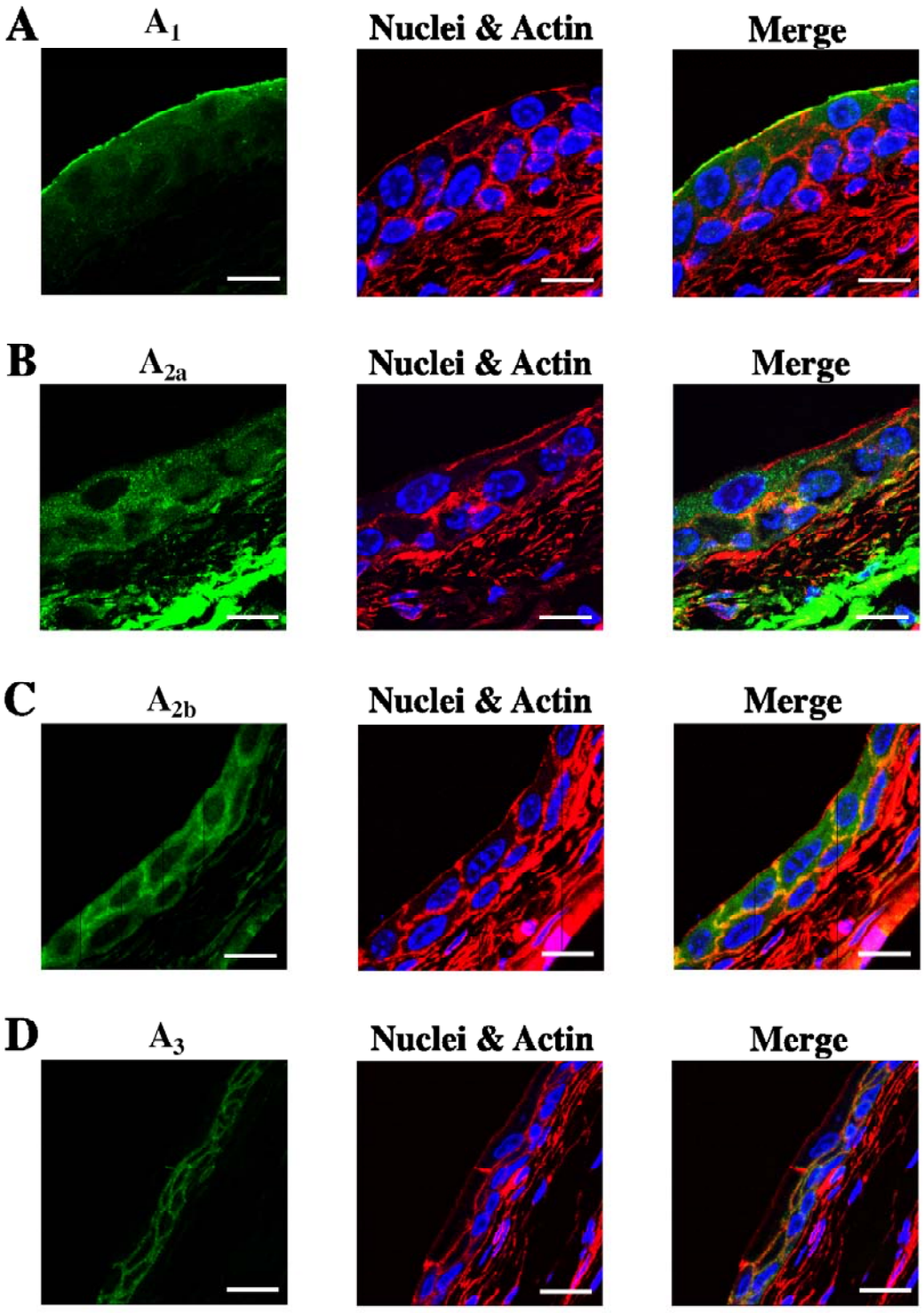

Figure 3.2. Localization of adenosine receptors in rat uroepithelium

Cryosections of rat bladder tissue were labeled with antibodies to A_1 (**A**), A_{2a} (**B**), A_{2b} (**C**), or A_3 (**D**) receptors (green), rhodamine phalloidin to label the actin cytoskeleton (red) and Topro-3 to label nuclei (blue). A merged panel is shown at the right. Bar = 10 μm.

3.3.3 The uroepithelium is a site of adenosine biosynthesis

High concentrations of adenosine have been reported in urine (165, 166); however, it is unknown whether the uroepithelium produces adenosine and contributes to this pool. The uroepithelium was mounted in Ussing stretch chambers and following extensive washing was incubated in the presence of 100 nM iodotubericidin, an inhibitor of adenosine kinase, and 10 μM EHNA, an inhibitor of adenosine deaminase. The mucosal hemichamber of the Ussing stretch chamber is a closed system and can be filled with additional buffer, which increases the hydrostatic pressure, bows the uroepithelium, and simulates bladder filling (18). Buffer samples were taken from the mucosal and serosal hemichambers (± pressure), and mass spectroscopy analysis was used to measure the concentration of adenosine, AMP, and inosine in the fluid. In the absence of pressure, adenosine was found at low concentrations in the mucosal hemichamber, and increased over time in the serosal hemichamber (Fig. 3.3A). The addition of pressure resulted in a significant rise in the concentration of adenosine found in the mucosal and serosal hemichambers (Fig. 3.3A). The highest concentrations of adenosine were recorded at the serosal surface of the tissue with concentrations approaching 200 nM. In the absence of pressure, AMP and inosine concentrations in the mucosal hemichamber remained

relatively low. However, AMP and inosine concentrations at this surface rose significantly in tissue exposed to pressure (Fig. 3.3B-C). Little AMP was observed in the serosal hemichamber either in the absence or presence of pressure (Fig. 3.3B). With time the concentration of inosine increased in the serosal hemichamber, but pressure had no significant effect on serosal release (Fig. 3.3C).

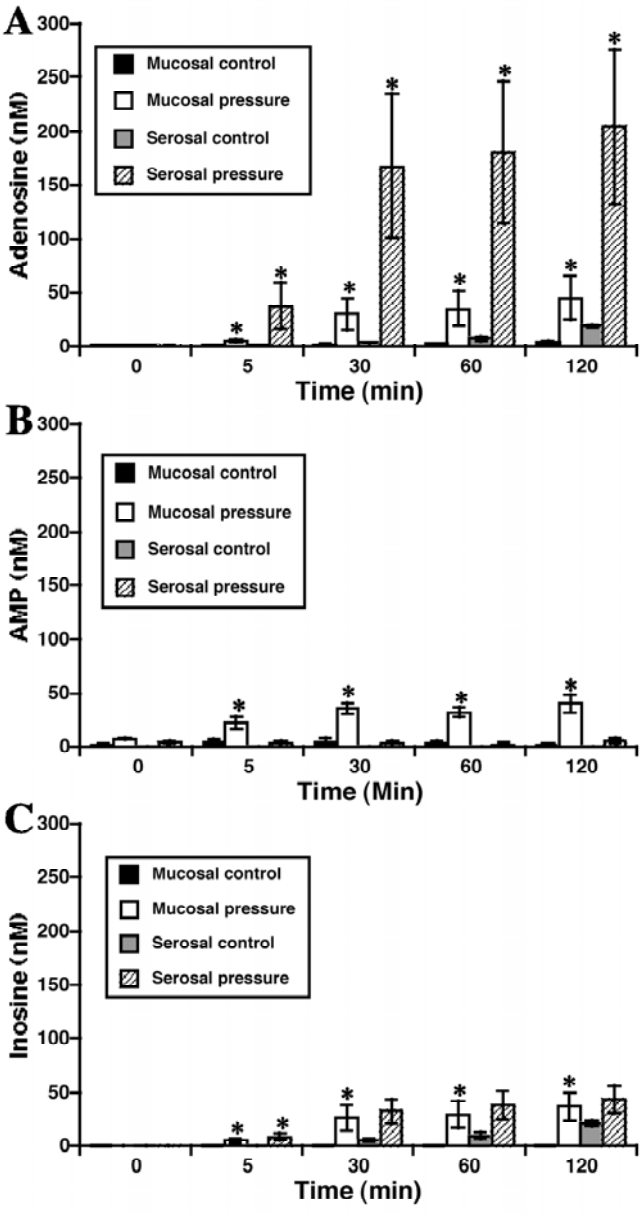

Figure 3.3. Production of adenosine, AMP, and inosine by uroepithelium

Rabbit uroepithelium was mounted in Ussing stretch chambers and then incubated in the presence or absence of pressure. At the indicated time points samples were taken from the mucosal or serosal hemichamber and the concentration of adenosine (**A**), AMP (**B**), or inosine (**C**) was measured. Data are mean ± SEM (n = 4). Statistically significant differences ($p < 0.05$), relative to untreated control tissue, are marked with an asterisk.

3.3.4 Adenosine stimulates umbrella cells exocytosis

An important role of all epithelial cells, including umbrella cells, is to regulate the composition and size of their apical membrane domains, a function that depends on exocytosis and endocytosis. We determined if adenosine regulated exocytosis in the umbrella cells by monitoring changes in membrane capacitance (where 1 μF of capacitance ≈ 1 cm^2 of tissue area). In isolated rabbit uroepithelium, capacitance primarily reflects the apical plasma membrane surface area of the umbrella cell layer (18), and increased capacitance correlates well with other measures of exocytosis (7). In control tissue, not exposed to adenosine, no change in capacitance was observed after 5 h (Fig. 3.4). However, addition of 1 μM adenosine to either the mucosal or serosal hermichamber resulted in an increase in membrane capacitance (Fig. 3.4A-B). The increase in capacitance was linear over 5 h with a change of ~ 30% observed when added to the serosal hemichamber (Fig. 3.4A), and a change of ~ 24% when added to the mucosal hemichamber (Fig. 3.4B). The EC_{50} for adenosine-induced changes in capacitance was similar for both serosal and mucosal surfaces of the tissue, 0.17 μM and 0.14 μM respectively.

In control experiments, 0.03 U/ml deaminase, an enzyme that converts adenosine into inosine, was added in conjunction with adenosine to either hemichamber to confirm that the changes in capacitance were dependent on adenosine and not its byproduct inosine. In the presence of deaminase, 1 μM adenosine had no significant effect on tissue capacitance (Fig. 3.4A-B). We also treated tissue with brefeldin A (BFA), an inhibitor of secretion (i.e. exocytosis) in many cell types including umbrella cells (7). BFA treatment inhibited increases in capacitance that occurred upon addition of adenosine to the mucosal hemichamber (Fig. 3.4B). A significant decrease in capacitance was noted when adenosine was added to the serosal surface of BFA-treated tissue (Fig. 3.4A), possibly indicating a shift toward endocytosis under these conditions.

In summary, the above results indicate that the uroepithelium is responsive to adenosine, and that adenosine may increase exocytosis in the uroepithelium.

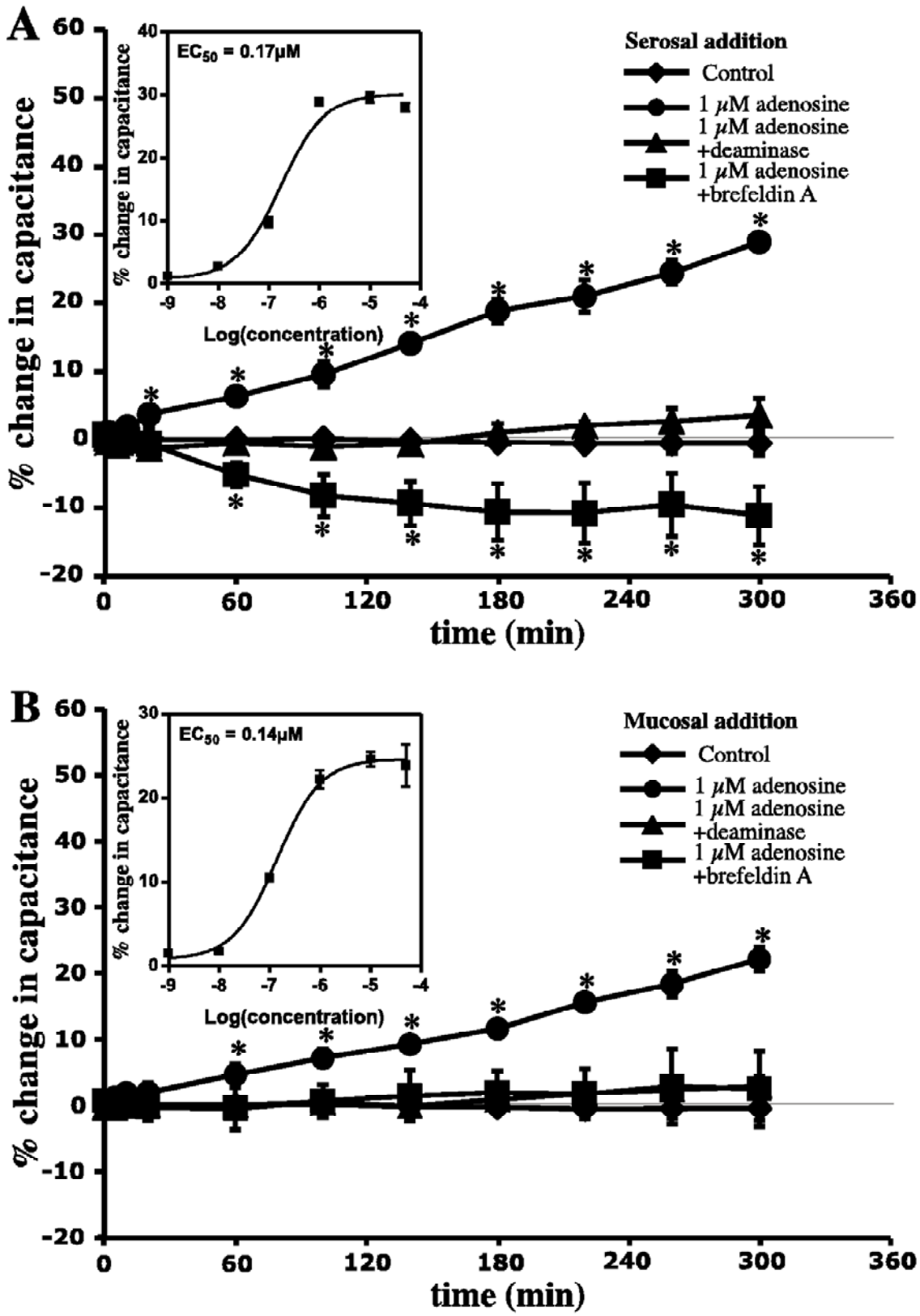

Figure 3.4. Stimulation of capacitance by adenosine

Rabbit uroepithelium was mounted in Ussing stretch chambers and incubated in the absence of pressure. Adenosine (1 μM) alone, a mixture of 1 μM adenosine and 0.03 U/ml deaminase, or a mixture of 1 μM adenosine and 10 μg/ml BFA was added to the serosal (**A**) or mucosal (**B**) hemichamber and capacitance was recorded. Control reactions were not exposed to adenosine. The inset shows a dose-response curve for the change in capacitance recorded 300 min after the addition of the specified concentration of adenosine. Data are mean ± SEM ($n \geq 4$) and statistically significant differences ($p < 0.05$) relative to control reactions are marked with an asterisk.

3.3.5 Multiple adenosine receptors may modulate umbrella cells exocytosis

To assess which adenosine receptors were responsible for the changes in capacitance described above, we measured the ability of the following adenosine receptor selective agonists to induce changes in membrane capacitance: the A_1-selective agonist CCPA (A_1 K_D ~ 0.2-1.3 nM), the A_{2a}-selective agonist CGS21680 (A_{2a} K_D ~ 25 nM), and the A_3-selective receptor agonist Cl-IB-MECA (A_3 K_D ~ 1-10 nM) (144). At present, no A_{2b}-selective agonists are available. Consistent with the immunofluoresence analysis presented above, the A_1-selective agonist CCPA caused the most marked increase in capacitance upon mucosal addition (~ 40%) with an EC_{50} of ~ 3 nM (Fig. 3.5A), a value similar to the reported K_D (~ 1 nM) this agonist has for A_1 receptors (144). The A_{2a}-selective agonist CGS21680 induced an ~ 10% change in capacitance with and EC_{50} of ~ 30 nM. Again, the observed EC_{50} was close to the reported K_D (~ 25 nM) reported for A_{2a} receptors (Fig. 3.5B) (144). The A_3-selective agonist Cl-IB-MECA was the least potent

agonist with an EC_{50} value of ~ 700 nM, which is significantly larger than the reported K_D (~ 1-10 nM) (144). Cl-IB-MECA treatment resulted in an ~ 10% capacitance change when added to the mucosal hemichamber (Fig. 3.5C).

CCPA also stimulated changes in capacitance when added to the serosal hemichamber, and was 10 times more potent at this surface than the mucosal surface (EC_{50} of ~ 0.3 nM at the serosal surface versus ~ 3.0 nM at the mucosal surface) (Fig. 3.5D). However the maximal change in capacitance was less than that observed upon mucosal addition (~ 20 % vs ~ 40%). The most effective serosal agonist was CGS21680, which caused an ~ 30% change in capacitance with an EC_{50} of ~ 35 nM (Fig. 3.5E). Cl-IB-MECA treatment resulted in a maximal ~ 25% change in capacitance with an EC_{50} of ~ 190 nM (Fig. 3.5F). Again, the measured EC_{50} for CCPA and CGS21680 approximated the measured K_D of these agonists for A_1/A_{2a} receptors, while the EC_{50} for Cl-IB-MECA was significantly greater than the reported K_D for this agonist and A_3 receptors.

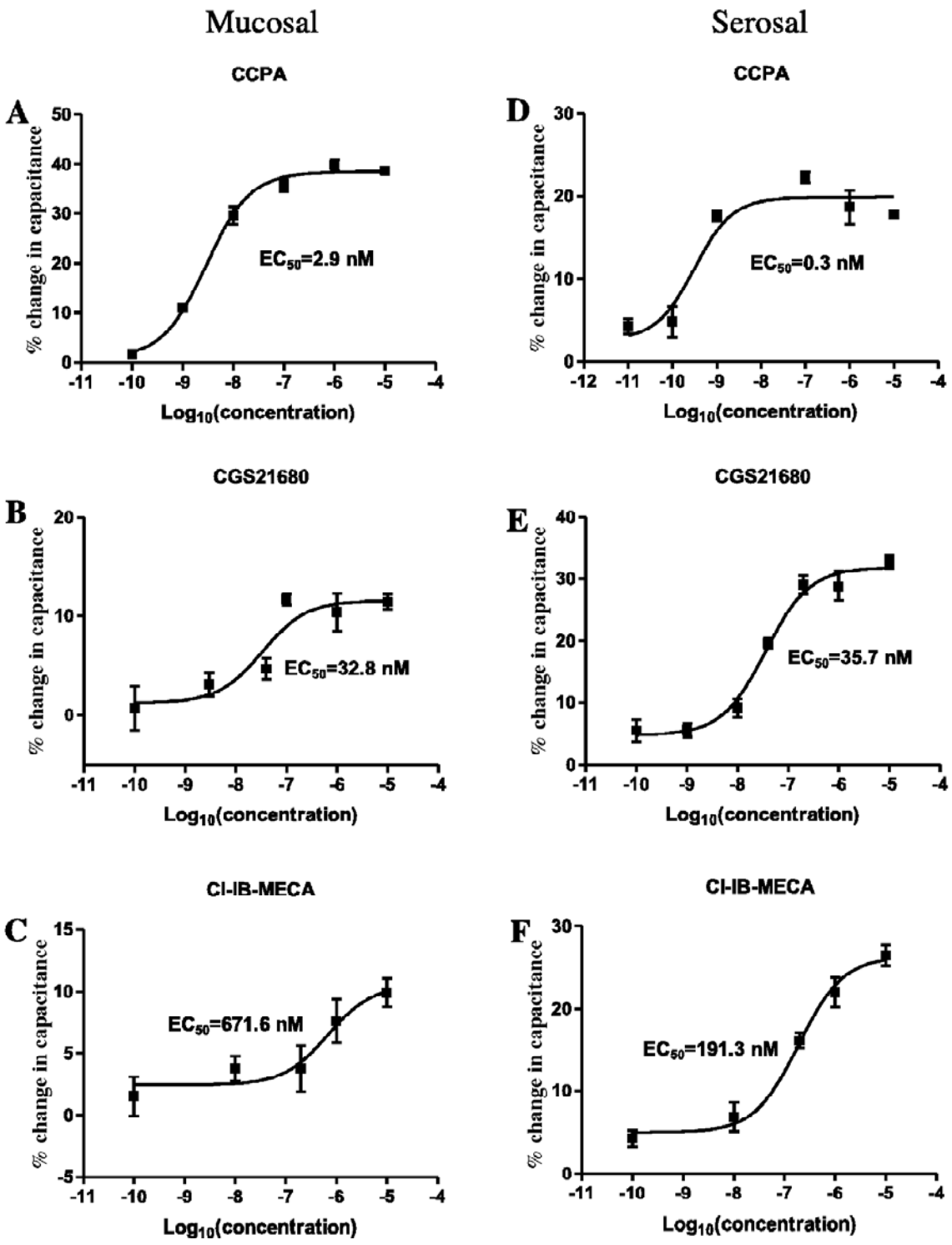

Figure 3.5. Effect of adenosine receptor agonists on capacitance

Rabbit uroepithelium, mounted in Ussing stretch chambers in the absence of pressure, were exposed to the A_1-selective agonist CCPA added to the mucosal (**A**) or serosal (**D**) hemichambers, the A_{2a}-selective agonist CGS21680 added to the mucosal (**B**) or serosal (**E**) hemichambers, or the A_3-selective agonist Cl-IB-MECA added to the mucosal (**C**) or serosal (**F**) hemichambers. The capacitance was recorded 300 min after the addition of the specified concentration of agonist. Data are mean ± SEM (n ≥ 3).

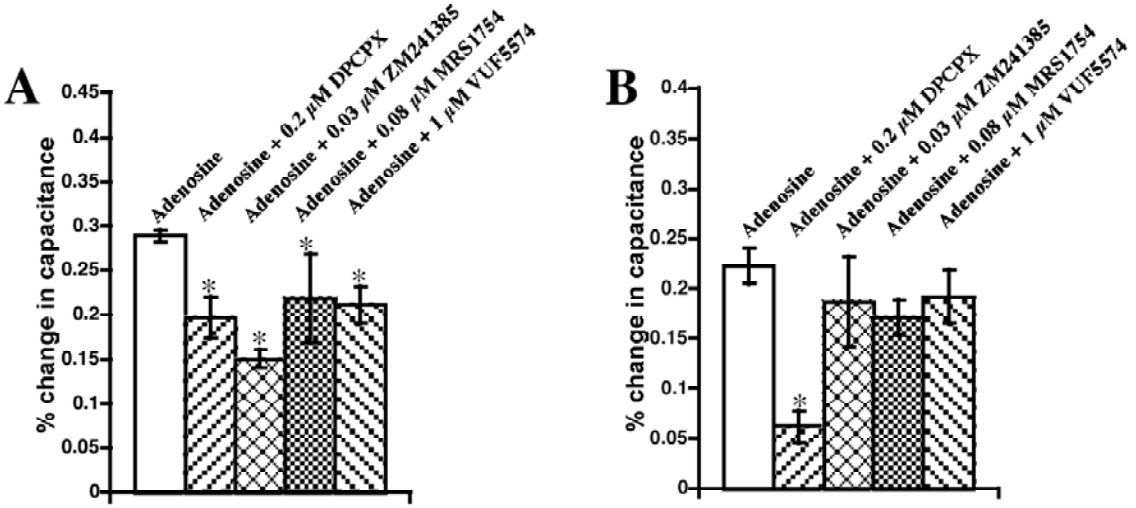

Figure 3.6. Inhibition of adenosine-stimulated capacitance changes by adenosine receptor antagonists

Rabbit uroepithelium, mounted in Ussing stretch chambers in the absence of pressure, was pretreated with the A_1-selective antagonist DPCPX (0.2 μM), the A_{2a}-selective antagonist ZM241385 (0.03 μM), the A_{2b}-selective antagonist MRS1754 (0.08 μM), or the A_3-selective antagonist VUF5574 (1.0 μM) for 15 min. Adenosine (1 μM) was added to the serosal (**A**) or mucosal (**B**) hemichambers and the percent change in capacitance was recorded 5 h later. Data are mean ± SEM (n ≥ 3). Statistically significant differences ($p < 0.05$) relative to adenosine alone are marked with an asterisk.

To further define the receptor subtypes responsible for the adenosine-dependent changes in capacitance, specific adenosine receptor antagonists were added in combination with adenosine (1 μM) to either the serosal or mucosal hemichamber. The receptor-selective antagonists used were: DPCPX (A_1 selective; K_i = 0.3-4.0 nM), ZM241385 (A_{2a} selective; K_i = ~ 0.5 nM), MRS1754 (A_{2b} selective; K_i = 2.0 nM), and VUF5574 (A_3 selective; K_i = 4.0 nM) (144, 167). The Gaddum equation was used to calculate the concentration of antagonist that would ideally give a ≥ 90% reduction in adenosine-induced changes in capacitance. The most effective antagonist, when added in combination with adenosine at the serosal surface, was the A_{2a}-selective agonist ZM241385, which inhibited adenosine-induced changes in capacitance by ~ 50% (Fig. 3.6A). DPCPX, MRS1754, and VUF557 also significantly decreased adenosine-induced changes in membrane capacitance by ~ 25%. While mucosal addition of ZM241385, MRS1754, and VUF5574 did not significantly inhibit adenosine-induced changes in capacitance at the 5-h time point (Fig. 3.6B), the A_1 receptor-selective antagonist DPCPX significantly decreased adenosine-induced effects by ~ 80% (Fig 3.6B).

On the whole, the agonist/antagonist studies indicated that the activity of A_1 receptors may predominate at the mucosal surface with some contribution from A_{2A} receptors. In contrast A_{2A} receptors may predominate at the serosal surface with a significant contribution by A_1 and possibly A_{2b} and A_3 receptors.

3.3.6 Stretched-induced changes in capacitance are modulated by, but do not require adenosine

We have previously shown that the stretch associated with bladder filling is a physiologically relevant stimulus for exocytosis in the umbrella cell layer, and that ATP release is an important upstream signal in this process (7, 108). Whether other upstream stimuli modulate stretch-induced membrane turnover in the umbrella cells is unknown. We exposed isolated uroepithelium to increased hydrostatic pressure in the presence or absence of 1 μM CGS15943, a broad-spectrum adenosine receptor antagonist (144). Increased pressure stimulated changes in capacitance of ~ 50% (Fig. 3.7A). However, treatment with CGS15943 had no significant effect on pressure-induced capacitance changes. Nor was any significant effect noted when the receptor selective agonists DPCPX, ZM241385, MRS1754, and VUF5574 were tested (Fig. 3.7A). Furthermore, deaminase had no significant effect on capacitance when added during the pressure stimulus (Fig. 3.7B). Intriguingly, when adenosine (1μM) was added to either the serosal or mucosal surface of tissue exposed to increased pressure, it significantly potentiated both the kinetics of the resulting capacitance change, and the plateau levels after 5 h incubation (Fig. 3.7C). These data indicate that although adenosine signaling is not required for pressure-induced changes in capacitance, adenosine may act to modulate the rate and the extent of these surface area changes.

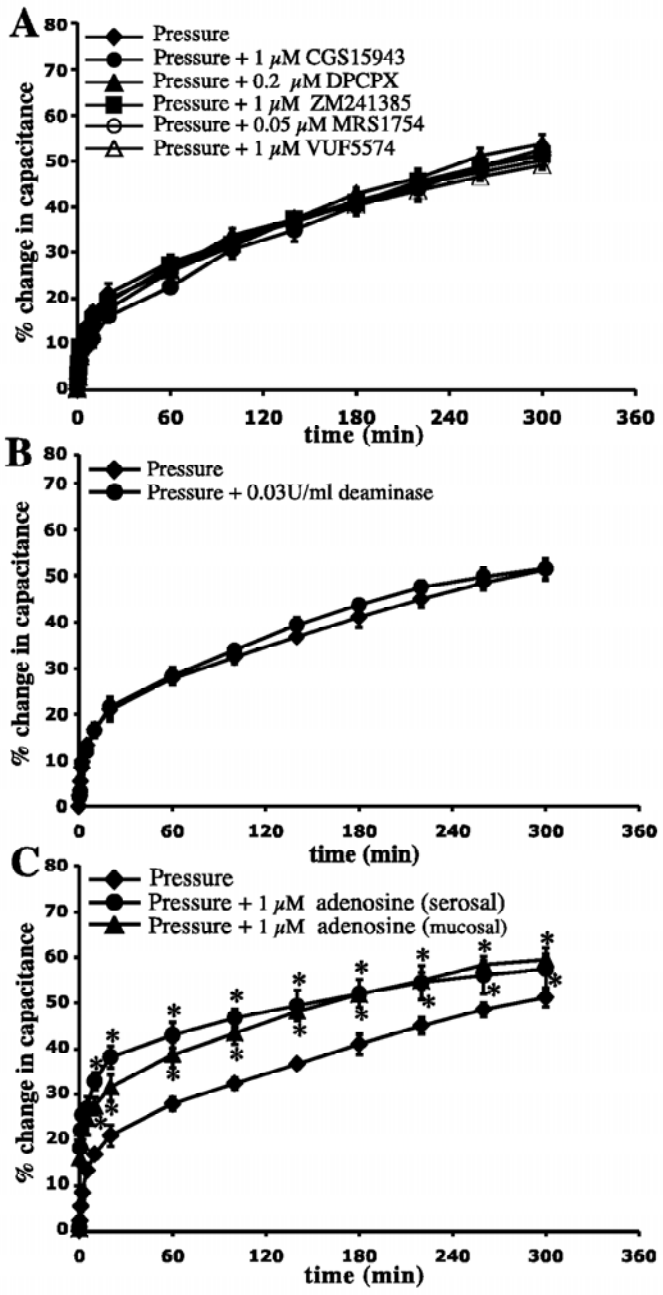

Figure 3.7. Effect of adenosine receptor antagonists, deaminase, and adenosine on pressure-induced changes in capacitance

Rabbit uroepithelium was mounted in Ussing stretch chambers, exposed to increased pressure, and the capacitance recorded. (**A**) The indicated adenosine receptor antagonist was added to both hemichambers for 15-min prior to increasing hydrostatic pressure at t=0. (**B**) Pressure was increased across the mucosal surface of the tissue (± deaminase) at t=0. (**C**) Tissue was exposed to increased pressure in the presence of 1μM adenosine added to the mucosal or serosal hemichamber of the tissue. Data are mean ± SEM ($n \geq 4$). Statistically significant differences ($p < 0.05$) relative to pressure alone are marked with an asterisk.

3.3.7 Ca^{2+} is essential for adenosine-modulated umbrella cell exocytosis

Elevated intracellular Ca^{2+} is a well-characterized stimulus for exocytosis in many cell types, including umbrella cells (18). Adenosine is known to increase free Ca^{2+} though a PLC/IP_3 pathway (146, 148), and we observed that 10 μM U73122, a PLC inhibitor, significantly impaired adenosine-induced increases in capacitance (Fig. 3.8A-B). Consistent with a role for PLC/IP_3 in this process, we observed that 2.5 μM xestospongin C, a marine toxin that inhibits IP_3-dependent Ca^{2+} release (168), also significantly decreased adenosine-mediated increases in capacitance (Fig. 3.8C), as did 75 μM 2-APB (Fig. 3.8C), an additional IP_3 receptor antagonist (169). Intriguingly, in the presence of 2-APB there was a consistent decrease in capacitance of ~ 10% after 5 h (Fig. 3.8C), indicating that under these conditions agonists shifted the equilibrium between exocytosis and endocytosis, so that the latter predominated. We also observed a potential role for extracellular Ca^{2+} in this process. When tissue was incubated in nominally Ca^{2+}-free

Krebs buffer, the adenosine-induced capacitance changes in capacitance were completely inhibited (Fig. 3.8D-E). However, if Ca^{2+} was added back to the Ca^{2+}-free Krebs solution after 4 h, there was a rapid increase in capacitance during the subsequent 1 h, indicating that the inhibition observed in Ca^{2+}-free medium was rapidly reversible. In summary, both intracellular and extracellular Ca^{2+} may be essential for adenosine receptor-modulated umbrella cell exocytosis.

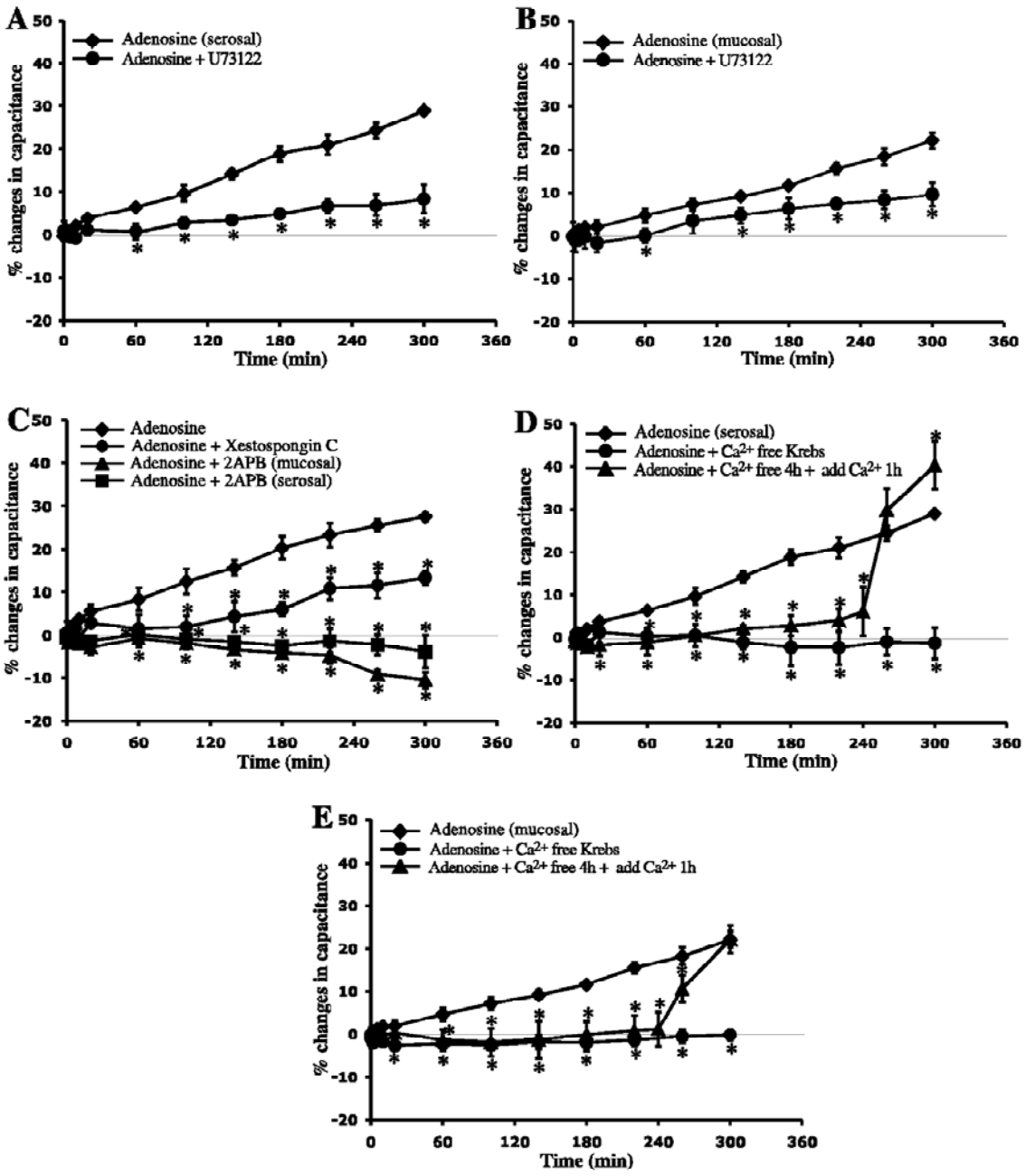

Figure 3.8. Role of Ca^{2+} in adenosine-induced changes in capacitance

Adenosine was added to the serosal (**A**) or mucosal (**B**) hemichamber in the presence or absence of 10 μM U73112 and the change of capacitance was recorded for 5 h. (**C**) Adenosine (1 μM) was added to the mucosal and serosal surfaces of the tissue in the absence (control) or presence of 2.5 μM xestospongin C. Alternatively, adenosine was

added to the mucosal or serosal hemichamber in the presence of 75 μM 2-APB. (**D**-**E**) Adenosine was added to the serosal (**D**) or mucosal (**E**) hemichamber of tissue incubated in normal Krebs solution, or Ca^{2+}-free Krebs solution. Alternatively, 2 mM Ca^{2+} was added to the Ca^{2+}-free Krebs solution after 4 h of incubation. Capacitance was recorded at the indicated time points. Data are mean ± SEM ($n \geq 4$). Statistically significant differences ($p < 0.05$) relative to adenosine alone are marked with an asterisk.

3.4 DISCUSSION

Adenosine plays an important role in regulating a variety of normal cellular functions in the urinary tract including release of renin, tubuloglomerular feedback, renal medullary blood flow, and renal tubular transport (144-146). However, little is known about the function of adenosine in the uroepithelium. Our analysis indicates that the uroepithelium is an important site of adenosine biosynthesis and adenosine receptor expression, and that adenosine may function as an autocrine/paracrine regulator of exocytosis in the umbrella cell layer.

3.4.1 Adenosine biosynthesis occurs in the uroepithelium

Although adenosine is found in the urine (at concentrations of ~ 1 μM) (165, 166), it was unknown if the bladder mucosa contributes to the pool of urinary adenosine. Our data indicates that adenosine may be produced in significant quantities by the uroepithelium. We observed adenosine biosynthesis under baseline conditions, which significantly increased in response to stretch. Under the latter condition, maximum concentrations of adenosine in the mucosal chamber approached ~ 50 nM, while in the serosal chamber they approached ~ 200 nM. The actual concentration of adenosine near the uroepithelial cell membranes is difficult to discern because of the relatively large volume of our

chamber system, unstirred layer effects, and the action of nucleoside transporters that may have caused us to underestimate adenosine biosynthesis at either or both tissue surfaces. While our results indicate that the epithelium is the primary source of adenosine, there are scattered endothelial cells, fibroblasts, immune cells, and smooth muscle cells in the connective tissue underlying the epithelium that may contribute to the serosal adenosine release *in vivo*.

The mechanism of adenosine biosynthesis in the uroepithelium is unknown. While the role of nucleoside transporters cannot be ruled out, it seems unlikely that hydrolysis of ATP by ecto/exo-nucleotidases plays a major role. We have previously shown that increased pressure stimulates ATP release from both surfaces of the uroepithelium, but mucosal release is 50-fold greater than serosal release (108). In contrast, we found that the majority of adenosine biosynthesis occurred at the serosal surface of pressure-treated tissue. Increased pressure stimulated inosine biosynthesis at both cell surfaces, but the mechanism of inosine biosynthesis is not clear as the experiments were performed in the presence of the adenosine deaminase inhibitor EHNA. It is possible that the inhibitory activity of EHNA was not complete, or that inosine was produced by some other mechanism, e.g. release from nucleotide transporters at the cell surface. Pressure also stimulated the biosynthesis of AMP at the mucosal surface of the tissue, possibly via the extracellular-cAMP-adenosine pathway (147). In this pathway, cAMP that is produced in response to adenlyl cyclase activation is released by the cell and converted to adenosine by the serial action of ectophosphodiesterase (cAMP to AMP) and ecto-5'-nucleotidase (AMP to adenosine). Interestingly, cAMP production is rapidly increased within the uroepithelium in response to increased hydrostatic pressure, and cAMP is an important

second messenger that stimulates exocytosis in the umbrella cell (7). Future experiments will define whether pressure stimulates release of cAMP into the extracellular fluid of umbrella cells and whether the extracellular-cAMP-adenosine pathway contributes to AMP or adenosine biosynthesis by the uroepithelium.

3.4.2 The uroepithelium expresses multiple adenosine receptors

Gene expression of all four adenosine receptors has been described previously in the bladder (149), but the distribution of these receptors was unexplored until this analysis. A_1 receptors were expressed at the apical pole of the umbrella cells, and to a lesser extent at the basolateral surface of the umbrella cell and in the connective tissue underlying the uroepithelium. As noted below, functional A_1 receptors may also be present on the serosal surface of the uroepithelium. Studies in cat indicate that A_1 receptors may also be present on the detrusor muscle (156). While we did not observe significant staining for A_1 receptors in the muscle tissue of rat or mice bladders (our unpublished observations), we can not rule out that other antibodies may give different staining patterns, or that the distribution of A_1 receptors is different in cat bladders.

In a similar fashion, functional A_{2a} receptors have been detected on guinea pig detrusor (73), but our analysis indicated that A_{2a} receptors were found predominantly on the uroepithelium and the underlying connective tissue elements, but not the detrusor muscle. Again, this could reflect the antibodies used in this analysis and/or species differences. We observed significant A_{2b} receptor expression along the basolateral surface of the umbrella cells, and consistent with previous Northern blot analysis (150),

we observed significant A_{2b} protein expression in the detrusor muscle. Surprisingly, there is no data implicating A_{2b} receptors in bladder detrusor function. A_3 receptors were predominantly expressed along the umbrella cell basolateral membrane, and to a lesser extent in the subepithelial connective tissue. The apical distribution of A_1 receptors, the cytoplasmic distribution of A_{2a} receptors, and the basolateral distribution of A_{2b} and A_3 receptors we observed in the umbrella cell is consistent with previous reports that A_1 receptors are found on the apical surface of polarized Madin-Darby canine kidney cells, and the other receptors are found intracellularly or at the basolateral surface of these cells (170).

3.4.3 Regulation of exocytosis in the uroepithelium by adenosine

Other than a small number of studies implicating adenosine receptor signaling in detrusor muscle contraction and innervation (73, 151, 153, 154, 156), little else is known about the function of adenosine in the bladder. By monitoring changes in capacitance we observed that adenosine, as well as adenosine receptor agonists, all stimulated exocytosis in the umbrella cell layer.

Consistent with the apical distribution of A_1 receptors on the apical surface of the umbrella cell layer, the A_1-selective agonist CCPA was the most potent stimulator of exocytosis when added to the mucosal surface of the tissue (EC_{50} = ~ 3 nM). Furthermore, the A_1-selective antagonist DPCPX was most effective at inhibiting adenosine-induced capacitance changes when added to the mucosal surface of the tissue. We also observed that the A_{2a}-selective agonist CGS21680 stimulated modest changes in

capacitance (~ 10%) with an EC_{50} of ~ 30 nM, consistent with the reported K_D for this receptor agonist (144), and the A_{2a}-selective antagonist ZM241385 inhibited adenosine-induced changes in capacitance at early time points. The lack of A_3 receptor expression at the apical surface of the umbrella cells, the very high EC_{50} measured for the A_3-selective agonist Cl-IB-MECA (~ 700 nM), several hundred-fold higher than the reported K_D for this agonist (~ 1-10 nM)(144), and the lack of effect of VUF5574 makes it unlikely that A_3 receptors play a significant role in modulating exocytosis at the apical surface of the umbrella cells. Overall, the data indicate that A_1 receptors are the predominant regulators of exocytosis at the mucosal surface, and that A_{2a} receptors may play a lesser role.

The most effective serosal agonist was the A_{2a}-selective agonist CGS21680, which caused an ~ 30% change in capacitance. Furthermore, ZM241385 was the most effective inhibitor of adenosine-induced capacitance at the serosal surface of the tissue. Surprisingly, the A_1-selective agonist CCPA was the most potent agonist with an EC_{50} of 0.3 nM. However the maximal change in capacitance was less than that observed upon mucosal addition (~ 20 % vs ~ 40%) and CCPA was less effective than CGS21680 at promoting capacitance changes. One possibility is that there are smaller numbers of A_1 receptors on the serosal surface of the tissue, which would explain why they were not readily detectable by immunofluorescence and why they are less effective at stimulating exocytosis at the serosal surface of the tissue. The A_{2b}-selective antagonist MRS1754 caused a significant inhibition of adenosine-induced capacitance changes at the serosal surface, implicating this receptor in adenosine-mediated regulation of exocytosis. A_3-selective agonist Cl-IB-MECA caused an ~ 25% change in capacitance. However, the EC_{50} value for Cl-IB-MECA was significantly higher than the reported K_D (~ 200 nM vs

1-10 nM)(144), possibly indicating that A_3 receptors are not effective transducers of adenosine-mediated changes in exocytosis. The functional role of A_3 receptors in the uroepithelium remains to be defined. In summary, A_{2a} receptors are the major contributors to adenosine-induced changes in exocytosis at the serosal surface of tissue, with a lesser input from A_1 and possibly A_{2b} receptors.

An important issue is the apparent discrepancy between the measured K_D of A_1 receptors for adenosine (~ 10 nM) in rat cortical membranes (171), and the EC_{50} of ~ 140 nM we measured when adenosine was added to the mucosal surface of the uroepithelial tissue. One possibility is that there are multiple adenosine receptors active at the mucosal surface that give an aggregate response that is greater than the K_D of an individual receptor. This is possible because both A_1- and A_{2a}-selective agonists gave responses when added to the mucosal surface. An alternative possibility is that the K_D for rabbit A_1 receptors is different than the rat receptor. In fact, there are known species differences in agonist affinity (144). An additional possibility is that adenosine turnover may decrease the effective concentration of the agonist in the bath. Although A_1 receptors are resistant to downregulation, the high concentrations of adenosine in extracellular fluids (in the 50 – 200 nM range) and urine (165, 166), would likely lead to chronic activation and/or desensitization/downregulation of the A_1 receptors unless significant adenosine turnover occurred in the tissue. Although the other receptors have lower affinities for adenosine, a similar requirement for adenosine turnover may exist.

Although A_1/A_3 receptors and A_{2a}/ A_{2b} receptors often have opposing effects on cellular function (e.g. generation of cAMP), activation of either A_1, A_{2a}, or A_3 receptors in the uroepithelium resulted in increased capacitance, indicating that a common

secondary messenger cascade acted downstream of receptor activation to regulate exocytosis. All four receptors are known to couple to PLC, which generates IP_3 and can result in increased cytoplasmic Ca^{2+} (144, 146). Consistent with this mechanism we observed that inhibitors of PLC or IP_3-receptor dependent Ca^{2+} release pathways blocked adenosine-induced exocytosis. However, our data indicate that extracellular Ca^{2+} may also play a role, as incubation in Ca^{2+}-free Krebs solution inhibited adenosine-induced exocytosis. Although adenosine is generally thought to inhibit voltage-sensitive channels in many tissues (144), in the uroepithelium adenosine could act to depolarize the cell, activating voltage sensitive Ca^{2+} channels, which, in turn, would result in Ca^{2+}-dependent Ca^{2+} release. Alternatively, depletion of Ca^{2+} from intracellular stores could active Ca^{2+} influx via plasma membrane-associated store-operated channels, a pathway commonly found in non-excitable cells that couples PLC/IP_3 pathways to influx of extracellular Ca^{2+} (172).

We also assessed whether adenosine played a role in the pressure-induced changes in exocytosis we measured previously (7, 18, 19). Although the uroepithelial tissue is responsive to low concentrations of adenosine and its agonists, and the tissue can produce adenosine (especially in the presence of hydrostatic pressure), adenosine did not seem to be important for the basal levels of pressure-induced changes in capacitance. However, addition of exogenous adenosine promoted increased rates of capacitance change above those observed for tissue exposed to hydrostatic pressure alone. This additive effect could be explained if adenosine induced second messengers distinct form those generated by stretch, or that the effects of stretch and adenosine may act in a synergistic manner to raise the amount of second messengers such as Ca^{2+} to levels greater than stretch or

adenosine alone. Finally, we note that the serosal surface of the tissue has numerous cell types (e.g. uroepithelial cells, endothelial cells, fibroblasts, macrophages, smooth muscle cells, and myofibroblasts) and we can not rule out that adenosine binds to and stimulates release of secretegogues from these cell types that then indirectly stimulate exocytosis in the umbrella cell layer.

3.4.4 Adenosine as an autocrine/paracrine regulator of uroepithelial function

Other than bladder filling, and the attendant activation of downstream signaling cascades such as cAMP and Ca^{2+} (7, 18), the nature of the physiological stimuli that modulate membrane traffic in the umbrella cell are poorly understood. We recently identified extracellular ATP (released from the uroepithelium) as an important autocrine factor that acts as a proximal signal for both pressure-induced exocytosis and endocytosis (108). The data presented in this paper indicate that adenosine, acting through cell surface receptors, may also act in an autocrine/paracrine manner to regulate exocytosis in the umbrella cell layer both in response to, and independently of bladder filling.

Exocytic and related endocytic pathways are crucial because they regulate turnover of the apical membrane and proteins that comprise the apical membrane barrier of the umbrella cell (1). Furthermore, exocytosis/endocytosis in umbrella cells may modulate the sensory function of the uroepithelium, a recently described function of the epithelium that allows it to communicate the state of the external environment to the underlying nervous system and possibly the musculature as well (3, 173). The uroepithelium is now known to release various transmitters including nitric oxide, acetylcholine, and ATP, and

the uroepithelium expresses several neurotransmitter receptors including adrenergic, nicotinic, muscarinic, neurokinin, transient receptor potential channel 1 (VR1), P2X, and P2Y receptors (3, 4, 17, 54, 173-175), and now adenosine receptors (this paper). An important function of adenosine-induced membrane turnover could be to regulate the release of transmitters, and modulate the density of receptors at the surface of the umbrella cell. Finally, while we have identified one function for adenosine in the uroepithelium, modulation of exocytic traffic, it is likely that adenosine will regulate other functions of the uroepithelium and bladder including ion transport, urothepithelial-afferent nerve signaling, and bladder contraction.

4.0 CONCLUSIONS

The urinary bladder is an organ for urine storage and elimination. The fulfillment of this function requires the finely regulated action of several different tissues including the uroepithelium, detrusor, and nerves. Umbrella cells, once thought to be an inert barrier for toxic urine, may actively participate in multiple aspects of bladder function, including mechanically regulated responses.

My work clearly defines the umbrella cell response to different mechanical forces and force parameters, and provided a model for how umbrella cells accommodate increased urine volume and how the fullness of urine is then sensed. I also explored possible mechanosensors, transducers, and secondary messengers that function in this mechanotransduction pathway. The better understanding of this urinary bladder physiology may provide beneficial value for the treatment of bladder dysfunction, such as overactive bladder and urinary outlet obstruction.

4.1 MECHANICAL-REGULATED RESPONSES OF UMBRELLA CELLS

By monitoring electrophysiological parameters and apical membrane capacitance, umbrella cells showed significant sensitivity to mechanical stretch. My experiments indicate that the modulation of umbrella cell electrophysiological parameters and apical membrane capacitance is force direction dependent and stretch speed is the key modulating factor. By analyzing these data with different mechanical conditions, I proposed a two-membrane model whereby stretch of the apical membrane caused TEV hyperpolarization, TER decrease, Isc increase, and apical membrane capacitance increase, while stretch of the basolateral membrane caused the opposite responses. Although this model is supported by mathematical calculating and in vitro experiments, a direct observation is still needed. One possible approach is to selectively stretch just the umbrella cell apical or basolateral membrane using micro-aspiration technique, and analyze the corresponding umbrella cell electrophysiological responses. This may directly provide extra solid proof for my proposed umbrella cell mechanotransduction model. Besides, micro-aspiration technique (95, 96) and other methods such as atomic force microscope (AFM) can also be used to provide further information about mechanical properties of the apical and basolateral membrane, such as visoelasticity. Umbrella cells show distinct morphological and biochemical differences between their

apical and basolateral membrane. For example, apical membrane is rich in cholesterol and lacks actin filaments, while the basolateral membrane is rich in actin filaments. This may enable apical membrane to be extremely sensitive to mechanical stretch, because actin filaments generate a resistive force to external mechanical stimuli and control the cell's elasticity (176). Cholesterol also plays an important role in membrane function, and depletion of cholesterol increases membrane stiffness (177). These properties strongly suggest that the apical and basolateral membranes of umbrella cells have distinct mechanical properties, including a viscous apical membrane that enables a time dependent strain (mechanically termed as creep), and a basolateral membrane with very low elastic modulus that enables a strain-stiffing behavior. By investigating these properties and the underlying mechanisms, we may further understand the mechanical basis for stretch-induced responses.

4.2 MECHANOSENSORS, TRANSDUCERS, AND SECOND MESSENGERS IN STRETCH-REGULATED UMBRELLA CELL RESPONSES

Multiple factors have been identified to play a role in stretch-regulated umbrella cell responses, including ion channels, the cytoskeleton, and signaling molecules such as ATP, adenosine and Ca^{2+} (6, 17, 19, 113, 132).

Cation channels have long been described in the apical membrane of umbrella cells, but their identity is not clear. My functional data indicated that cation channels play an important role in apical membrane mechanotransduction and exocytosis/endocytosis. In preliminary experiments, I identified PKD1/PKD2 in umbrella cell apical membrane. The mechanotransduction functions of this complex in other cells strongly suggested that they might also play a similar function in the umbrella cell apical membrane (52, 53). PKD1/PKD2 mutants cause serious kidney disease that is related to mechanotransduction, while their possible function and relationship with mechanotransduction in bladder has never been investigated. Intriguingly, results of yeast two-hybrid analysis indicated that UPIII, an apical membrane protein in umbrella cells, interacts with PKD2, confirmed that PKD2 is also localized to the apical membrane and may interact with AUM particles. Interestingly, the umbrella cells of UPIII knockout mice show small or no plaques on their apical membrane (with accumulated cytoplasmic

vesicles) and the bladders develop vesicoureteral reflux (11), suggesting a phenotype that may result from abnormal mechanotransduction and vesicle fusion. As the possible mechanosensor/transducer for apical membrane Ca^{2+} influx and vesicle fusion, PKD2 may contribute to the development of this knockout phenotype by loss of interacting with UPIII.

Because of the relative complexity of the basolateral membrane compared to the apical membrane, multiple mechanosensors must exist and work in a coordinated fashion. For example, the integrin-mediated focal adhesion kinase may play a role in modulating the umbrella cell cytoskeleton and intracellular pathways through the force transmission from the extracellular matrix when the basolateral membrane is fully stretched. Selective inhibitive peptide may be used to examine this possible mechanotransduction function of integrins, such as Arg-Gly-Asp (RGD). Actin filaments and myosins are more likely to be involved in this process. Blebbistatin, a selective inhibitor of nonmuscle myosin II and inhibited myosin II-mediated mechanotransduction pathways in multiple cellular systems (75, 76, 95, 96), may be a useful tool to test the role of myosin-II in umbrella cell mechanotransduction. Ion channels are also involved, such as SK/IK and K_{ATP}, while their molecular mechanism in umbrella cell mechanotransduction is still not fully understood. Further investigation may reveal more interesting details for their functions in umbrella cell mechanotransduction, such as whether they have cross talk or they work independently.

Adenosine receptors are identified in umbrella cells, and umbrella cells also release significant adenosine. Adenosine receptors are shown to increase the apical membrane capacitance by an IP_3 and Ca^{2+} dependent pathway, and this pathway is also

required by stretch-induced apical membrane exocytosis. How these different upstream signals induce same downstream pathway and what relationship they may have is an interesting question. It is interesting to investigate whether adenosine receptor can also modulate umbrella cell electrophysiological properties. This is possible, as A2a is known to modulate K_{ATP} channels and cause membrane hyperpolarization and bladder smooth muscle relaxation (73). My data also show that K_{ATP} plays a role in modulating umbrella cell electrophysiological parameters.

Thus far, my data indicates the possible coordinated work of ion channels, receptors, cytoskeleton, and signal molecules in umbrella cell mechanotransduction. It is important to further define the inter-relationship among these components and how these coordinated work achieved.

4.3 MECHANOSENSORY TRANSDUCTION

As a non-excitable epithelial cell, umbrella cells provide an excellent model for mechanical manipulation, and the electrophysiological properties of the apical and basolateral membranes enable one to explore their distinctive responses to mechanical forces. The force direction dependence of umbrella cells responses is similar to that of hair cells (24). Furthermore, the modulation of umbrella cell's responses by stretch speed and a constant increase in apical membrane capacitance of ~100%, indicates that the basolateral membrane functions as a limiting factor of the mechanosensory machinery. It may also modulate ATP release. More direct experiments may further confirm this idea, such as the selective stretch of the apical or basolateral membranes and monitoring the release of ATP and other neurotransmitter.

In the gastrointestinal tract, mechanical forces play an important role in modulating gastrointestinal motor and secretory function. Epithelia line the inner wall of these organs and play an essential function in nutrient absorption and enzyme release in response to mechanical forces and chemical stimuli (nutrients) (118, 119). In the vascular system, shear stress regulates the function of endothelial cells, which also receives cycles of pulse that stretches their basolateral membrane. In the respiratory tract, in addition to sensing air flowing by apical cilia present on epithelial cell, air pressure causes distention

and stretch of the basolateral membrane. As polarized cells, epithelia cells have distinctive apical and basoalteral membranes, while their differentiate function in mechanotransduction, especially in mechanosensory transduction is poorly defined, and these epithelial cells are usually considered as an isotropic material in respond to external forces. My work clearly defined an anisotropic property and elaborately regulated responses of umbrella cells, and this may provide a new direction for the studies of mechanosensory transduction in other epithelial cells described above.

BIBLIOGRAPHY

1. Apodaca G. The uroepithelium: not just a passive barrier. Traffic. 2004 Mar;5(3):117-28.

2. Apodaca G, Balestreire E, Birder LA. The uroepithelial-associated sensory web. Kidney Int. 2007 Nov;72(9):1057-64.

3. Birder LA. More than just a barrier: urothelium as a drug target for urinary bladder pain. Am J Physiol Renal Physiol. 2005 Sep;289(3):F489-95.

4. Birder LA, Ruan HZ, Chopra B, Xiang Z, Barrick S, Buffington CA, et al. Alterations in P2X and P2Y purinergic receptor expression in urinary bladder from normal cats and cats with interstitial cystitis. Am J Physiol Renal Physiol. 2004 Nov;287(5):F1084-91.

5. Lewis SA. Everything you wanted to know about the bladder epithelium but were afraid to ask. Am J Physiol Renal Physiol. 2000 Jun;278(6):F867-74.

6. Lewis SA, de Moura JL. Incorporation of cytoplasmic vesicles into apical membrane of mammalian urinary bladder epithelium. Nature. 1982 Jun 24;297(5868):685-8.

7. Truschel ST, Wang E, Ruiz WG, Leung SM, Rojas R, Lavelle J, et al. Stretch-regulated exocytosis/endocytosis in bladder umbrella cells. Mol Biol Cell. 2002;13:830-46.

8. Hurst RE, Roy JB, Min KW, Veltri RW, Marley G, Patton K, et al. A deficit of chondroitin sulfate proteoglycans on the bladder uroepithelium in interstitial cystitis. Urology. 1996 Nov;48(5):817-21.

9. Parsons CL, Boychuk D, Jones S, Hurst R, Callahan H. Bladder surface glycosaminoglycans: an epithelial permeability barrier. J Urol. 1990 Jan;143(1):139-42.

10. Duncan MJ, Li G, Shin JS, Carson JL, Abraham SN. Bacterial penetration of bladder epithelium through lipid rafts. J Biol Chem. 2004 Apr 30;279(18):18944-51.

11. Hu P, Meyers S, Liang FX, Deng FM, Kachar B, Zeidel ML, et al. Role of membrane proteins in permeability barrier function: uroplakin ablation elevates urothelial permeability. Am J Physiol Renal Physiol. 2002 Dec;283(6):F1200-7.

12. Kong XT, Deng FM, Hu P, Liang FX, Zhou G, Auerbach AB, et al. Roles of uroplakins in plaque formation, umbrella cell enlargement, and urinary tract diseases. J Cell Biol. 2004 Dec 20;167(6):1195-204.

13. Lewis SA, Eaton DC, Clausen C, Diamond JM. Nystatin as a probe for investigating the electrical properties of a tight epithelium. J Gen Physiol. 1977 Oct;70(4):427-40.

14. Lewis SA, Wills NK. Apical membrane permeability and kinetic properties of the sodium pump in rabbit urinary bladder. J Physiol. 1983 Aug;341:169-84.

15. Lewis SA, Wills NK, Eaton DC. Basolateral membrane potential of a tight epithelium: ionic diffusion and electrogenic pumps. J Membr Biol. 1978 Jun 28;41(2):117-48.

16. Horisberger JD. Apical and basolateral membrane conductances in the TBM cell line. Am J Physiol. 1991 Jun;260(6 Pt 1):C1172-81.

17. Ferguson DR, Kennedy I, Burton TJ. ATP is released from rabbit urinary bladder epithelial cells by hydrostatic pressure changes--a possible sensory mechanism? J Physiol. 1997 Dec 1;505 (Pt 2):503-11.

18. Wang E, Truschel S, Apodaca G. Analysis of hydrostatic pressure-induced changes in umbrella cell surface area. Methods. 2003 Jul;30(3):207-17.

19. Wang EC, Lee JM, Johnson JP, Kleyman TR, Bridges R, Apodaca G. Hydrostatic pressure-regulated ion transport in bladder uroepithelium. Am J Physiol Renal Physiol. 2003 Oct;285(4):F651-63.

20. de Groat WC, Yoshimura N. Pharmacology of the lower urinary tract. Annu Rev Pharmacol Toxicol. 2001;41:691-721.

21. Gabella G, Davis C. Distribution of afferent axons in the bladder of rats. J Neurocytol. 1998 Mar;27(3):141-55.

22. Chien S. Mechanotransduction and endothelial cell homeostasis: the wisdom of the cell. Am J Physiol Heart Circ Physiol. 2007 Mar;292(3):H1209-24.

23. Chien S. Molecular basis of rheological modulation of endothelial functions: importance of stress direction. Biorheology. 2006;43(2):95-116.

24. Holt JR, Corey DP. Two mechanisms for transducer adaptation in vertebrate hair cells. Proc Natl Acad Sci U S A. 2000 Oct 24;97(22):11730-5.

25. Xu J, Liu M, Tanswell AK, Post M. Mesenchymal determination of mechanical strain-induced fetal lung cell proliferation. Am J Physiol. 1998 Sep;275(3 Pt 1):L545-50.

26. Zeichen J, van Griensven M, Bosch U. The proliferative response of isolated human tendon fibroblasts to cyclic biaxial mechanical strain. Am J Sports Med. 2000 Nov-Dec;28(6):888-92.

27. Matsuda N, Yokoyama K, Takeshita S, Watanabe M. Role of epidermal growth factor and its receptor in mechanical stress-induced differentiation of human periodontal ligament cells in vitro. Arch Oral Biol. 1998 Dec;43(12):987-97.

28. Lin SY, Corey DP. TRP channels in mechanosensation. Curr Opin Neurobiol. 2005 Jun;15(3):350-7.

29. Anishkin A, Kung C. Microbial mechanosensation. Curr Opin Neurobiol. 2005 Aug;15(4):397-405.

30. Kung C. A possible unifying principle for mechanosensation. Nature. 2005 Aug 4;436(7051):647-54.

31. Syntichaki P, Tavernarakis N. Genetic models of mechanotransduction: the nematode Caenorhabditis elegans. Physiol Rev. 2004 Oct;84(4):1097-153.

32. Sukharev S, Corey DP. Mechanosensitive channels: multiplicity of families and gating paradigms. Sci STKE. 2004 Feb 10;2004(219):re4.

33. Corey DP. New TRP channels in hearing and mechanosensation. Neuron. 2003 Aug 14;39(4):585-8.

34. Gillespie PG, Walker RG. Molecular basis of mechanosensory transduction. Nature. 2001 Sep 13;413(6852):194-202.

35. Lewis SA, Hanrahan JW. Apical and basolateral membrane ionic channels in rabbit urinary bladder epithelium. Pflugers Arch. 1985;405 Suppl 1:S83-8.

36. Clapham DE. TRP channels as cellular sensors. Nature. 2003 Dec 4;426(6966):517-24.

37. Montell C. Physiology, phylogeny, and functions of the TRP superfamily of cation channels. Sci STKE. 2001 Jul 10;2001(90):RE1.

38. Montell C. The TRP superfamily of cation channels. Sci STKE. 2005 Feb 22;2005(272):re3.

39. Montell C, Birnbaumer L, Flockerzi V, Bindels RJ, Bruford EA, Caterina MJ, et al. A unified nomenclature for the superfamily of TRP cation channels. Mol Cell. 2002 Feb;9(2):229-31.

40. Vriens J, Owsianik G, Voets T, Droogmans G, Nilius B. Invertebrate TRP proteins as functional models for mammalian channels. Pflugers Arch. 2004 Dec;449(3):213-26.

41. Howard J, Bechstedt S. Hypothesis: a helix of ankyrin repeats of the NOMPC-TRP ion channel is the gating spring of mechanoreceptors. Curr Biol. 2004 Mar 23;14(6):R224-6.

42. Walker RG, Willingham AT, Zuker CS. A Drosophila mechanosensory transduction channel. Science. 2000 Mar 24;287(5461):2229-34.

43. Sidi S, Friedrich RW, Nicolson T. NompC TRP channel required for vertebrate sensory hair cell mechanotransduction. Science. 2003 Jul 4;301(5629):96-9.

44. Strotmann R, Harteneck C, Nunnenmacher K, Schultz G, Plant TD. OTRPC4, a nonselective cation channel that confers sensitivity to extracellular osmolarity. Nat Cell Biol. 2000 Oct;2(10):695-702.

45. Suzuki M, Mizuno A, Kodaira K, Imai M. Impaired pressure sensation in mice lacking TRPV4. J Biol Chem. 2003 Jun 20;278(25):22664-8.

46. Vriens J, Watanabe H, Janssens A, Droogmans G, Voets T, Nilius B. Cell swelling, heat, and chemical agonists use distinct pathways for the activation of the cation channel TRPV4. Proc Natl Acad Sci U S A. 2004 Jan 6;101(1):396-401.

47. Birder L, Kullmann FA, Lee H, Barrick S, de Groat W, Kanai A, et al. Activation of urothelial transient receptor potential vanilloid 4 by 4alpha-phorbol 12,13-didecanoate contributes to altered bladder reflexes in the rat. J Pharmacol Exp Ther. 2007 Oct;323(1):227-35.

48. Torres VE, Harris PC. Mechanisms of Disease: autosomal dominant and recessive polycystic kidney diseases. Nat Clin Pract Nephrol. 2006 Jan;2(1):40-55; quiz

49. Koulen P, Cai Y, Geng L, Maeda Y, Nishimura S, Witzgall R, et al. Polycystin-2 is an intracellular calcium release channel. Nat Cell Biol. 2002 Mar;4(3):191-7.

50. Teilmann SC, Byskov AG, Pedersen PA, Wheatley DN, Pazour GJ, Christensen ST. Localization of transient receptor potential ion channels in primary and motile cilia of the female murine reproductive organs. Mol Reprod Dev. 2005 Aug;71(4):444-52.

51. Li Q, Montalbetti N, Wu Y, Ramos A, Raychowdhury MK, Chen XZ, et al. Polycystin-2 cation channel function is under the control of microtubular structures in primary cilia of renal epithelial cells. J Biol Chem. 2006 Dec 8;281(49):37566-75.

52. Nauli SM, Alenghat FJ, Luo Y, Williams E, Vassilev P, Li X, et al. Polycystins 1 and 2 mediate mechanosensation in the primary cilium of kidney cells. Nat Genet. 2003 Feb;33(2):129-37.

53. Nauli SM, Zhou J. Polycystins and mechanosensation in renal and nodal cilia. Bioessays. 2004 Aug;26(8):844-56.

54. Birder LA, Nakamura Y, Kiss S, Nealen ML, Barrick S, Kanai AJ, et al. Altered urinary bladder function in mice lacking the vanilloid receptor TRPV1. Nat Neurosci. 2002 Sep;5(9):856-60.

55. Miller C. An overview of the potassium channel family. Genome Biol. 2000;1(4):REVIEWS0004.

56. Goldstein SA, Bayliss DA, Kim D, Lesage F, Plant LD, Rajan S. International Union of Pharmacology. LV. Nomenclature and molecular relationships of two-P potassium channels. Pharmacol Rev. 2005 Dec;57(4):527-40.

57. Gutman GA, Chandy KG, Adelman JP, Aiyar J, Bayliss DA, Clapham DE, et al. International Union of Pharmacology. XLI. Compendium of voltage-gated ion channels: potassium channels. Pharmacol Rev. 2003 Dec;55(4):583-6.

58. Gutman GA, Chandy KG, Grissmer S, Lazdunski M, McKinnon D, Pardo LA, et al. International Union of Pharmacology. LIII. Nomenclature and molecular relationships of voltage-gated potassium channels. Pharmacol Rev. 2005 Dec;57(4):473-508.

59. Kubo Y, Adelman JP, Clapham DE, Jan LY, Karschin A, Kurachi Y, et al. International Union of Pharmacology. LIV. Nomenclature and molecular relationships of inwardly rectifying potassium channels. Pharmacol Rev. 2005 Dec;57(4):509-26.

60. Wei AD, Gutman GA, Aldrich R, Chandy KG, Grissmer S, Wulff H. International Union of Pharmacology. LII. Nomenclature and molecular relationships of calcium-activated potassium channels. Pharmacol Rev. 2005 Dec;57(4):463-72.

61. Nichols CG. KATP channels as molecular sensors of cellular metabolism. Nature. 2006 Mar 23;440(7083):470-6.

62. Seino S. ATP-sensitive potassium channels: a model of heteromultimeric potassium channel/receptor assemblies. Annu Rev Physiol. 1999;61:337-62.

63. Inagaki N, Seino S. ATP-sensitive potassium channels: structures, functions, and pathophysiology. Jpn J Physiol. 1998 Dec;48(6):397-412.

64. Babenko AP, Aguilar-Bryan L, Bryan J. A view of sur/KIR6.X, KATP channels. Annu Rev Physiol. 1998;60:667-87.

65. Baukrowitz T, Fakler B. KATP channels gated by intracellular nucleotides and phospholipids. Eur J Biochem. 2000 Oct;267(19):5842-8.

66. Campbell JD, Sansom MS, Ashcroft FM. Potassium channel regulation. EMBO Rep. 2003 Nov;4(11):1038-42.

67. Herrera GM, Heppner TJ, Nelson MT. Regulation of urinary bladder smooth muscle contractions by ryanodine receptors and BK and SK channels. Am J Physiol Regul Integr Comp Physiol. 2000 Jul;279(1):R60-8.

68. Mora TC, Suarez-Kurtz G. Effects of NS1608, a BK(Ca) channel agonist, on the contractility of guinea-pig urinary bladder in vitro. Br J Pharmacol. 2005 Mar;144(5):636-41.

69. Darblade B, Behr-Roussel D, Oger S, Hieble JP, Lebret T, Gorny D, et al. Effects of potassium channel modulators on human detrusor smooth muscle myogenic phasic contractile activity: potential therapeutic targets for overactive bladder. Urology. 2006 Aug;68(2):442-8.

70. Tertyshnikova S, Knox RJ, Plym MJ, Thalody G, Griffin C, Neelands T, et al. BL-1249 [(5,6,7,8-tetrahydro-naphthalen-1-yl)-[2-(1H-tetrazol-5-yl)-phenyl]-amine] : a putative potassium channel opener with bladder-relaxant properties. J Pharmacol Exp Ther. 2005 Apr;313(1):250-9.

71. Pandita RK, Ronn LC, Jensen BS, Andersson KE. Urodynamic effects of intravesical administration of the new small/intermediate conductance calcium activated potassium channel activator NS309 in freely moving, conscious rats. J Urol. 2006 Sep;176(3):1220-4.

72. Bonev AD, Nelson MT. ATP-sensitive potassium channels in smooth muscle cells from guinea pig urinary bladder. Am J Physiol. 1993 May;264(5 Pt 1):C1190-200.

73. Gopalakrishnan M, Whiteaker KL, Molinari EJ, Davis-Taber R, Scott VE, Shieh CC, et al. Characterization of the ATP-sensitive potassium channels (KATP) expressed in guinea pig bladder smooth muscle cells. J Pharmacol Exp Ther. 1999 Apr;289(1):551-8.

74. Petkov GV, Heppner TJ, Bonev AD, Herrera GM, Nelson MT. Low levels of K(ATP) channel activation decrease excitability and contractility of urinary bladder. Am J Physiol Regul Integr Comp Physiol. 2001 May;280(5):R1427-33.

75. Engler AJ, Sen S, Sweeney HL, Discher DE. Matrix elasticity directs stem cell lineage specification. Cell. 2006 Aug 25;126(4):677-89.

76. Frey MT, Tsai IY, Russell TP, Hanks SK, Wang YL. Cellular responses to substrate topography: role of myosin II and focal adhesion kinase. Biophys J. 2006 May 15;90(10):3774-82.

77. Geiger B, Bershadsky A. Exploring the neighborhood: adhesion-coupled cell mechanosensors. Cell. 2002 Jul 26;110(2):139-42.

78. Giannone G, Dubin-Thaler BJ, Rossier O, Cai Y, Chaga O, Jiang G, et al. Lamellipodial actin mechanically links myosin activity with adhesion-site formation. Cell. 2007 Feb 9;128(3):561-75.

79. Ingber DE. Mechanosensation through integrins: cells act locally but think globally. Proc Natl Acad Sci U S A. 2003 Feb 18;100(4):1472-4.

80. Ingber DE. Cellular mechanotransduction: putting all the pieces together again. Faseb J. 2006 May;20(7):811-27.

81. Tzima E, Irani-Tehrani M, Kiosses WB, Dejana E, Schultz DA, Engelhardt B, et al. A mechanosensory complex that mediates the endothelial cell response to fluid shear stress. Nature. 2005 Sep 15;437(7057):426-31.

82. Mobasheri A, Carter SD, Martin-Vasallo P, Shakibaei M. Integrins and stretch activated ion channels; putative components of functional cell surface mechanoreceptors in articular chondrocytes. Cell Biol Int. 2002;26(1):1-18.

83. Schwarz US, Erdmann T, Bischofs IB. Focal adhesions as mechanosensors: the two-spring model. Biosystems. 2006 Feb-Mar;83(2-3):225-32.

84. Tamada M, Sheetz MP, Sawada Y. Activation of a signaling cascade by cytoskeleton stretch. Dev Cell. 2004 Nov;7(5):709-18.

85. Altmann SM, Lenne PF. Forced unfolding of single proteins. Methods Cell Biol. 2002;68:311-35.

86. Oberhauser AF, Marszalek PE, Erickson HP, Fernandez JM. The molecular elasticity of the extracellular matrix protein tenascin. Nature. 1998 May 14;393(6681):181-5.

87. Rief M, Gautel M, Oesterhelt F, Fernandez JM, Gaub HE. Reversible unfolding of individual titin immunoglobulin domains by AFM. Science. 1997 May 16;276(5315):1109-12.

88. De La Rosette J, Smedts F, Schoots C, Hoek H, Laguna P. Changing patterns of keratin expression could be associated with functional maturation of the developing human bladder. J Urol. 2002 Aug;168(2):709-17.

89. Veranic P, Jezernik K. Trajectorial organisation of cytokeratins within the subapical region of umbrella cells. Cell Motil Cytoskeleton. 2002 Dec;53(4):317-25.

90. Romih R, Veranic P, Jezernik K. Actin filaments during terminal differentiation of urothelial cells in the rat urinary bladder. Histochem Cell Biol. 1999 Nov;112(5):375-80.

91. Berg JS, Powell BC, Cheney RE. A millennial myosin census. Mol Biol Cell. 2001 Apr;12(4):780-94.

92. Altman D, Sweeney HL, Spudich JA. The mechanism of myosin VI translocation and its load-induced anchoring. Cell. 2004 Mar 5;116(5):737-49.

93. Purcell TJ, Sweeney HL, Spudich JA. A force-dependent state controls the coordination of processive myosin V. Proc Natl Acad Sci U S A. 2005 Sep 27;102(39):13873-8.

94. Veigel C, Molloy JE, Schmitz S, Kendrick-Jones J. Load-dependent kinetics of force production by smooth muscle myosin measured with optical tweezers. Nat Cell Biol. 2003 Nov;5(11):980-6.

95. Effler JC, Iglesias PA, Robinson DN. A mechanosensory system controls cell shape changes during mitosis. Cell Cycle. 2007 Jan 1;6(1):30-5.

96. Effler JC, Kee YS, Berk JM, Tran MN, Iglesias PA, Robinson DN. Mitosis-specific mechanosensing and contractile-protein redistribution control cell shape. Curr Biol. 2006 Oct 10;16(19):1962-7.

97. Gupton SL, Waterman-Storer CM. Spatiotemporal feedback between actomyosin and focal-adhesion systems optimizes rapid cell migration. Cell. 2006 Jun 30;125(7):1361-74.

98. Mannikarottu AS, Hypolite JA, Zderic SA, Wein AJ, Chacko S, Disanto ME. Regional alterations in the expression of smooth muscle myosin isoforms in response to partial bladder outlet obstruction. J Urol. 2005 Jan;173(1):302-8.

99. Rhee AY, Ogut O, Brozovich FV. Nonmuscle myosin, force maintenance, and the tonic contractile phenotype in smooth muscle. Pflugers Arch. 2006 Sep;452(6):766-74.

100. Tschumperlin DJ, Dai G, Maly IV, Kikuchi T, Laiho LH, McVittie AK, et al. Mechanotransduction through growth-factor shedding into the extracellular space. Nature. 2004 May 6;429(6987):83-6.

101. Alexander LD, Alagarsamy S, Douglas JG. Cyclic stretch-induced cPLA2 mediates ERK 1/2 signaling in rabbit proximal tubule cells. Kidney Int. 2004 Feb;65(2):551-63.

102. Yano S, Komine M, Fujimoto M, Okochi H, Tamaki K. Mechanical stretching in vitro regulates signal transduction pathways and cellular proliferation in human epidermal keratinocytes. J Invest Dermatol. 2004 Mar;122(3):783-90.

103. Nguyen HT, Adam RM, Bride SH, Park JM, Peters CA, Freeman MR. Cyclic stretch activates p38 SAPK2-, ErbB2-, and AT1-dependent signaling in bladder smooth muscle cells. Am J Physiol Cell Physiol. 2000 Oct;279(4):C1155-67.

104. Balestreire EM, Apodaca G. Apical epidermal growth factor receptor signaling: regulation of stretch-dependent exocytosis in bladder umbrella cells. Mol Biol Cell. 2007 Apr;18(4):1312-23.

105. Ralevic V, Burnstock G. Receptors for purines and pyrimidines. Pharmacol Rev. 1998 Sep;50(3):413-92.

106. Bucheimer RE, Linden J. Purinergic regulation of epithelial transport. J Physiol. 2004 Mar 1;555(Pt 2):311-21.

107. Khakh BS, Burnstock G, Kennedy C, King BF, North RA, Seguela P, et al. International union of pharmacology. XXIV. Current status of the nomenclature and properties of P2X receptors and their subunits. Pharmacol Rev. 2001 Mar;53(1):107-18.

108. Wang EC, Lee JM, Ruiz WG, Balestreire EM, von Bodungen M, Barrick S, et al. ATP and purinergic receptor-dependent membrane traffic in bladder umbrella cells. J Clin Invest. 2005 Sep;115(9):2412-22.

109. Ruan HZ, Birder LA, Xiang Z, Chopra B, Buffington T, Tai C, et al. Expression of P2X and P2Y receptors in the intramural parasympathetic ganglia of the cat urinary bladder. Am J Physiol Renal Physiol. 2006 May;290(5):F1143-52.

110. Burnstock G. Release of vasoactive substances from endothelial cells by shear stress and purinergic mechanosensory transduction. J Anat. 1999 Apr;194 (Pt 3):335-42.

111. Chen CC, Akopian AN, Sivilotti L, Colquhoun D, Burnstock G, Wood JN. A P2X purinoceptor expressed by a subset of sensory neurons. Nature. 1995 Oct 5;377(6548):428-31.

112. Lewis C, Neidhart S, Holy C, North RA, Buell G, Surprenant A. Coexpression of P2X2 and P2X3 receptor subunits can account for ATP-gated currents in sensory neurons. Nature. 1995 Oct 5;377(6548):432-5.

113. Lewis SA, Lewis JR. Kinetics of urothelial ATP release. Am J Physiol Renal Physiol. 2006 Aug;291(2):F332-40.

114. Cockayne DA, Hamilton SG, Zhu QM, Dunn PM, Zhong Y, Novakovic S, et al. Urinary bladder hyporeflexia and reduced pain-related behaviour in P2X3-deficient mice. Nature. 2000 Oct 26;407(6807):1011-5.

115. Cook SP, McCleskey EW. ATP, pain and a full bladder. Nature. 2000 Oct 26;407(6807):951-2.

116. Fredholm BB, AP IJ, Jacobson KA, Klotz KN, Linden J. International Union of Pharmacology. XXV. Nomenclature and classification of adenosine receptors. Pharmacol Rev. 2001 Dec;53(4):527-52.

117. Lumpkin EA, Caterina MJ. Mechanisms of sensory transduction in the skin. Nature. 2007 Feb 22;445(7130):858-65.

118. Raybould HE. Does Your Gut Taste? Sensory Transduction in the Gastrointestinal Tract. News Physiol Sci. 1998 Dec;13:275-80.

119. Raybould HE. Visceral perception: sensory transduction in visceral afferents and nutrients. Gut. 2002 Jul;51 Suppl 1:i11-4.

120. Peier AM, Reeve AJ, Andersson DA, Moqrich A, Earley TJ, Hergarden AC, et al. A heat-sensitive TRP channel expressed in keratinocytes. Science. 2002 Jun 14;296(5575):2046-9.

121. Tian W, Salanova M, Xu H, Lindsley JN, Oyama TT, Anderson S, et al. Renal expression of osmotically responsive cation channel TRPV4 is restricted to water-impermeant nephron segments. Am J Physiol Renal Physiol. 2004 Jul;287(1):F17-24.

122. Gevaert T, Vriens J, Segal A, Everaerts W, Roskams T, Talavera K, et al. Deletion of the transient receptor potential cation channel TRPV4 impairs murine bladder voiding. J Clin Invest. 2007 Nov 1;117(11):3453-62.

123. Apodaca G. Modulation of membrane traffic by mechanical stimuli. Am J Physiol Renal Physiol. 2002 Feb;282(2):F179-90.

124. Minsky BD, Chlapowski FJ. Morphometric analysis of the translocation of lumenal membrane between cytoplasm and cell surface of transitional epithelial cells during the expansion-contraction cycles of mammalian urinary bladder. J Cell Biol. 1978 Jun;77(3):685-97.

125. Chlapowski FJ, Bonneville MA, Staehelin LA. Lumenal plasma membrane of the urinary bladder. II. Isolation and structure of membrane components. J Cell Biol. 1972 Apr;53(1):92-104.

126. Staehelin LA, Chlapowski FJ, Bonneville MA. Lumenal plasma membrane of the urinary bladder. I. Three-dimensional reconstruction from freeze-etch images. J Cell Biol. 1972 Apr;53(1):73-91.

127. Sarikas SN, Chlapowski FJ. Effect of ATP inhibitors on the translocation of luminal membrane between cytoplasm and cell surface of transitional epithelial cells during the expansion-contraction cycle of the rat urinary bladder. Cell Tissue Res. 1986;246(1):109-17.

128. Blankson H, Holen I, Seglen PO. Disruption of the cytokeratin cytoskeleton and inhibition of hepatocytic autophagy by okadaic acid. Exp Cell Res. 1995 Jun;218(2):522-30.

129. Swingle M, Ni L, Honkanen RE. Small-molecule inhibitors of ser/thr protein phosphatases, use and common forms of abuse. Methods Mol Biol. 2007;365:23-38.

130. Mohanty MJ, Li X. Stretch-induced Ca(2+) release via an IP(3)-insensitive Ca(2+) channel. Am J Physiol Cell Physiol. 2002;283:C456-C62.

131. Henquin JC. Pathways in beta-cell stimulus-secretion coupling as targets for therapeutic insulin secretagogues. Diabetes. 2004;53 (Suppl. 3):S48-S58.

132. Yu W, Zacharia LC, Jackson EK, Apodaca G. Adenosine receptor expression and function in bladder uroepithelium. Am J Physiol Cell Physiol. 2006 Aug;291(2):C254-65.

133. Moe P, Blount P. Assessment of potential stimuli for mechano-dependent gating of MscL: effects of pressure, tension, and lipid headgroups. Biochemistry. 2005 Sep 13;44(36):12239-44.

134. Kwak BR, Silacci P, Stergiopulos N, Hayoz D, Meda P. Shear stress and cyclic circumferential stretch, but not pressure, alter connexin43 expression in endothelial cells. Cell Commun Adhes. 2005 Jul-Dec;12(5-6):261-70.

135. Laine M, Arjamaa O, Vuolteenaho O, Ruskoaho H, Weckstrom M. Block of stretch-activated atrial natriuretic peptide secretion by gadolinium in isolated rat atrium. J Physiol. 1994;480:553-61.

136. Jiao JH, Baumann P, Baron A, Roatti A, Pence RA, Baertschi AJ. Sulfonylurea receptor ligands modulate stretch-induced ANF secretion in rat atrial myocyte culture. Am J Physiol Heart Circ Physiol. 2000;278:H2028-H38.

137. Kim SH, Cho KW, Chang SH, Kim SZ, Chae SW. Glibenclamide suppresses stretch-activated ANP secretion: involvements of K+ATP channels and L-type Ca2+ channel modulation. Plugers Arch. 1997;434:362-72.

138. Sand P, Anger A, Rydqvist B. Hypotonic stress activates an intermediate conductance K+ channel in human colonic crypt cells. Acta Physiol Scand. 2004 Dec;182(4):361-8.

139. Ibraghimov-Beskrovnaya O, Dackowski WR, Foggensteiner L, Coleman N, Thiru S, Petry LR, et al. Polycystin: in vitro synthesis, in vivo tissue expression, and subcellular localization identifies a large membrane-associated protein. Proc Natl Acad Sci U S A. 1997 Jun 10;94(12):6397-402.

140. Ferguson DR. Urothelial function. B J U Int. 1999 Aug;84:235-42.

141. Althaus M, Bogdan R, Clauss WG, Fronius M. Mechano-sensitivity of epithelial sodium channels (ENaCs): laminar shear stress increases ion channel open probability. Faseb J. 2007 Aug;21(10):2389-99.

142. Carattino MD, Sheng S, Kleyman TR. Epithelial Na+ channels are activated by laminar shear stress. J Biol Chem. 2004 Feb 6;279(6):4120-6.

143. Carattino MD, Sheng S, Kleyman TR. Mutations in the pore region modify epithelial sodium channel gating by shear stress. J Biol Chem. 2005 Feb 11;280(6):4393-401.

144. Fredholm BB, Ijzerman AP, Jacobson KA, Klotz K-N, Linden J. International union of pharmacology. XXV. Nomenclature and classification of adenosine receptors. Pharmacol Rev. 2001;53:527-52.

145. Hansen PB, Schnermann J. Vasoconstrictor and vasodialator effects of adenosine in the kidney. Am J Physiol. 2003;285:F590-F9.

146. Klinger M, Freissmuth M, Nanoff C. Adenosine receptors: G protein-mediated signalling and the role of accessory proteins. Cell Signaling. 2002;14:99-108.

147. Jackson EK, Raghvendra DK. The extracellular cyclic AMP-adenosine pathway in renal physiology. Annu Rev Physiol. 2004;66:571-99.

148. Schulte G, Fredholm BB. Signalling from adenosine receptors to mitogen-activated protein kinases. Cell Signaling. 2003;15:813-27.

149. Dixon AK, Gubitz AK, Sirinathsinghji JS, Richardson PJ, Freeman TC. Tissue distribution of adenosine receptor mRNA in the rat. B J Pharm. 1996;118:1461-8.

150. Stehle JH, Rivkees SA, Lee JJ, Weaver DR, Deeds JD, Reppert SM. Molecular cloning and expression of the cDNA for a novel A2-adenosine receptor subtype. Mol Endo. 1992;6:384-93.

151. Ikeda Y, Wu C, Fry CH. Role of P1-receptors in the contractile function of guinea-pig and human detrusor smooth muscle. Proc Physiol Society - Physiology Online. 2003;551P:C9.

152. Brown C, Burnstock G, Cocks T. Effects of adenosine-5-triphophate (ATP) and b,g -methylene ATP on the rat urinary bladder. Br J Pharmacol. 1979;65:97-102.

153. Nicholls J, Hourani SMO, Kitchen I. Characterization of P1-purinoceptors on rat duodenum and urinary bladder. Br J Pharmacol. 1992;105:639-42.

154. King JA, Huddart H, Staff WG. Purinergic modulation of rat urinary bladder detrusor smooth muscle. Gen Pharmacol. 1997;29:597-604.

155. Werkstrom V, Andersson K-E. ATP- and adenosine-induced relaxation of the smooth muscle of the pig urethra. BJU Int. 2005;96:1386-91.

156. Yang SJ, An JY, Shim JO, Park CH, Huh IH, Sohn UD. The mechanism of contraction by 2-chloroadenosine in cat detrusor muscle cells. J Urol. 2000;163:652-8.

157. Fry CH, Ikeda Y, Harvey R, Wu C, Sui GP. Control of bladder function by peripheral nerves: avenues for novel drug targets. Urology. 2004;63 (supplement 1):24-31.

158. Oka M, Kimura Y, Itoh Y, Sasaki Y, Taniguchi N, Ukai Y, et al. Brain pertussis toxin-sensitive G proteins are involved in the flavoxate hydrocholoride-induced suppression of the micturition reflex. Brain Res. 1996;727:91-8.

159. Sosnowski M, Yaksh TL. The role of spinal and brainstem adenosine receptors in the modulation of the volume-evoked micturition reflex in the unanesthetized rat. Brain Res. 1990;515:207-13.

160. Jackson EK, Zhu C, Tofovic SP. Expression of adenosine receptors in the preglomerular microcirculation. Am J Physiol. 2002;283:F42-F51.

161. Tan-Allen KY, Sun XC, Bonanno JA. Characterization of adenosine receptors in bovine corneal endothelium. Exp Eye Res. 2005;80:687-96.

162. Nanoff C, Jacobson KA, Stiles GL. The A2 adenosine receptor: guanine nucleotide modulation of agonist binding is ehnaced by proteolysis. Mol Pharmacol. 1991;39:130-5.

163. Rosin DL, Robeva A, Woodard RL, Guyenet PG, Linden J. Immunohistochemical localization of adenosine A2A receptors in the rat central nervous system. J Compar Neurol. 1998;401:163-86.

164. Acharya P, Beckel J, Ruiz WG, Wang E, Rojas R, Birder L, et al. Distribution of the tight junction proteins ZO-1, occludin, and claudin-4, -8, and -12 in bladder epithelium. Am J Physiol Renal Physiol. 2004 Aug;287(2):F305-18.

165. Heyne N, Benöhr P, Mühlbauer B, Delabar U, Risler T, Osswald H. Regulation of renal adenosine excretion in humans - role of sodium and fluid homeostasis. Nephrol Dial Transplant. 2004;19:2737-41.

166. Vidotto C, Fousert D, Akkermann M, Griesmacher A, Müller MM. Purine and pyrimidine metabolites in children's urine. Clinica Chimica Acta. 2003;335:27-32.

167. von Muijlwijk-Koezen JE, Timmerman H, van der Goot H, Menge WMPB, von Drabbe Künzel JF, de Groote M, et al. Isoquinoline and quinazoline urea analogues as antagonists for the human adenosine A3 receptor. J Med Chem. 2000;43:2227-38.

168. Gafni J, Munsch JA, Lam TH, Catlin MC, Costa LG, Molinski TF, et al. Xestospongins: potent membrane permeable blockers of the inositol 1,4,5-trisphosphate receptor. Neuron. 1997 Sep;19(3):723-33.

169. Maruyama T, Kanaji T, Nakade S, Kanno T, Mikoshiba K. 2APB, 2-aminoethoxydiphenyl borate, a membrane-penetrable modulator of Ins(1,4,5)P3-induced Ca^{2+} release. J Biochem (Tokyo). 1997;1997:498-505.

170. Saunders C, Keefer JR, Kennedy AP, Wells JN, Limbird LE. Receptors coupled to pertussis toxin-sensitive G-proteins traffic to opposite surfaces in Madin-Darby canine kidney cells. J Biol Chem. 1996;271:995-1002.

171. Jacobson KA, van Rhee AM. Development of selective purinoceptor agonists and antagonists. In: Jacobson KA, Jarvis MF, editors. Purinergic approches in experimental therapeutics. New York: Wiley-Liss, Inc.; 1997. p. 101-28.

172. Parekh AB, Putney JW, Jr. Store-operated calcium channels. Physiol Rev. 2005 Apr;85(2):757-810.

173. de Groat WC. The urothelium in overactive bladder: passive bystander or active participant? Urology. 2004 Dec;64(6 Suppl 1):7-11.

174. Birder LA, Apodaca G, De Groat WC, Kanai AJ. Adrenergic- and capsaicin-evoked nitric oxide release from urothelium and afferent nerves in urinary bladder. Am J Physiol. 1998 Aug;275(2 Pt 2):F226-9.

175. Birder LA, Nealen ML, Kiss S, de Groat WC, Caterina MJ, Wang E, et al. Beta-adrenoceptor agonists stimulate endothelial nitric oxide synthase in rat urinary bladder urothelial cells. J Neurosci. 2002 Sep 15;22(18):8063-70.

176. Janmey PA, McCulloch CA. Cell mechanics: integrating cell responses to mechanical stimuli. Annu Rev Biomed Eng. 2007;9:1-34.

177. Byfield FJ, Aranda-Espinoza H, Romanenko VG, Rothblat GH, Levitan I. Cholesterol depletion increases membrane stiffness of aortic endothelial cells. Biophys J. 2004 Nov;87(5):3336-43.